Integrated Detection, Estimation, and Guidance in Pursuit of a Maneuvering Target

by

Dany Dionne

Department of Electrical and Computer Engineering
McGill University
Montreal

A thesis submitted to the
Faculty of Graduate Studies and Research
in partial fulfillment of the requirements for the degree of
Doctor of Philosophy

Your file Votre référence
ISBN: 0-494-12832-1
Our file Notre référence
ISBN: 0-494-12832-1

ABSTRACT

The thesis focuses on efficient solutions of non-cooperative pursuit-evasion games with imperfect information on the state of the system. This problem is important in the context of interception of future maneuverable ballistic missiles. However, the theoretical developments are expected to find application to a broad class of hybrid control and estimation problems in industry. The validity of the results is nevertheless confirmed using a benchmark problem in the area of terminal guidance. A specific interception scenario between an incoming target with no information and a single interceptor missile with noisy measurements is analyzed in the form of a linear hybrid system subject to additive abrupt changes.

The general research is aimed to achieve improved homing accuracy by integrating ideas from detection theory, state estimation theory and guidance. The results achieved can be summarized as follows. (i) Two novel maneuver detectors are developed to diagnoze abrupt changes in a class of hybrid systems (detection and isolation of evasive maneuvers): a new implementation of the GLR detector and the novel adaptive-$\mathscr{H}_0$ GLR detector. (ii) Two novel state estimators for target tracking are derived using the novel maneuver detectors. The state estimators employ parameterized family of functions to described possible evasive maneuvers. (iii) A novel adaptive Bayesian multiple model predictor of the ballistic miss is developed which employs semi-Markov models and ideas from detection theory. (iv) A novel integrated estimation and guidance scheme that significantly improves the homing accuracy is also presented. The integrated scheme employs banks of estimators and guidance laws, a maneuver detector, and an on-line governor; the scheme is adaptive with respect to the uncertainty affecting the probability density function of the filtered state. (v) A novel discretization technique for the family of continuous-time, game theoretic, bang-bang guidance laws is introduced. The performance of the novel algorithms is assessed for the scenario of a pursuit-evasion engagement between a randomly maneuvering ballistic missile and an interceptor. Extensive Monte Carlo simulations are employed to evaluate the main statistical properties of the algorithms.

The thesis demonstrates the following. (1) The adaptive-$\mathscr{H}_0$ GLR detector delivers a more efficient and reliable diagnosis of evasive maneuvers than the original GLR detector. (2) Modeling of the target behavior by parametric families of functions permits to improve the accuracy of the state estimate. (3) Modeling of the future evasive maneuvers by semi-Markov models and their prediction by a Bayesian multiple model approach improves the homing accuracy of the terminal guidance. (4) The adaptation of the state estimator and the guidance law with respect to the probability density of the filtered state within the integrated scheme provides for further tuning of the terminal guidance scheme. (5) The discretization scheme for the bang-bang guidance laws is important and much simpler in application. Moreover, the homing accuracy achieved by using the discretized law is

at least as good as that achieved by the original game theoretic guidance laws.

RÉSUMÉ

Le focus de la thèse vise la solution efficace de jeux de poursuite-évasion non-coopératifs dans le contexte d'une information imparfaite sur l'état du système. Ce problème est important dans le cadre de l'interception de future missiles ballistiques maneuverables. Cependant, il est attendu que les développements théoriques de la thèse trouveront application dans une vaste classe de problèmes de commande hybride et d'estimation affectant l'industrie. La validité des résultats est néanmoins confirmée en utilisant un problème type du domaine du guidage terminal. Spécifiquement, un scénario d'interception entre une cible entrante, ayant accès à aucune information, et un seul missile intercepteur, avec des mesures bruitées, est analysée sous la forme d'un système linéaire hybride sujet à des changements additifs brusques.

L'ensemble de la recherche vise à atteindre une amélioration de la précision de guidage en intégrant des idées provenant de la théorie de la détection, de la théorie de l'estimation and du guidage. Les résultats obtenus peuvent être résumé comme suit. (i) Deux nouveaux détecteurs de maneuvre sont développés pour diagnoser les changements brusques dans une classe de systèmes hybrides (détection et isolation de maneuvres): une nouvelle implantation du détecteur GLR et le nouveau détecteur GLR adaptatif-$\mathscr{H}_0$. (ii) Deux nouveaux estimateurs d'état pour la poursuite de cible sont dérivés en utilisant les nouveaux détecteurs de maneuvre. Les estimateurs d'état emploient des familles paramétrisées de function pour décrire les possibles maneuvres d'évasion. (iii) Un nouveau prédicteur bayésien adaptatif à modèle multiple de la distance de passage ballistique est développé en employant des modèles semi-markoviens et des idées provenant de la théorie de la détection. (iv) Une nouvelle approche intégrée de l'estimation et du guidage permettant d'améliorer significativement la précision du guidage est aussi présentée. (v) Une nouvelle technique de discrétisation pour une famille de lois de guidage en temps continu de type bang-bang et provenant de la théorie des jeux est introduite. La performance des nouveaux algorithmes est déterminée pour le scénario d'engagement de poursuite-évasion entre un missile ballistique maneuvrant au hasard et un intercepteur. Des simulations Monte Carlo extensives sont employées pour évaluer les propriétés statistiques principales des algorithmes.

La thèse démontre ce qui suit. (1) Le détecteur GLR adaptatif-$\mathscr{H}_0$ délivre un diagnostic des maneuvres d'évasion plus efficace et fiable que le détecteur GLR original. (2) La modélisation du comportement de la cible par des familles paramétrisées de function permet d'améliorer la précision de l'estimation d'état. (3) La modélisation des maneuvres d'évasion futures par des modéles semi-markoviens et leur prediction par une approache bayésienne à modèle multiple améliore la précision guidage ter-

minal. (4) L'adaptation de l'estimateur d'état et de la loi de guidage par rapport à la densité de probabilité de l'état filtré livre, à l'intérieur de l'approche intégrée, un réglage supplémentaire du système de guidage terminal. (5) La technique de discrétisation pour les lois de guidage de type bang-bang est importante en ce qu'elle simplifie leur application. De plus, la précision du guidage obtenue par l'utilisation des lois discrétisées est au moins aussi bonne que celle obtenue par les lois de guidage originales provenant de la théorie des jeux.

ORIGINALITY AND CONTRIBUTIONS

The original contributions of the thesis comprises the development and the analysis of:

- Two novel maneuver detector algorithms that significantly extend the work of Willsky and Jones (1976) to the detection and isolation of target maneuvers in the situation when the value of the target acceleration is unknown at all times. The novel detectors are adaptive in the sense that they estimate on-line the parameters required for the isolation procedures, see Refs. [21, 28].

- Two novel state estimators for jump-Gaussian linear systems. The novel estimators are finite dimensional and recursive Gaussian sum filters that employ an adaptive and variable bank of models to approximate the probability distribution function of the state, see Refs. [20, 22, 23, 24]

- A novel algorithm to calculate the ballistic miss in pursuit-evasion scenarios involving a maneuvering target. The novel algorithm is a multiple model Bayesian predictor employing a set of adaptive semi-Markov models to describe the target behavioral pattern, see Ref. [27].

- A novel design of a guidance law which takes into account the uncertainty in the estimate of the target acceleration and which compensates for the interactions between the guidance systems and the estimation systems. The novel design employs a maneuver detector, banks of estimators and guidance laws, and an on-line governor, see Refs. [25, 26, 21, 29].

- A novel discretization scheme for continuous-time stabilizing bang-bang control laws. The discretized control law takes the form of a bounded linear guidance law and is a discrete-time analytical equivalent of the original nonlinear, continuous-time, control law, see Ref. [19].

LIST OF PUBLICATIONS

(A) Articles published or accepted in refereed journals:

1. Dionne D., Michalska H., Oshman Y. and Shinar J. (2005), A Novel Adaptive Generalized Likelihood Ratio Detector with Application to Maneuvering Target Tracking, AIAA Journal of Guidance, Control, and Dynamics, in press.
2. Dionne D., and Michalska H. (2005), An Adaptive Proportional Navigation Law for Interception of a Maneuvering Target, CSME Transactions on Industrial Automation and Control, in press.
3. Dionne D. and Michalska H. (2004), A Multiple Reference GLR State Estimator for Hybrid Systems, WSEAS Transactions on Circuits and Systems, v. 3, pp. 711-716.
4. Dionne D. and Michalska H. (2004), Integrated Estimation and Guidance for Target Interception, in Data Fusion for Situation Monitoring, Incident Detection, Alert and Response Management, NATO ASI Series Book, Kluwer, in press.
5. Michalska H. and Dionne D. (2004), An Adaptive, Variable Structure, Multiple Model Estimator, in Data Fusion for Situation Monitoring, Incident Detection, Alert and Response Management, NATO ASI Series Book, Kluwer, in press.

(B) Articles submitted to refereed journals:

1. Dionne D., Michalska H., Shinar J. and Oshman Y., Decision-Directed Adaptive Estimation and Guidance for an Interception Endgame, submitted to the AIAA Journal of Guidance, Control, and Dynamics.
2. Dionne D. and Michalska H., Cost-Equivalent Guidance Laws, submitted to the AIAA Journal of Guidance, Control, and Dynamics.

(C) Other referred contributions:

1. Dionne D. and Michalska H. (2005), An Adaptive GLR Estimator for State Estimation of a Maneuvering Target, Proceedings of the American Control Conference, in press.
2. Dionne D. and Michalska H. (2004), An Adaptive Multiple Reference GLR State Estimator for Hybrid Systems, Proceedings of the International Conference on Computing, Communications and Control Technologies, Austin, Texas, pp. 107–112.
3. Dionne D. and Michalska H. (2004), A Multiple Reference GLR State Estimator for Hybrid Systems, Proceedings of the WSEAS International Conference on Instrumentation, Measurements, Control, Circuits and Systems, Miami, Florida, paper n. 484-360.

4. Dionne D., Michalska H. and Oshman Y. (2004), Terminal Missile Guidance Using a Semi-Markov Target Model, Proceedings of the 16th IFAC Symposium on Automatic Control in Aerospace, St-Petersburg, Russia, June, v. 2, pp. 56-61.

STATEMENT OF THE AUTHOR'S CONTRIBUTIONS

The work presented in the thesis has been carried out almost entirely by the doctoral student alone. This include the original ideas, the derivation of the algorithms, and the production and analysis of the results.

Contents

List of Figures

List of Tables

The realization of this thesis spawn over several years during which numerous persons and organisms provided appreciable help. Notably, I would like to mention:

1. Hannah Michalska. As the supervisor of my Ph.D., her help and support permitted the realization of this thesis.
2. Josef Shinar and Yaakov Oshman who supervised my internship in the Faculty of Aerospace Engineering at Technion - Israel Institute of Technology.
3. My parents who encouraged and supported me in pursuing my career.
4. Stéphane Marquis, my boyfriend, for his patience and his understanding over the years.
5. Isabelle Bégin and Melita Hadzagic, my friends and colleagues, for all the good moments and mutual support while working on our respective theses.
6. Finally, the NSERC and FCAR organisms as they provided financial support for this thesis.

Chapter 1

Introduction

THIS chapter discusses the most important results reported in the literature and concerning change detection and state estimation in linear jump-Gaussian systems, as well as guidance in terminal pursuit evasion problems, in as far as they are relevant for the problems considered in this thesis. The motivation for the research is then provided.

1.1 Detection

Many stochastic processes encountered in applications such as target tracking, pattern recognition, and fault detection are characterized by the occurrence of abrupt changes at unknown time instants. An abrupt change is defined as a rapid change (a change which occurs over a single time interval) in the probability density function of a process, cf. [10]. The detection is the task of deciding whether an abrupt change occurred in a given observed process. There is a vast number of references in both the statistics and engineering literature concerning the detection of sudden changes occurring in either signals or systems. Recent surveys of the various approaches are provided in Refs. [9, 10, 37, 48, 81]. As is pointed out in Ref. [9], p. 5, the basic strategy used in many change detection problems typically consists of two steps. First, the problem is transformed into a standard form by generating certain "residuals". The residuals are artificial measurements designed to reflect possible changes of interest in the analyzed signal or system. The value of the residuals is, for example, zero while no change occurs. Next, sophisticated statistical methods solve the detection problem in terms of the residuals. The first step very much depends on the model used for the specific application under consideration while the second step, referred to as the "change detection problem", is performed by the detection algorithm. There are many diverse detection algorithms presented in the literature. These algorithms can be classified in terms of the following requirements:

- **Discrete versus continuous time.** Observations may be acquired continuously in time or, else, at discrete time instants. The length of the time intervals between discrete time measurements is either constant or, else, varies according to some rules.

- **On-line versus off-line detection.** All observations may be available in advance so that they can be processed simultaneously, or they may have to be processed on-line.

- **Performance criterion.** All algorithms contain a statistical trade-off between the speed at which changes are detected and the risk of generating "false alarms". The exact formulation of this trade-off may differ between the algorithms.

- **Information concerning the change.** By the very nature of the problem, the time at which a change occurs is unknown a priori, but the assumptions concerning the signal before and after the change vary widely. Important distinctions include the number of change points and the possible knowledge of the statistical distributions of the signal before and after the change.

- **Isolation of the change.** The isolation is the task of characterizing the nature of the abrupt change after its detection. Most detection algorithms cannot isolate the detected changes. The joint task of detecting and isolating a change is referred to as the diagnosis of a change, cf. [37].

In this thesis, the research concerning the detection of abrupt changes is limited to on-line detection and isolation methods for discrete-time observations containing one or more additive abrupt changes. The exact statistical distribution of the signal before and after the change is unknown but is assumed to belong to a parametric family of distributions. In the case of multiple change points, only "slowly-varying" systems are considered, i.e., systems for which the ratio between the largest time constant in the dynamics and the lower bound for the length of the time interval between the sequential changes is sufficiently small. The slowly-varying assumption permits to diagnoze individually the multiple change points.

The restriction to on-line algorithms implies the study of sequential detection methods. Such methods are necessary when an early warning of a change needs to be generated from data that are flowing in, and processed, as time progresses. Most sequential detection methods compare, at every time instant, a certain functional of the measurements with a certain a priori specified threshold. To position the contributions of this thesis in a broader context, various likelihood based and Bayesian based methods are reviewed below.

1.1.1 Bayesian Methods

For a given fixed probability of false alarm, the Bayesian methods provide the optimal detection rule minimizing the expected delay of detection, cf. [87]. The main idea of these methods is to use the a posteriori probability calculations to decide that a change has occurred, i.e., a detection occurs when the conditional probability of a change exceeds a conveniently chosen threshold. The performance criterion of the Bayesian methods is such that that the cost of a false alarm is one and that the cost of each observation after an abrupt change is c. Hence, the Bayesian cost function to be minimized is:

$$J(k) = \Pr(k < k^\star | \mathcal{Y}^k) + cE(k - k^\star | \mathcal{Y}^k)^+, \qquad c > 0 \tag{1.1}$$

where $k^\star$ is the time instant of the abrupt change and $\mathcal{Y}^k$ is the σ-algebra of all the measurements collected up to k. The Bayesian cost function can be rewritten in terms of the conditional probability, $\Pr(k > k^\star|\mathcal{Y}^k)$, that a change has occurred before time instant k:

$$J(k) = E\left[(1 - \Pr(k > k^\star|\mathcal{Y}^k)) + c\sum_{k=0}^{k-1} \Pr(k > k^\star|\mathcal{Y}^k) \right] \tag{1.2}$$

Assuming that the distributions of the observations before and after the change are known, it can be shown that the process $\{\Pr(k > k^\star|\mathcal{Y}^k), k > 0\}$ is a sub-martingale with respect to the filtration generated by the observations and that the conditional probabilities can be recursively calculated using the Bayes' rule, cf. [81]. Then, for some a priori distributions of the time of change, a recursive optimal detection rule with the cost as in (1.1) can be explicitly derived; for example, in Ref. [74] the optimal detection rule was obtained in the case when $\Pr(k < k^\star)$ has a geometric distribution.

Assuming that the distribution of the observations after the change is unknown, the conditional probability of a change loses, in general, its Markov property, cf. [81] and references therein. The latter fact disallows a recursive optimal detection rule. An important exception occurs in the case of hidden Markov models for which the distribution of the observations after the change is a member of a known finite set. Then, the conditional probability of a change point can be recursively calculated and recursive optimal detection rules can be formulated, cf. [31].

1.1.2 Likelihood Methods

The likelihood methods employ a set of likelihood functions associated to a set of hypotheses. The hypotheses describe admissible abrupt changes in the input. These methods diagnoze abrupt changes in a suitably chosen process with the aid of a sequential probability ratio test (SPRT) applied to likelihood functions. When the distribution of the observations before and after the change are known and when the observations are discrete, the CUSUM algorithm, a likelihood based method introduced in Ref. [60], provides the recursive optimal detector in terms of the worst mean detection delay, cf. [59, 62]. A continuous-time analogue was recently presented in Ref. [75] with similar recursive and optimal properties as its discrete-time counterpart.

When the exact distribution of the observations after the change is unknown, two possible solutions were suggested provided that the distribution belongs to a parametric family of distributions, cf. [83]. Both solutions are recursive if the number of considered hypotheses is bounded from above. The first solution relies on weighting the likelihood ratios with respect to all admissible distribution of the observations after the change using a probability measure. In the second solution, the unknown distribution is replaced by its maximum likelihood estimate and basically results in a generalized likelihood ratio (GLR) algorithm, first introduced in Ref. [85]. For a fixed false alarm probability, the GLR algorithm is asymptotically optimal in terms of the minimum average delay of detection as the false alarm probability goes to zero, cf. [49].

1.2 State Estimation

The state estimation problem is to estimate sequentially the state of a dynamical system using a sequence of noisy measurements of the output from the system. The probabilistic formulation of the problem and the requirement for updating the information on receipt of new measurements render the problem well suited for a solution via the Bayesian approach. The Bayesian approach to dynamic state estimation constructs the posterior probability density function (pdf) of the state based on all available information. This pdf embodies all available statistical information and it may be regarded as to be the complete solution to the estimation problem, cf. [61].

At time instant k when a measurement $y(k)$ becomes available, the pdf of the state can be expressed using the Bayes' rule:

$$\mathrm{p}\left(x(k)\left|\mathcal{Y}^k\right.\right) = \frac{\mathrm{p}\left(y(k)|x(k)\right)\mathrm{p}\left(x(k)\left|\mathcal{Y}_1^{k-1}\right.\right)}{\mathrm{p}\left(y(k)\left|\mathcal{Y}_1^{k-1}\right.\right)} \tag{1.3}$$

where $\mathcal{Y}_1^k$ is the σ-algebra generated by the measurements:

$$\mathcal{Y}_1^k \triangleq \sigma\{y(s) : 1 < s \leq k\} \tag{1.4}$$

Suppose that the pdf of the state at time $k-1$ is available, then the predicted pdf at time k, $\mathrm{p}\left(x(k)\left|\mathcal{Y}_1^{k-1}\right.\right)$, is obtained via the Chapman-Kolmogorov equation, cf. [61]:

$$\mathrm{p}\left(x(k)\left|\mathcal{Y}_1^{k-1}\right.\right) = \int \mathrm{p}(x(k)|x(k-1))\mathrm{p}\left(x(k-1)\left|\mathcal{Y}_1^{k-1}\right.\right)\,\mathrm{d}x(k-1) \tag{1.5}$$

and the normalizing constant in (1.3), $\mathrm{p}\left(y(k)\left|\mathcal{Y}_1^{k-1}\right.\right)$, is given by:

$$\mathrm{p}\left(y(k)\left|\mathcal{Y}_1^{k-1}\right.\right) = \int \mathrm{p}\left(y(k)|x(k)\right)\mathrm{p}\left(x(k)\left|\mathcal{Y}_1^{k-1}\right.\right)\,\mathrm{d}x(k) \tag{1.6}$$

The recursive propagation of the posterior pdf given by (1.3)-(1.6) is only a conceptual solution in the sense that it cannot be determined analytically. The implementation of the conceptual solution requires the storage of the entire pdf which is, in general, equivalent to an infinite dimensional vector. Only in a restrictive set of cases can the pdf be exactly and completely characterized by a sufficient statistic of fixed and finite dimension. Such is the case of a finite dimensional Gaussian linear system which gives rise to the Kalman filter, cf. [2].

Many continuous-time dynamical systems have often a time-variable structure in the sense that they are subject to structural changes occurring at discrete points in time and with only partly known characteristics. The latter are conveniently represented as hybrid systems which are combinations of continuous-time systems and discrete-event systems. The major challenge in state estimation for such systems arises from the presence of two types of uncertainties: the measurement uncertainty and the uncertainty about the current structure of the system. Optimal state estimation in stochastic linear hybrid systems is, in general, computationally intractable as it often fails to translate into a finite recursive state estimation scheme, cf. [47].

In this thesis, state estimation is limited to jump-Gaussian linear systems. The latter are hybrid systems characterized by an input which is both unknown and subject to abrupt changes. Several suboptimal state estimators have been proposed for jump-Gaussian linear systems. To situate the contributions of this thesis in a broader context, the following practical approaches for state estimation in jump-Gaussian linear systems are reviewed: Gaussian approximations, Gaussian sum filters, decision-directed approaches, grid-based methods, and particle filters.

1.2.1 Gaussian Approximations

The members of this class of suboptimal filters are analytic approximations which enforce the pdf of the state to be Gaussian. To yield a Gaussian pdf, the original system is first approximated by a linear Gaussian system. Then, a Kalman filter is applied to the approximate linear Gaussian system. For our purpose, the relevant members of this class of filters are the extended Kalman filter (EKF), cf. [2], and the Kalman filter augmented with a, so-called, shaping filter, cf. [7]. These two filters differ in the way the approximate linear Gaussian system is generated.

The EKFs approximate the original system by use of a local linearization technique, cf. [2]. The EKF can be an adequate approach when the original system is not subject to abrupt changes. In the presence of abrupt changes, the pdf of the state is in general multi-modal and the local linearization technique does not capture adequately the dynamics of the system, cf. [61].

The Kalman filter augmented with a shaping filter applies to linear Gaussian systems with an unknown input. This filter obtains a linear Gaussian approximation by removing the unknown input and by augmenting the system with a companion linear system (the so-called shaping filter). The companion Gaussian linear system is selected in such a way that the distribution of its companion state matches the first two moments of the distribution of the unknown input process. For jump-Gaussian linear systems, the most common shaping filters are the Wiener process input model shaping filter, cf. [7], and the Singer's shaping filter, cf. [76]. The Wiener process input model shaping filter approximates the unknown input by a Brownian motion. This model is appropriate when the distribution of the jumps follows a Poisson distribution since the two first moments of the Wiener and Poisson processes are the same, cf. [32]. The Singer's shaping filter approximates the unknown input by a correlated process noise. The distribution of this correlated process noise is selected to have the same first two moments as the distribution of a random telegraph wave.

1.2.2 Gaussian Sum Filters

The Gaussian sum filters are analytical approximations to (1.3)-(1.6) in which the pdf of the state is approximated by a Gaussian mixture:

$$\mathrm{p}\left(x \left| \mathcal{Y}^k \right.\right) \approx \sum_{i=1}^{q^k} w_i^k \mathcal{N}\left(x_i^k; \hat{x}_i(k|k), \mathbf{P}_i(k|k)\right) \tag{1.7}$$

where w_i^k are normalizing weights and $\hat{x}_i(k|k)$ and $\mathbf{P}_i(k|k)$ are outputs of filters matched to given linear Gaussian models. Such an approximation can be made as accurate as desired by employing a sufficient number of mixture components and it can naturally approximate a multi-modal pdf. The problem resides in designing a recursive and finite dimensional procedure to calculate w_i^k, $\hat{x}_i(k|k)$, and $\mathbf{P}_i(k|k)$.

In jump-Gaussian linear systems, the bank of model-matched filters is introduced to describe possible behaviors of the system. However, a perfect description of the pdf of the state by (1.7) is impractical since it requires an exponentially growing number of models, cf. [52]. Hence, certain model management techniques are required to limit the number of models. The model management techniques usually involve either the merging of similar models or the pruning of unlikely models. A comparison of both techniques is provided in Ref. [42].

The interacting multiple model (IMM) estimator is an acclaimed procedure for state estimation in jump-Gaussian linear systems. The IMM estimator employs a merging technique for model management and was first presented in Refs. [13, 14]. The IMM estimator consists of a bank of q models selected a-priori. The model-matched filters are then re-initialized at each time instant by "mixing" of the models:

$$\hat{x}_i(k-1|k-1) = \sum_{j=1}^{q} \mu_{ij}^{k-1} \hat{x}_j(k-1|k-1) \tag{1.8}$$

$$\begin{aligned}\mathbf{P}_i(k-1|k-1) = \sum_{j=1}^{q} \mu_{ij}^{k-1} \Big[&\mathbf{P}_j(k-1|k-1) + (\hat{x}_j(k-1|k-1) - \hat{x}_i(k-1|k-1)) \times \\ &(\hat{x}_j(k-1|k-1) - \hat{x}_i(k-1|k-1))^T \Big]\end{aligned} \tag{1.9}$$

The mixing probabilities, μ_{ij}^{k-1}, are calculated from the Markovian transition probabilities between the models (a priori known) and from the conditional probability of each model being true. The state estimate is obtained by a probabilistic mixture of the model-matched estimates weighted using the conditional probabilities of the models.

1.2.3 Decision Directed Methods

This class of suboptimal filters employs a governor which selects on-line (at each time instant) a model from a pre-defined bank of models. The state estimate is the model-matched estimate of the selected model. The selection is based on the output from a detector. The most notable members of this class of estimators are the decision directed adaptive estimator, cf. [58], and the variable state dimension (VSD) estimator, cf. [5]. Both estimators employ a detector to detect the occurrence of a maneuver. The detector detects changes in the mean of the pdf of the state. Whenever a maneuver is detected, a new model is selected from the bank and the most recent measurements are re-processed. However, the detectors employed are non-parametric and hence cannot isolate the characteristics of the maneuver. Thus, whenever a new model is selected, the number of observations to be re-processed is unknown and must be estimated from a-priori information.

The decision directed adaptive estimator employs a Kalman filter augmented with a shaping filter. The shaping filter requires the selection of some parameters, most notably the variance parameter. The underlying assumption is that the Kalman filter with a shaping filter should act as a whitening filter while minimizing the value of the variance parameter. The decision directed adaptive estimator employs a bank of values for the variance parameter and the value in effect is selected on-line as follows. First, the detector monitors the residuals of the filter. Next, whenever the detected mean of the residuals deviates from zero, a higher value for the variance parameter is selected.

The VSD estimator employs a bank of models which have different state dimensions and a detector which monitors the residuals of the filter. When the detector detects a deviation from zero in the means of the residuals, the governor triggers the selection of a model of a higher dimension and re-processes the most recent observations using the newly selected model.

1.2.4 Input Estimation Methods

In this class of methods, an estimate of the value of the unknown input is obtained by inversion of the dynamical system and yields a state estimate associated with the value of the estimated input, cf. [15]. This technique requires to perform a least square fit over the measurements conditioned on a dynamical system model and thus requires an assumption concerning the dynamical profile of the unknown input (the usual assumption is that the value of the unknown input is constant). Also, the least square fit can be performed only over a sliding window of the most recent measurements in order to avoid a continuous increase of the computational requirements. This class of estimators is generally characterized by slower convergence as compared to other techniques such as the IMM estimator and is also more computationally demanding, cf. [6, 7].

1.2.5 Grid-Based Methods

This class of nonlinear filters performs a numerical integration in order to solve the multidimensional integrals in (1.3)-(1.6). These methods can provide an exact pdf of the state if the state space is discrete. Then, the approach is finite dimensional if the number of states is finite. For continuous state space, the grid-based methods requires the discretization of the state space into N cells and the discretization of the integrals (1.5) and (1.6) over the trellis of cells, as follows:

$$\mathrm{p}(x(k)|\mathcal{Y}_1^{k-1}) = \int \mathrm{p}(x(k)|x(k-1))\mathrm{p}(x(k-1)|\mathcal{Y}_1^{k-1})\,\mathrm{d}x(k-1) \tag{1.10a}$$

$$\approx \sum_{i=1}^{N} w_i(k|k-1)\delta(x(k)-x_i(k)) \tag{1.10b}$$

$$\mathrm{p}(y(k)|\mathcal{Y}_1^{k-1}) = \int \mathrm{p}(y|x(k))\mathrm{p}(x(k)|\mathcal{Y}_1^{k-1})\,\mathrm{d}x(k) \tag{1.11a}$$

$$\approx \sum_{i=1}^{N} w_i(k|k-1) \int\limits_{x\in x_i(k)} \mathrm{p}\left(y(k)|x\right)\,\mathrm{d}x \tag{1.11b}$$

$$\approx \sum_{i=1}^{N} w_i(k|k-1)\mathrm{p}\left(y(k)|\bar{x}_i(k-1)\right) \tag{1.11c}$$

$$w_i(k|k-1) \triangleq \sum_{j=1}^{N} w_j(k-1|k-1) \int \mathrm{p}\left(x|\bar{x}_j(k-1)\right)\,\mathrm{d}x \tag{1.12a}$$

$$\approx \sum_{j=1}^{N} w_j(k-1|k-1)\mathrm{p}\left(\bar{x}_i(k)|\bar{x}_j(k-1)\right) \tag{1.12b}$$

$$w_i(k|k) \triangleq \frac{w_i(k|k-1) \int\limits_{x\in x_i(k)} \mathrm{p}\left(y(k)|x\right)\,\mathrm{d}x}{\mathrm{p}(y(k)|\mathcal{Y}_1^{k-1})} \tag{1.13a}$$

$$\approx \frac{w_i(k-1|k-1)\mathrm{p}\left(y(k)|\bar{x}_i(k-1)\right)}{\mathrm{p}(y(k)|\mathcal{Y}_1^{k-1})} \tag{1.13b}$$

where $\bar{x}_i(k-1)$ denotes the center of the ith cell at time instant $k-1$.

For systems which can be represented by a hidden Markov model, the grid-based methods can successfully find the full pdf of the system, cf. [57]. However, the grid-based methods have several disadvantages, cf. [61]. The grid must be sufficiently dense to deliver a good approximation of a continuous state space. As the dimensionality of the state space increases the computational cost of the approach increases dramatically. If the state space is not finite, a grid-based approach necessitates some imposed limitation of the state space. The state space must also be partitioned into cells a priori; the last implies that the resolution of the discretization cannot be later enhanced in the regions with high conditional probabilities.

The Viterbi algorithm, first presented in Ref. [82], is one of the most popular grid-based methods and is extensively used in speech processing. The state estimate is obtained from the path of the maximum a posteriori probability through the trellis.

That is, the state estimate is the last component of the sequence of discrete states that, given the measurements, maximizes the probability of the state sequence.

1.2.6 Particle Filters

This class of nonlinear filters performs numerical integrations in order to solve the multi-dimensional integrals in (1.3)-(1.6) to yield a pdf of the state. The numerical integrations are carried out by a sequential Markov chain Monte Carlo (MCMC) technique which can be viewed as a randomized adaptive grid approximation. The MCMC technique employs N particles which evolve randomly in time according to some a priori selected dynamics and, at each time instant, the population of particles is re-sampled using an importance sampling procedure. The pdf of the state is approximated by:

$$\mathrm{p}\left(x|\mathcal{Y}_1^k\right) \approx \sum_{i=1}^{N} w_i^k \delta\left(x(k) - x_i(k)\right) \mathrm{d}x_i \tag{1.14}$$

where w_i^k is the weight of particle i.

In analogy with the grid-based methods, the particles can be viewed as the centers of the grid cells that also have the capacity to evolve, cf. [61]. The advantage of filters based on such evolving particles rather than on a fixed grid is that they do not require truncation of infinite state spaces, permits the resolution of the numerical integration to be increased in regions with high conditional probabilities (by increasing the number of particles evolving in these regions), and are characterized by a limited computational cost that does not increase exponentially with the dimensionality of the state space. The main disadvantage is that, over time, the particles tend to degenerate in the sense that the particles follow the same path; The degeneracy of the particles renders the estimated description of the pdf unreliable.

The MCMC technique leads to several types of particle filters such as the filter presented in Ref. [35] which is similar to a Viterbi algorithm, but which employs evolving particles rather than a fixed trellis. See Ref. [61] and references therein for a review of several different implementations.

1.3 Guidance

Guidance is the process of modifying the trajectory of a vehicle in motion to reach a pre-specified target. In the most general sense, the target can be defined in terms of its state which can vary with time.

In application to a pursuit-evasion engagement, the guidance and control problem is usually separated into two phases: the midcourse phase and the terminal phase, cf. [36]. The midcourse phase occurs between the launch of the pursuer and the terminal phase. The midcourse phase has for its main objective to bring the pursuer in position that allows to reach the evader by the pursuer's on-board sensors. Once the target is detected by the pursuer, the terminal phase is initiated. The terminal guidance aims to minimize the miss distance of the pursuer with respect to the detected target. In this thesis, only the terminal guidance problem is considered.

Whenever the target is a moving object (an evader), the solution to the terminal guidance problem is difficult due to imperfect information about the target dynamics and its future evasive strategy. In particular, the interception of a highly maneuvering target such as a tactical ballistic missile (TBM) is an open problem. A highly maneuvering target is a target over which the interceptor does not enjoy a significant maneuverability advantage. The optimal solution to the finite horizon control problem with bounded controls and a terminal cost function for linear stochastic systems has been studied by Striebel in Ref. [78]. The theorem 1 in Ref. [78] demonstrates that the optimal control solution is in general a function of the whole pdf of the state rather than just its mean, i.e., the separation principle does not apply in general.

Nevertheless, this theorem demonstrates that, at least in certain cases, the optimal state estimator is still independent of the control law.

The two common solution approaches to the terminal guidance problem are based on deterministic optimal control formulations, cf. [90], and on deterministic game theoretic formulations, cf. [65, 67]. These approaches yield closed form guidance laws which are functions of an auxiliary variable called the zero effort miss (ZEM) and also known as the ballistic miss. The ZEM is the miss distance obtained from the homogenous solution of the system equations of motion; thus, the ZEM is dependent on the formulation of the problem and the system model. In a one-sided optimal control optimization problem, the ZEM at time instant t has the physical meaning of being the miss distance if, from the current time onwards, the interceptor does not apply controls ($u(l) = 0$, $l = t, ..., t_f$, where u is the interceptor's control and t_f is the final time instant of the engagement) and the target performs the expected maneuvers. In a two-sided game differential problem, the ZEM is the miss distance if, from the current time onwards, both players do not apply controls.

1.3.1 Optimal Control Formulations

Optimal control techniques assume that the future evasive strategy is completely defined, either in open-loop or close-loop form. The feedback nature of the guidance law then allows the pursuer to correct for inaccurate predictions of target maneuvers. The closed form guidance laws based on optimal control theory guidance are usually based on the application of linear quadratic optimal control theory and requires assuming full state observation and an unbounded control command. The difference between the various guidance laws then depends on the model employed to describe the system. The models can use various assumptions about the evader's acceleration and the pursuer's airframe/autopilot response. In all cases, the resulting optimal guidance law can be viewed as a modified form of proportional navigation, cf. [36].

The proportional navigation guidance (PN) law is a prominent member of this family of guidance laws, cf. [88, 90]. The characteristic assumption used in the PN law is that the future evader's acceleration is zero and that there is no lag in the autopilot response. Extensions to the PN law to an autopilot response represented by a first order transfer function (the MEL law) and to a non-zero (but constant) future target maneuver (the APN law) are provided in Refs. [18, 34], respectively.

In practice, three of the assumptions of deterministic optimal control formulations can never be met: the pursuer's command is always bounded, the state of the system cannot be fully and exactly observed, and the future target maneuvers are unknown. Hence, the solutions obtained using deterministic optimal control formulations are suboptimal and yield an acceptable terminal cost only when the interceptor enjoys a large maneuverability advantage over the evader, cf. [72].

1.3.2 Game Theoretic Formulations

The mathematical framework for analyzing conflicts controlled by independent agents is in the realm of dynamic games. The concept of such a formulation dates back to the fifties and was published in the seminal book of Isaacs [41]. Using this approach, the scenario of intercepting a maneuverable target is formulated as a zero-sum pursuit-evasion game:

$$J = \inf_{u \in \mathcal{A}_P^c} \sup_{z \in \mathcal{A}_E^c} |x_1(t_f)| \tag{1.15}$$

Here, $x_1(t_f)$ is the miss distance, u and z are the pursuer and evader controls, respectively, and $\mathcal{P}$ denotes the family of piecewise continuous functions. The symbols $\mathcal{A}_P^c$ and $\mathcal{A}_E^c$ represent the feasible sets for the pursuer and evader strategies, respectively. As compared to the deterministic control formulation, there is no information required about the future target maneuvers. The game solution provides simultaneously the missile's guidance law (the optimal pursuer strategy), the worst target maneuver (the optimal evader strategy) and the resulting guaranteed miss distance (the value of the game). However, a unique optimal (saddle-point) strategy does not always exists, and even if it exist, obtaining the solution can be challenging.

The game-theoretic saddle-point solutions are found to exist only into a part of the game space referred to as the *regular area.* Outside the regular area, i.e., in the so-called *singular area*, the value of the game is constant so the optimal strategies are arbitrary. The specific saddle-point strategies are functions of the information available to the evader, the dynamics of the system, and the maneuverability of the opponent. Whenever the information available to one the parties is imperfect, the solution of the game might involve a mixed strategy, i.e., the optimal solution might be of stochastic nature and be defined by a probabilistic distribution, cf. [8].

In the literature, there are two major formulations of a zero-sum pursuit-evasion game which delivers game-theoretic saddle-point analytical solutions. Both formulations assume full state observation (with a possible delay) and the original nonlinear dynamics is linearized along the collision course. The two formulations differ with respect to the type of bound affecting the acceleration of the two players. In the first formulation, called "linear quadratic differential game" (LQDG), a soft bound is employed, i.e., the control commands are theoretically unbounded, but effectively restricted through the employed cost function. The LQDG cost function penalizes the control energy of the players, cf. [11, 12, 51]. The resulting guidance laws require solving a Riccati equation. The second formulation, called "normed differential game" (NDG), employs a hard bound on the controls of both players, cf. [38, 39, 65, 67, 68]. The resulting guidance laws are of the bang-bang type and are a function of the ZEM; the explicit formulae for calculating the ZEM in these double-sided game differential formulations depend on the employed system models and are obtained by assuming that, from the current time onwards, both players do not apply control. A comparison of the two formulations is provided in Ref. [80].

In practice, the assumption of full state observation (delayed or not) is never met. Hence, the analytical saddle-point solutions of the game problem formulations are suboptimal. Simulation results show that the game theoretic guidance laws yield a lower terminal cost as compared with the guidance laws derived from deterministic optimal control problem, cf. [3].

1.4 Motivation for the Research Reported in this Thesis

The modern ballistic missile (BM) presents a great challenge to the guided missile community. Successful interception of a BM, carrying probably an unconventional warhead, requires a very small miss distance, or even a direct hit. This challenge motivated an intensive development of several ballistic missile defense (BMD) systems. All of them were designed by using state of the art technology, but conventional guidance and estimation concepts. Against non-maneuvering targets, flying on predictable ballistic trajectories, these systems succeeded to demonstrate "hit-to-kill" performance. Consequently, with the deployment of these BMD systems the threat of the currently operational BMs will be minimized or even eliminated.

However, in the future, highly maneuvering BMs can be anticipated. Re-entering ballistic missiles fly at very high speeds and their atmospheric maneuvering potential is comparable to that of the interceptors. Since non-maneuvering targets can be easily intercepted, the designer of a future BM will have the option of making this inherent maneuver potential usable by only a modest technical effort. Whether a BM is maneuvering in a fixed direction, or not maneuvering at all, its trajectory can be considered predictable, thus allowing successful interception. Optimal control and differential game formulations of the interception problem, cf. [67, 70], as well as extensive simulation studies, cf. [90], indicate that the most effective evasion is achieved by a well-timed direction reversal of the maximum maneuver. However, due to the lack of information about the state of the pursuer, the evader cannot accurately time the required direction change. Since no maneuvering, or maneuvering in a fixed direction might lead to a certain interception, the evasive strategy of the evader has to be random.

Previous studies of the terminal interception problem of a maneuvering BM pointed out that the main error sources responsible for a non-zero miss distance are, cf. [66]:

(a) The noisy measurements, i.e., imperfect information on the current evader's state, see Ref. [40] for a detailed description of the corruptions affecting the collected information,

(b) The non-ideal dynamics of the control system.

(c) The evasive maneuvers.

(d) The limited maneuverability of the pursuer.

The research presented in the thesis directly addresses the error sources (a) and (c). The error source (b) is partially treated in the thesis in the sense that the dynamics of the control system is represented by a transfer function. The error source (d) is also partially treated whenever the presented guidance schemes are combined with the solutions to normed bounded games of the type presented in Refs. [38, 39, 65, 67, 68]. The thesis presents the following novel algorithms.

- Two novel maneuver detectors which significantly extend the work of Willsky and Jones 1976 to the detection and isolation of target maneuvers in the situation when the value of the target acceleration is unknown at all times. The novel detectors are adaptive in the sense that they estimate on-line the parameters required for the detection and isolation procedures, see § 3.

- Two novel state estimators for jump-Gaussian linear systems. The novel estimators are finite dimensional and recursive Gaussian sum filters which employ an adaptive and variable bank of models to approximate the probability distribution function of the state, see § 4.

- A novel algorithm to calculate the ballistic miss in pursuit-evasion scenarios involving a maneuvering target. The novel algorithm is a multiple model Bayesian predictor employing a set of adaptive semi-Markov models to describe the target behavioral pattern, see § 5.

- A novel design of a guidance law which takes into account the uncertainty in the estimate of the target acceleration and which compensates for the interactions between the guidance systems and the estimation systems. The novel design employs a maneuver detector, banks of estimators and guidance laws, and an on-line govenor, see § 5.

- A novel discretization scheme of continuous-time stabilizing bang-bang control laws. The discretized control law takes the form of a bounded linear guidance law and is a discrete-time analytical equivalent of the original nonlinear continuous-time control law, see § 5.

The novel algorithms presented in this thesis apply to a class of problem broader than the one defined by the guidance and interception problem. The algorithms apply to the class of linear hybrid systems with additive inputs subject to parametric abrupt changes, as mathematically described in § 2. This class of systems is commonly encountered in several applications, most notably in quality control, recognition-oriented signal processing, fault detection, and monitoring and control of industrial plants.

Chapter 2

The Benchmark Problem: A Terminal Interception Engagement

TERMINAL interception engagements are short-horizon terminal control problems describing the pursuit of a maneuverable target by a guided missile. The information structure in such scenarios is generally imperfect as it is characterized by noise-corrupted measurements of the relative position of the target (evader) acquired by the guided missile (pursuer). The evader has no information on the pursuer, but, being aware that an interception may occur, is likely to perform evasive maneuvers.

In § 2.1, the terminal interception problem is formulated as a stochastic time-varying linear control problem. In the following sections, two specific time-invariant pursuit-evasion problems are considered: an engagement with nonlinear planar kinematics and an engagement with linear time-invariant planar kinematics. In the following chapters, the novel detection, estimation, and guidance algorithms are developed for the stochastic time-varying linear system of § 2.1, while the specific linear and nonlinear pursuit-evasion models are employed for the purpose of numerical simulations.

2.1 A Stochastic Problem

Consider a stochastic time-varying linear system with a continuous-valued base state x, sampled at intervals Δ, and modeled by:

$$x(k+1) = \mathbf{F}(k)x(k) + \mathbf{G}_1(k)u(k) + \mathbf{G}_2(k)z(k) + w(k) \tag{2.1a}$$

$$y_m(k) = \mathbf{H}(k)x(k) + \eta(k) \tag{2.1b}$$

with $x \in \mathbb{R}^n$, $u \in \mathbb{R}^{i_u}$, $z \in \mathbb{R}^p$, $y_m \in \mathbb{R}^r$. The process and measurement noises, w and η, are assumed to be normally distributed and independent: $w(k) \sim \mathcal{N}(0, \mathbf{Q}_w(k))$ and $\eta(k) \sim \mathcal{N}(0, \mathbf{Q}_\eta(k))$. The state and measurement variables, x and y_m, are random time series and the magnitude of the inputs u and z is bounded by $u^{\max}$ and $z^{\max}$, respectively. The input u is a known external input. The random process z is an unknown input whose behavior is subject to additive abrupt changes of unknown magnitude. The additive abrupt changes belong to a parametric family of functions and the time interval between the sequential changes exceeds a given lower bound $w^\star$ sufficiently larger than the sampling time interval, i.e., $w^\star >> \Delta$. Moreover, the system is slowly-varying in structure in the sense that the ratio between the largest time constant in the dynamical description of the system and the lower bound $w^\star$ is sufficiently small. The process z is not directly observed but the system (2.1) is assumed observable.

In the pursuit-evasion problem, the known input u in system (2.1) is the pursuer's command acceleration, also denoted by a_P^c, while the unknown input z represents the evader's command acceleration. The cost function, J, to be minimized by the pursuer is the miss distance. Due to the uncertainties, the miss distance is a random variable and the cost function has to be stated in a stochastic setting which also respects the definition of a successful interception model.

A realistic interception model depends on many physical parameters and is very complex. In this point-mass study, the probability of interception is determined by the following

$$P_d = \begin{cases} 1 & |M| \leq R_k \\ 0 & |M| > R_k \end{cases} \tag{2.2}$$

where R_k is the lethal (kill) radius of the interceptor and M is the miss distance. This model assumes an overall entire reliability of the guidance system equal to one.

The objective of the interceptor (pursuer) is to intercept the target (evader) with a predetermined probability of success, using the smallest possible lethal radius R_k. This probability, termed the single shot kill probability (SSKP), is defined by

$$\text{SSKP} = E\{P_d(R_k)\} \tag{2.3}$$

where E is the mathematical expectation taken with respect to the probability density of the noise against any given feasible target maneuver. Using this definition, the stochastic cost function, J', for some prescribed value SSKP $= P_{\text{pr}}$ is

$$J' = \inf\{R_k \text{ with respect to } a_P^c \in \mathcal{A}_P^c\} \tag{2.4a}$$

$$\text{where} \tag{2.4b}$$

$$P_{\text{pr}} = E(P_d(R_k)) \tag{2.4c}$$

$$\mathcal{A}_P^c \triangleq \left\{a_P^c \in \mathcal{P} \,\middle|\, |a_P^c(t)| \leq (a_P^c)^{\max} \;\text{ a.e. }\; t \in [0, t_f]\right\} \tag{2.4d}$$

Here, $\mathcal{A}_P^c$ is the set of feasible control command acceleration strategies for the pursuer and $\mathcal{P}$ denotes the family of piecewise functions. The cost function is to be minimized by the pursuer against all the disturbances created by the evader's acceleration commands.

For further use, let $\mathcal{Y}_{k_0}^k$ denote the σ-algebra generated by the measurements:

$$\mathcal{Y}_{k_0}^k \triangleq \sigma\{y_m(s) : k_0 \leq s \leq k\} \tag{2.5}$$

2.2 A Pursuit-Evasion Scenario with Nonlinear Planar Kinematics

The dynamics of the terminal interception problem is modeled mathematically in 3D by a set of nonlinear differential equations which can be linearized about a nominal collision trajectory, determined by the initial line of sight and by the initial velocity vector of the evader. The pursuer's heading angle, $\phi_{P_{\text{col}}}$, required for collision, is determined by

$$\sin(\phi_{P_{\text{col}}}) = \frac{V_E}{V_P}\sin(\phi_E(0)) \tag{2.6}$$

where V_P and V_E are the pursuer and evader velocities, respectively, and ϕ_E is the heading angle of the evader. The linearization allows for a decomposition of the three-dimensional model into two identical sets of planar equations lying in two perpendicular planes, cf. [1]; thus, in further studies, a single model of linearized planar motion can be considered. A schematic view of the planar end-game geometry is displayed in Fig. 2.1. The X axis is aligned with the initial line of sight that serves as the reference direction. Note that the respective velocity vectors are generally not aligned with the reference line of sight, but they remain close to the directions of the collision course indicated by Eq. (2.6). It is assumed that both the pursuer and the evader move with constant speeds and have bounded lateral accelerations $|a_j^c| < (a_j^c)^{\max}$, $j = \{E, P\}$. Moreover, the maneuvering dynamics of both opponents can be approximated by first-order transfer functions with time constants τ_P and τ_E, respectively.

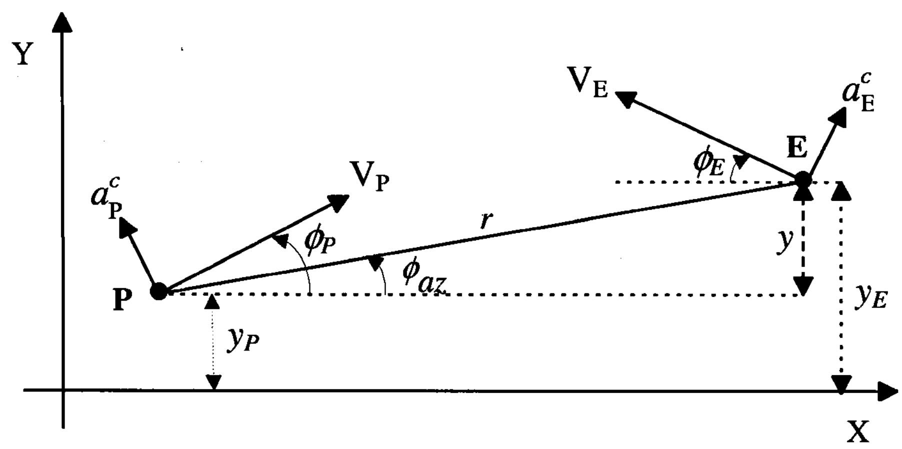

Figure 2.1: Planar engagement geometry. The pursuer is denoted by "P" and the evader by "E". The angles ϕ_P and ϕ_E are the heading angles for the pursuer and the evader, respectively, and ϕ_{az} is the line of sight angle. The acceleration a_P^c (respectively, a_E^c) is applied perpendicularly to the velocity vector of the pursuer V_P (respectively, to the velocity of the evader V_E).

The (deterministic) nonlinear equations of the planar interception are

$$\dot{x}_P = V_P\cos(\phi_P), \qquad \dot{x}_E = V_E\cos(\phi_E) \tag{2.7a}$$

$$\dot{y}_P = V_P\sin(\phi_P), \qquad \dot{y}_E = V_E\sin(\phi_E) \tag{2.7b}$$

$$\dot{\phi}_P = \frac{a_P}{V_P}, \qquad \dot{\phi}_E = \frac{a_E}{V_E} \tag{2.7c}$$

$$\dot{a}_P = \frac{a_P^c - a_P}{\tau_P}, \qquad \dot{a}_E = \frac{a_E^c - a_E}{\tau_E} \tag{2.7d}$$

where x_P and y_P are the positions of the pursuer along the X and Y axes, respectively, x_E and y_E are the positions of the evader along the X and Y axes, respectively, and a_P and a_E are the lateral accelerations of the pursuer and evader, respectively.

2.3 A Pursuit-Evasion Scenario with Linearized Planar Kinematics

For the linearization, it is assumed that the heading angles, ϕ_P and ϕ_E, are close to the direction of the collision course as indicated by Eq. (2.6). The linearized differential equations of relative planar motion normal to the reference line and the respective initial conditions are then

$$\dot{x}_1 = x_2; \qquad x_1(0) = 0 \tag{2.8a}$$

$$\dot{x}_2 = x_3 - x_4; \qquad x_2(0) = \left.\frac{\mathrm{d}y}{\mathrm{d}t}\right|_{t=0} \tag{2.8b}$$

$$\dot{x}_3 = \frac{a_E^c - x_3}{\tau_E}; \qquad x_3(0) = a_E(0) \tag{2.8c}$$

$$\dot{x}_4 = \frac{a_P^c - x_4}{\tau_P}; \qquad x_4(0) = a_P(0) \tag{2.8d}$$

and define a four-dimensional state vector

$$x^T = (x_1, x_2, x_3, x_4) \triangleq \left(y, \frac{\mathrm{d}y}{\mathrm{d}t}, a_E, a_P\right) \tag{2.9}$$

where $y \triangleq y_E - y_P$ is the lateral separation between the evader and the pursuer, and $\mathrm{d}y/\mathrm{d}t$ is the relative lateral velocity. The non-zero initial condition $x_2(0)$ represents the difference between the respective initial velocity components which are not aligned with the initial (reference) line of sight. Due to the assumption of small deviations from the collision geometry, this difference is small compared with the components along the line of sight. The linearization also yields a constant closing velocity, V_c

$$V_c = V_P \cos(\phi_{P\mathrm{col}}) + V_E \cos(\phi_E(0)) \tag{2.10}$$

allowing to compute the final time of the interception, t_f, for a given initial distance, X_0, as:

$$t_f = \frac{X_0}{V_c} \tag{2.11}$$

The matrix representation of the continuous time-invariant linearized dynamics (2.8) is

$$\dot{x}\,(t) = \mathbf{A}x(t) + \mathbf{B}_1 a_P^c(t) + \mathbf{B_2} a_E^c(t) \tag{2.12}$$

where

$$\mathbf{A} = \begin{bmatrix} 0 & 1 & 0 & 0 \\ 0 & 0 & 1 & -1 \\ 0 & 0 & \frac{-1}{\tau_E} & 0 \\ 0 & 0 & 0 & \frac{-1}{\tau_P} \end{bmatrix}, \quad \mathbf{B}_1 = \begin{bmatrix} 0 \\ 0 \\ 0 \\ \frac{1}{\tau_P} \end{bmatrix}, \quad \mathbf{B}_2 = \begin{bmatrix} 0 \\ 0 \\ \frac{1}{\tau_E} \\ 0 \end{bmatrix} \tag{2.13}$$

The corresponding matrices $\mathbf{F}$, $\mathbf{G}_1$, and $\mathbf{G}_2$ of the discrete-time representation of the linear dynamics over a sampling time interval Δ are, cf. [7], p. 192,

$$\mathbf{F} = \Phi(t+\Delta, t) = \mathcal{L}^{-1}\Big((s\mathbf{I} - \mathbf{A})^{-1}\Big)\Big|_{\Delta} = \begin{bmatrix} 1 & \Delta & \tau_E(\Delta - \Psi_E) & -\tau_P(\Delta - \Psi_P) \\ 0 & 1 & \Psi_E & -\Psi_P \\ 0 & 0 & e^{-\Delta/\tau_E} & 0 \\ 0 & 0 & 0 & e^{-\Delta/\tau_P} \end{bmatrix} \tag{2.14a}$$

$$\mathbf{G}_1 = \int_t^{t+\Delta} \Phi(t+\Delta, \tau)\mathbf{B}_1 \, \mathrm{d}\tau = \begin{bmatrix} \tau_P(\Delta - \Psi_P) - \frac{\Delta^2}{2} \\ \Psi_P - \Delta \\ 0 \\ 1 - e^{-\Delta/\tau_P} \end{bmatrix} \tag{2.14b}$$

$$\mathbf{G}_2 = \int_t^{t+\Delta} \Phi(t+\Delta, \tau)\mathbf{B}_2 \, \mathrm{d}\tau = \begin{bmatrix} -\tau_E(\Delta - \Psi_E) + \frac{\Delta^2}{2} \\ -\Psi_E + \Delta \\ 1 - e^{-\Delta/\tau_E} \\ 0 \end{bmatrix} \tag{2.14c}$$

where

$$\Psi_i \triangleq \tau_i(1 - e^{-\Delta/\tau_i}) \qquad i \in \{P, E\} \tag{2.14d}$$

2.4 The Measurement Model in the Pursuit-Evasion Scenarios

Using an on-board sensor, the only measurements available to the pursuer are the range, r, and the relative angular position, ϕ_{az}, of the evader with respect to an inertially fixed reference (e.g., the initial line of sight). The angle measurement ϕ_{az} is corrupted by a Gaussian noise μ while the range r is assumed to be measured perfectly. Using the small angle approximation, the linearized measurement of the lateral separation, y_m, is

$$y_m(t) = r(t)\sin\left(\phi_{\mathrm{az}}(t) + \mu(t)\right) \approx r(t)\phi_{\mathrm{az}}(t) + r(t)\mu(t), \qquad \mu(t) \sim \mathcal{N}(0, \sigma^2) \quad (2.15)$$

where μ is the angular measurement noise. Thus, the measurement matrix $\mathbf{H}$ and the linearized measurement noise η in Eq. (2.1b) are

$$\mathbf{H} = \begin{bmatrix} 1 & 0 & 0 & 0 \end{bmatrix}, \qquad \eta(t) = r(k)\mu \sim \mathcal{N}(0, (r(k)\sigma)^2) \quad (2.16)$$

where $r(k)$ is the distance to the evader in the discrete-time representation.

Remark The linearized pursuit-evasion model presented in § 2.3 and § 2.4, and slight variations of this model, have been broadly employed in several studies on guidance, see Refs. [11, 90] and references therein. The validity of this linearized model has been assessed for several types of pursuit-evasion scenarios and was found to be often acceptable during the last instants of a pursuit-evasion engagement, see Refs. [69, 90].

Chapter 3

Two Novel Detection Algorithms

MANY stochastic processes encountered in applications such as maneuvering target tracking, pattern recognition, and fault detection are characterized by the occurrence of abrupt changes at unknown time instants. Such abrupt changes are usually diagnosed by employing specialized detector algorithms, cf. [48]. The diagnosis task is performed in a two-stage manner, see Ref. [37], p. 218. In the first stage (referred to as detection), a decision is made whether an abrupt change has indeed occurred while in the second stage (referred to as isolation), the abrupt change is confirmed, and its estimated parametric characteristics are accepted as valid.

There is an inherent delay between the moment at which an abrupt change occurs and the time instant at which it is detected. This detection delay stems from the necessity of collecting sufficient information in order to render a detection with some reliability (usually, with respect to a pre-specified false alarm probability). It has been shown that the minimum average delay of detection is achieved by Bayesian detectors, cf. [73]. Unfortunately, optimal Bayesian detectors are in general not finite-dimensional whenever the value of the system input after the change is unknown, as is frequently the case in target tracking applications, see Ref. [81], p. 23. A finite-dimensional alternative for such systems is provided by the class of generalized likelihood ratio (GLR) type detectors. The GLR-type detectors have been shown to be asymptotically optimal under several criteria related to quickest detection, cf. [49]. In previous studies, the GLR detector algorithm, first presented in Ref. [85], has been applied successfully to maneuver detection, cf. [30, 46]. These studies assumed the system input to be unknown during the maneuver, however, the system inputs prior to the onset of the maneuver, referred to as the "reference realization", were assumed known. However, in situations where both the reference realization and the target maneuver are unknown, the GLR detector algorithm requires modifications.

This chapter presents two new detection algorithms suitable in situations when the system inputs are unknown both before and after an abrupt change. Both algorithms are equipped with the ability to adapt, on-line, the reference realization conditioned on the measurements and on the assumption that the reference realization is a member of a parametric family of functions. The first algorithm is a new implementation of the GLR detector that adaptively estimates the reference realization, but requires discarding the collected measurements intermittently. The second algorithm is a novel detector, termed adaptive-$\mathscr{H}_0$ GLR detector, that also adaptively estimates the reference realization but *which does not require discarding the collected measurements.* By preserving the collected measurements, a more accurate estimate of the reference realization can be achieved and the reliability of the detector is improved. The adaptive-$\mathscr{H}_0$ GLR detector can be viewed as a generalization of the GLR detector for isolation of additive abrupt changes in unknown inputs in linear systems.

The GLR detector is derived first. It is next followed in § 3.2 by a description of the novel implementation of the GLR detector for maneuver detection. The novel adaptive-$\mathscr{H}_0$ GLR detector is then derived in § 3.3.

3.1 The GLR Detector

The GLR detector addresses the basic problem of detecting changes in the mean value of an independent Gaussian sequence. As explained in Ref. [83], two possible solutions exist when the change is parametric but the parameter is unknown. Both solutions require calculating the ratio between the likelihood of a change and the likelihood that no change occurred. The first solution consists of weighting the likelihood ratio with respect to all possible values of the unknown parameter; however, it requires computing an integral of probability densities over the parameter space. The second solution replaces the unknown parameter by its maximum likelihood estimate, thus avoiding the integral operation. The second solution results in the generalized likelihood ratio (GLR) algorithm which was first presented in Ref. [85]. The GLR algorithm is described in detailed in Ref. [10].

The main ingredients of the GLR detector are parametric families of input functions. These input functions are translated into parametric families of distributions for the observations. The distributions of the observations are estimated on-line as members of these families of distributions. Based on the estimated distributions, a decision concerning the occurrence (or absence) of a maneuver is made, and the characteristics of the maneuver are derived. The basic tool employed by the GLR detector to estimate the distribution is the likelihood ratio defined as

$$L(\theta_1, \theta_0, \mathcal{Y}_{k_0}^k) \triangleq \frac{\mathrm{p}(\mathcal{Y}_{k_0}^k|\theta_1)}{\mathrm{p}(\mathcal{Y}_{k_0}^k|\theta_0)} \tag{3.1}$$

where θ_0, θ_1 are parameters. Whenever θ_0 is known, the likelihood ratio is a sufficient statistic for the parametric family θ_1. In other words, the information about θ_1 contained in the σ-algebra $\mathcal{Y}_{k_0}^k$ is concentrated in the statistic $L(\theta_1, \theta_0, \mathcal{Y}_{k_0}^k)$. For this reason, if the sufficient statistic $L(\theta_1, \theta_0, \mathcal{Y}_{k_0}^k)$ is available, it is not necessary to know the whole σ-algebra $\mathcal{Y}_{k_0}^k$ to make inference about θ_1.

The statistical approach of the GLR algorithm applies when the likelihood ratio is a function of two unknown independent parameters: the time instant of the change and the parameter describing the change θ_1. The parameter θ_0 is assumed known and describes the signal or system before the change. The statistical approach is then to use the maximum likelihood estimates of the two unknown parameters, and thus the double maximization

$$g_k = \max_{k_0 \leq j \leq k} \sup_{\theta_1} L(\theta_1, \theta_0, \mathcal{Y}_{k_0}^k) \tag{3.2}$$

where g_k is the decision function. The precise statement of the conditions on the probability densities $\mathrm{p}(\mathcal{Y}_{k_0}^k|\theta_i)$, $i \in \{0, 1\}$, under which this double maximization can be performed is found in Ref. [56]. The densities should belong to the so-called Koopman-Darmois family of probability densities

$$\mathrm{p}(\mathcal{Y}_{k_0}^k|\theta_i) = \mathfrak{h}(\mathcal{Y}_{k_0}^k) e^{\theta_i T(\mathcal{Y}_{k_0}^k) - \mathfrak{d}(\theta_i)} \tag{3.3}$$

where $\mathfrak{d}$ is a function strictly concave and infinitely many times differentiable over an interval of the real line, and T is a monotonic function. The detection of a change is proclaimed whenever the value of the decision function g_k reaches or exceeds a given threshold, h, as follows

$$g_k \underset{\theta_1}{\overset{\theta_0}{\lesseqgtr}} h \tag{3.4}$$

The scheme defined by the Eqs. (3.2) and (3.4) belongs to the class of sequential probability ratio tests (SPRT).

After a change is detected, the maximum likelihood estimates of the onset time instant of the change and of the parameter θ_1, denoted $\hat{k}^\star$, $\hat{\theta}_1$, respectively, are given by $\hat{k}^\star = j^{\max}$ and $\hat{\theta}_1 = \theta_1^{\sup}$ where

$$(j^{\max}, \theta_1^{\sup}) = \arg \max_{k_0 \leq j \leq k} \sup_{\theta_1} L(\theta_1, \theta_0, \mathcal{Y}_{k_0}^k) \tag{3.5}$$

3.1.1 The GLR Detector in Linear Systems

The GLR detector can be applied to Gaussian linear systems subject to additive abrupt changes, see Ref. [10], p. 209. The application of the GLR detector to such systems requires the generation of residuals, namely of artificial measurements that reflect the changes of interest. The residuals result from the transformation of the original sequence of dependent measurements into a sequence of independent Gaussian artificial measurements. These residuals are calculated to be the innovations of a Kalman filter. Let $k^\star$ be the onset time instant of the additive abrupt change θ_1, then the mean value of the innovation γ_1 delivered by a Kalman filter matched to θ_0 (referred to as the reference Kalman filter) is given by

$$E(\gamma_1(k)) = E(\gamma_0(k)) + \tilde{\rho}_1(k, k^\star) \tag{3.6}$$

where γ_0 is the innovation in absence of a change and the symbol $\tilde{\rho}_1$ denotes a drift in the mean (the so-called innovation signature, see § 3.1.2 for its calculation).[1]

The probability density $\mathrm{p}(\mathcal{Y}_{k_0}^k|\theta_i)$ can be calculated in terms of the innovations as follows

$$\mathrm{p}(\mathcal{Y}_{k_0}^k|\theta_i) = c e^{-\frac{1}{2}\sum\limits_{j=k_0}^{k} \gamma_i^T(j)\mathbf{V}^{-1}(j)\gamma_i(j)} \prod_{j=k_0}^{k} \sqrt{|\mathbf{V}^{-1}(j)|} \tag{3.7}$$

where $\mathbf{V}$ is the innovation covariance (the value of $\mathbf{V}$ is independent of θ_i) and c is a normalizing constant. The probability density is then a member of the Koopman-Darmois family of densities with the functions $\mathfrak{d}(\cdot)$ and $T(\cdot)$ being vector quadratic functions. Let the log-likelihood ratio, l, denote

$$l(\theta_1, \theta_0, \mathcal{Y}_{k_0}^k) \triangleq \ln L(\theta_1, \theta_0, \mathcal{Y}_{k_0}^k) \tag{3.8}$$

The log-likelihood ratio is calculated in terms of the innovations by:

$$l(\theta_1, \theta_0, \mathcal{Y}_{k_0}^k) = -\frac{1}{2}\left[\sum_{j=k_0}^{k} \gamma_1^T(j)\mathbf{V}^{-1}(j)\gamma_1(j) - \sum_{j=k_0}^{k} \gamma_0^T(j)\mathbf{V}^{-1}(j)\gamma_0(j)\right] \tag{3.9}$$

[1] Technically, only γ_0 is an innovation and γ_1 is a residual. For simplicity, both are referred to as innovations.

The supremum of the likelihood ratio can then be calculated analytically by noting that the log-likelihood ratio is a quadratic hypersurface. Before calculating the supremum, the quadratic hypersurface in Eq. (3.9) is expressed by employing Eq. (3.6) as

$$l(\theta_1, \theta_0, \mathcal{Y}_{k_0}^k) = \sum_{j=k_0}^{k} \tilde{\rho}_1^T(j,k^\star)\mathbf{V}^{-1}(j)\gamma_0(j) - \frac{1}{2}\sum_{j=k_0}^{k} \tilde{\rho}_1^T(j,k^\star)\mathbf{V}^{-1}(j)\tilde{\rho}_1(j,k^\star) \quad (3.10)$$

Then, the analytical unconstrained supremum of the quadratic hypersurface is

$$\sup_{\theta_1} l(\theta_1, \theta_0, \mathcal{Y}_{k_0}^k) = \frac{1}{2}\frac{\left(\sum\limits_{j=k_0}^{k} \tilde{\rho}_1^T(j,k^\star)\mathbf{V}^{-1}(j)\gamma_0(j)\right)^2}{\sum\limits_{j=k_0}^{k} \tilde{\rho}_1^T(j,k^\star)\mathbf{V}^{-1}(j)\tilde{\rho}_1(j,k^\star)} \quad (3.11)$$

The formula (3.11) is unusable as, by assumption, the parameter of the change θ_1 is unknown, hence its signature $\tilde{\rho}_1$ is unknown. However, a *normalized* signature, ρ_1, can be calculated by assuming some non-zero value for the parameter θ_1. Then, by linearity, any signature in the parametric family θ_1 can be calculated in terms of the normalized signature as follows, see Ref [10], p. 241,

$$\tilde{\rho}_1(j,k^\star) = \nu_1\rho_1(j,k^\star), \qquad j = k^\star, \cdots, k \quad (3.12)$$

where ν_1 is a scaling factor. By employing Eqs. (3.12) and (3.11), the supremum of the log-likelihood ratio can be calculated, without knowing the value of θ_1, as follows

$$\sup_{\theta_1} l(\theta_1, \theta_0, \mathcal{Y}_{k_0}^k) = \frac{1}{2}\frac{d^2(\theta_1, \theta_0, \mathcal{Y}_{k_0}^k)}{J(\theta_1, \theta_0)} \quad (3.13a)$$

$$d(\theta_1, \theta_0, \mathcal{Y}_{k_0}^k) \triangleq \sum_{j=k_0}^{k} \rho_1^T(j,k^\star)\mathbf{V}^{-1}(j)\gamma_0(j) \quad (3.13b)$$

$$J(\theta_1, \theta_0) \triangleq \sum_{j=k_0}^{k} \rho_1^T(j,k^\star)\mathbf{V}^{-1}(j)\rho_1(j,k^\star) \quad (3.13c)$$

and the maximum likelihood estimate, $\hat{\nu}_1$, of the scaling factor is given by

$$\hat{\nu}_1 \triangleq \arg\sup_{\nu_1} \mathrm{p}\left(\mathcal{Y}_{k_0}^k | \nu_1, \theta_1\right) \quad (3.14a)$$

$$= \frac{d(\theta_1, \theta_0, \mathcal{Y}_{k_0}^k)}{J(\theta_1, \theta_0)} \quad (3.14b)$$

In the above, d can be viewed as a correlation between the innovations and the normalized signature. This correlation property is typical of a matched filtering operation, see Ref. [10], p. 54. The quantity denoted by J is interpreted as the Kullback-Leibler divergence between the parameter θ_0 and the normalized value of θ_1. The Kullback-Leibler divergence is an information theoretic norm which acts as an index of the separability between two probability measures; it here provides the Euclidean distance between the parameter θ_0 and the normalized value of θ_1, see Ref. [10], p. 26.

3.1.2 Signature of the Change on the Innovations

Consider the following state space representation of a linear system subject to additive changes in the state or observation equation

$$x(k+1) = \mathbf{F}(k)x(k) + \mathbf{G}_1(k)u(k) + \mathbf{G}_2(k)f_x(k,k^\star) + w(k) \tag{3.15a}$$

$$y_m(k) = \mathbf{H}(k)x(k) + \mathbf{D}_1(k)u(k) + \mathbf{D}_2(k)f_y(k,k^\star) + \eta(k) \tag{3.15b}$$

where u is a known input, f_x and f_y are the dynamic profiles of the assumed change and $k^\star$ is the onset time instant of the change so that $f_x(k,k^\star) = f_y(k,k^\star) = 0$ for $k < k^\star$. The functions f_x and f_y are assumed to be parametric functions of time parameterized by θ_1. By linearity, the state, the state estimate from the reference Kalman filter, denoted $\hat{x}$, and its innovation can be decomposed as follows

$$x(k) = x_0(k) + \alpha(k,k^\star) \tag{3.16a}$$

$$\hat{x}(k|k) = \hat{x}_0(k|k) + \beta(k,k^\star) \tag{3.16b}$$

$$\gamma_1(k) = \gamma_0(k) + \tilde{\rho}_1(k,k^\star) \tag{3.16c}$$

where the subscript $(\cdot)_0$ denotes quantities calculated in absence of a change. The functions α, β, and $\tilde{\rho}$ are calculated recursively as follows, see Ref. [10], p. 239,

$$\alpha(k, k^\star) = \mathbf{F}(k)\alpha(k-1, k^\star) + \mathbf{G}_2(k-1)f_x(k-1, k^\star) \tag{3.17a}$$

$$\beta(k, k^\star) = \mathbf{F}(k)\beta(k-1, k^\star) + \mathbf{K}(k)\tilde{\rho}(k, k^\star) \tag{3.17b}$$

$$\tilde{\rho}(k, k^\star) = \mathbf{H}(k)\big(\alpha(k, k^\star) - \mathbf{F}(k)\beta(k-1, k^\star)\big) + \mathbf{D}_2(k)f_y(k, k^\star) \tag{3.17c}$$

with the initial conditions

$$\alpha(k^\star, k^\star) = 0 \tag{3.17d}$$

$$\beta(k^\star, k^\star) = 0 \tag{3.17e}$$

and where $\mathbf{K}$ is the Kalman gain of the reference Kalman filter.

3.2 The Original GLR Algorithm for Maneuver Detection

In the context of the problem specified in § 2.1, the task of the detector is to provide a full diagnosis of the unknown input maneuver z. The standard GLR detector tests a number of pre-specified hypotheses concerning the history of z after an abrupt change, but requires the knowledge of the input z before the change. Hence, the GLR detector, as first presented in Ref. [85], is not directly applicable to this problem because the input z is unknown at all time, i.e., z is unknown both before and after an abrupt change. This lack of information on z is common to many realistic detection scenarios.

This section presents an original implementation of the GLR detector for maneuver detection. The original GLR algorithm employs a re-initialization procedure to adapt on-line the estimated realization of z before an abrupt change, denoted by $\bar{z}$. Such an adaptation of the realization $\bar{z}$ provides the GLR detector with the ability to detect an abrupt change in z. It also provides the detector with the capacity to diagnoze more than one abrupt change. However, there are two trade-offs to this adaptation. First, all the measurements collected before the re-initialization must be discarded. Next, the adaptation of $\bar{z}$ is in general imperfect, hence the assumption of the GLR detector about a perfectly known $\bar{z}$ is invalid and the reliability of the detector degrades.

The following linear system, defined in § 2.1, is considered

$$x(k+1) = \mathbf{F}(k)x(k) + \mathbf{G}_1(k)u(k) + \mathbf{G}_2(k)z(k) + w(k) \tag{3.18a}$$

$$y_m(k) = \mathbf{H}(k)x(k) + \eta(k) \tag{3.18b}$$

where z is an unknown input subject to parametric additive abrupt changes. At any time instant k, the input signals to the GLR detection procedure are: 1) the measurements y_m, and 2) the set of hypotheses $S^k_{\mathscr{H}}$, for $k \geq 0$. Let $\mathcal{E}(k)$ be a binary indicator random variable (the detection indicator), such that

$$\mathcal{E}(k) \triangleq \begin{cases} 1 & \text{when an abrupt change has been detected at time } k \\ 0 & \text{otherwise} \end{cases} \tag{3.19}$$

Similarly, let $\mathcal{E}^R$ (k) be a binary indicator random variable (the isolation indicator), such that

$$\mathcal{E}^R(k) \triangleq \begin{cases} 1 & \text{when an abrupt change has been isolated at time } k \\ 0 & \text{otherwise} \end{cases} \tag{3.20}$$

The output signals from the GLR detection procedure are 1) the estimated onset time of the abrupt change, $\hat{k}^\star$, 2) the estimated value, $\hat{z}_{\mathrm{ML}}$, of the unknown input z after the change (this also necessitates identifying the class of parametric functions to which z belongs), 3) the state of the detection indicator $\mathcal{E}(k)$, and 4) the state of the isolation indicator $\mathcal{E}^R(k)$. The Figure 3.1 depicts a schematic block diagram of the original GLR algorithm for maneuver detection.

The state of the pair $\{\mathcal{E}(k), \mathcal{E}^R(k)\}$ describes one of the following mutually exclusive situations:

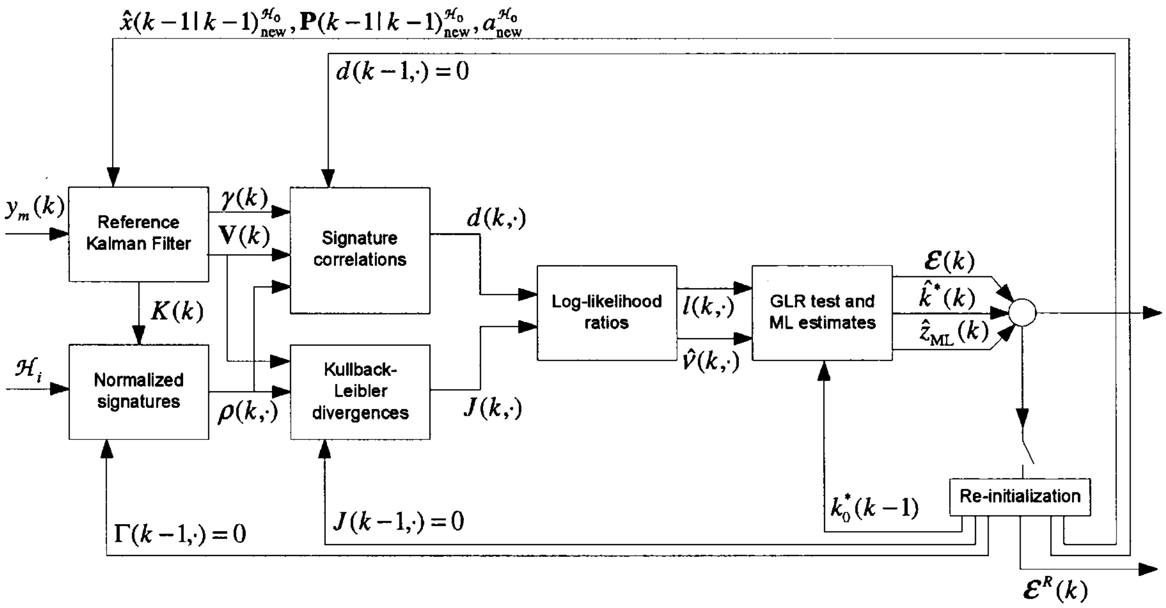

Figure 3.1: Schematic flow diagram of the a GLR detector for maneuver detection.

1. $\{\mathcal{E}(k), \mathcal{E}^R(k)\} = \{0,0\}$: in this case no abrupt change has been detected at $t = k$. All past detected abrupt changes, if any, have been isolated.

2. $\{\mathcal{E}(k), \mathcal{E}^R(k)\} = \{1,0\}$: in this case an abrupt change has been detected at time k, but not yet isolated.

3. $\{\mathcal{E}(k), \mathcal{E}^R(k)\} = \{1,1\}$: in this case an abrupt change has been detected and isolated at time k. To allow for the detection of subsequent abrupt changes, the states of both indicators are reset to zero at time instant $k+1$, i.e., $\{\mathcal{E}(k+1), \mathcal{E}^R(k+1)\} = \{0,0\}$ (unless another abrupt change has been detected at time $k+1$, in which case $\{\mathcal{E}(k+1), \mathcal{E}^R(k+1)\} = \{1,0\}$).

Using the detection and isolation indicators, a false detection (false alarm) event is defined as the event that results in the sequence $\{\mathcal{E}(k-1) = 1, \mathcal{E}^R(k-1) = 0, \mathcal{E}(k) = 0, \mathcal{E}^R(k) = 0\}$. The various cases described herein are shown schematically in Fig. 3.2. The procedures for determining the values of the binary variables $\mathcal{E}$, $\mathcal{E}^R$ are outlined in the sequel.

$\mathcal{E}$	0	0	0	0	0	0	1	1	1	0	0	0
$\mathcal{E}^R$	0	0	0	0	0	0	0	0	1	0	0	0
Event			J				D		I&R			

Time

(a) Detection and isolation of a single abrupt change

$\mathcal{E}$	0	0	0	0	0	0	1	0	0	0	0	0
$\mathcal{E}^R$	0	0	0	0	0	0	0	0	0	0	0	0
Event							D					

Time

(b) False detection

$\mathcal{E}$	0	0	0	0	1	1	1	1	1	0	0	0
$\mathcal{E}^R$	0	0	0	0	0	0	1	0	1	0	0	0
Event 1		J			D		I&R					
Event 2				J			D		I&R			

Time

(c) Detection and isolation of two close-by abrupt changes

Figure 3.2: Detection and isolation indicators' states. J: jump, D: detection, I&R: isolation and reset of both indicators.

The GLR algorithm is sequential in nature, as concisely detailed in the ensuing, and its computational load increases linearly with the number of considered hypotheses.

3.2.1 The Set of Hypotheses

A finite set of hypotheses $S^k_{\mathscr{H}} = \{\mathscr{H}_0, \mathscr{H}_1^k \ldots, \mathscr{H}_w^k\}$ is first introduced to adequately describe all relevant realizations of the time series z. This set of hypotheses must be updated at each current time instant k. Each hypothesis $\mathscr{H}_i^k \in S^k_{\mathscr{H}}$ corresponds to a different assumption about the onset time of the abrupt change, $k_i^\star(k)$, and an assumption about the possible class of parametric functions which adequately characterizes the shape of the change. Let $\{f_i(\cdot, k_i^\star)\}_{i=1}^w$ be a set of functions, representing all feasible classes of functions after the abrupt change. A particular shape of a change will then be referred to as $f_i(l, k_i^\star)$, $l \in [k_i^\star, k]$, for some $i \in \{1, 2, \ldots w\}$, whereas the actual change function would be $\nu_i f_i(l, k_i^\star)$, $l \in [k_i^\star, k]$, where ν_i is the change intensity. The GLR hypotheses do not require an assumption about the actual value of the change, as this value will be estimated later on by scaling. The members of the set of hypotheses $S^k_{\mathscr{H}}$ are, hence, defined as follows

$$\mathscr{H}_0: \quad z(l) = a^{\mathscr{H}_0}(l) \qquad l = k_0^\star, \ldots, k \tag{3.21a}$$

$$\mathscr{H}_i^k: \quad z(l) = a^{\mathscr{H}_0}(l) + \mathbf{1}(k_i^\star)\nu_i f_i(l, k_i^\star) \quad l \in \{k_0^\star, \ldots, k\}, \quad i \in \{1, \ldots, w\} \tag{3.21b}$$

where $\mathbf{1}(\cdot)$ is the unit step function. The hypothesis $\mathscr{H}_0$ is interpreted as the absence of any recent abrupt changes in the random process z and it assumes a specific realization $a^{\mathscr{H}_0}$ for the process z, whereas the hypothesis $\mathscr{H}_i^k$ corresponds to the occurrence of an abrupt change, of shape f_i, starting at time instant $k_i^\star$. It should be noted that all the hypotheses imply that only a single abrupt change can occur in the interval $[k_0^\star, k]$. In this context, it is clear how the parameters $k_i^\star(k)$ should be chosen at each k: since the length of the time interval between successive abrupt changes has been assumed to be bounded from below by $w^\star$, the parameters must be chosen so that $(k - w^\star) < k_i^\star(k) < k$ for all $i \in \{1, \ldots, w\}$. It is hence implied that all the abrupt changes outside the maximal sliding window $[k - w^\star, k]$ have been detected and isolated prior to k.

Effective Sliding Window of Hypotheses

In situations where $w^\star$ is large, it can be desirable to employ a sliding window smaller than the maximal sliding window to reduce the computational load. The resulting effective sliding window (ESW) has a width $w^\star_{\text{eff}} < w^\star$ and contains all the hypotheses with an onset time in the interval $(k - w^\star_{\text{eff}}) < k_i^\star(k) < k$. The detector loses little by employing an ESW provided that $w^\star_{\text{eff}}$ is sufficiently large and that some additional hypotheses are sparsely distributed over the interval $(k - w^\star) < k_i^\star(k) \leq (k - w^\star_{\text{eff}})$, as discussed in Ref. [49]. For the purpose of isolating the abrupt change, one of the hypotheses that has "slid out" of the ESW can be included as a member of the set of additional hypotheses. This additional hypothesis keeps track of a detected change whenever it slides out of the ESW.

3.2.2 The Reference Kalman Filter

To evaluate the likelihood of the individual hypotheses, a reference Kalman filter is implemented for the system (2.1a)-(2.1b), based on the assumption that hypothesis $\mathscr{H}_0$ is true

$$\hat{x}\,(k+1|k) = \mathbf{F}(k)\hat{x}\,(k|k) + \mathbf{G}_1(k)u(k) + \mathbf{G}_2(k)a^{\mathscr{H}_0}(k) \tag{3.22a}$$

$$\hat{x}\,(k|k) = \hat{x}\,(k|k-1) + \mathbf{K}(k)\gamma(k) \tag{3.22b}$$

where $a^{\mathscr{H}_0}$ is the assumed realization for the process z. The measurement residual, $\gamma(k)$, is

$$\gamma(k) = y_m(k) - \mathbf{H}(k)\hat{x}\,(k|k-1) \tag{3.23}$$

The gain, $\mathbf{K}$, the state estimation covariance, $\mathbf{P}$, and the residual covariance, $\mathbf{V}$, satisfy the Kalman filter Riccati equation, solved recursively by

$$\mathbf{K}(k) = \mathbf{P}(k|k-1)\mathbf{H}^T(k)\mathbf{V}^{-1}(k) \tag{3.24a}$$

$$\mathbf{P}(k+1|k) = \mathbf{F}(k)\mathbf{P}(k|k)\mathbf{F}^T(k) + \mathbf{Q}_w(k) \tag{3.24b}$$

$$\mathbf{P}(k|k) = \mathbf{P}(k|k-1) - \mathbf{K}(k)\mathbf{H}(k)\mathbf{P}(k|k-1) \tag{3.24c}$$

$$\mathbf{V}(k) = \mathbf{H}(k)\mathbf{P}(k|k-1)\mathbf{H}^T(k) + \mathbf{Q}_\eta(k) \tag{3.24d}$$

To calculate the likelihood ratios, the outputs needed from the reference Kalman filter are $\mathbf{K}$, γ, and $\mathbf{V}$. The reference Kalman filter is designed to act as a whitening filter over time intervals with no abrupt changes.

3.2.3 The Normalized Signatures: Novel Formulae

As mentioned earlier, the reference Kalman filter is matched to a hypothesis assuming a realization $a^{\mathscr{H}_0}$ for the process z. Whenever an abrupt change occurs, the difference between the true realization of z and the one employed by the Kalman filter manifests itself by a drift (the signature) in the mean of the residuals.

By assuming a normalized magnitude for the abrupt change, i.e., by employing a signature shape $f_i(k, k_i^\star)$, a normalized signature, $\rho(k,i)$, can be defined. The latter is recursively calculated as the product

$$\rho(k,i) = \mathbf{H}(k)\Gamma(k,i) \qquad i \in \{1, \dots, w\} \tag{3.25}$$

where

$$\Gamma(l,i) = \mathbf{G}_2(k) f_i(l, k_i^\star) + \mathcal{F}(l-1)\Gamma(l-1,i) \qquad l \in \{k_i^\star + 1, \dots, k\} \tag{3.26a}$$

$$\Gamma(k_i^\star, i) = 0 \tag{3.26b}$$

and

$$\mathcal{F}(l-1) \triangleq \mathbf{F}(k)[\mathbf{I} - \mathbf{K}(l-1)\mathbf{H}(k)] \tag{3.26c}$$

The Eqs. (3.25) and (3.26) introduced here to calculate an innovation signature are novel. They are mathematically equivalent to Eqs. (3.17) in case of an additive change in the state, but are simpler. The signature of an abrupt change and the normalized signature are related by a scaling factor. The value of this scaling factor is calculated as the ratio between the abrupt change and the shape of this abrupt change, as defined in Eq. (3.12).

Remark To facilitate the detection of a change, the signature of a change in the innovations should be large as it increases the Kullback-Leibler divergence between the hypotheses, see Eq. (3.13c). Hence, the reference Kalman filter should be characterized by a low bandwidth, as then the signature will be more pronounced after a change occurs.

3.2.4 The Log-Likelihood Ratios

To calculate the log-likelihood ratios, it is required to specify the realization of the process z after the abrupt change. Since the latter is unknown, its ML estimate is employed instead. The ML estimate of the process z is obtained under the assumption that hypothesis $\mathscr{H}_i^k$ is true. The log-likelihood ratio, $l(k,i)$, between the hypotheses $\mathscr{H}_i^k$ and $\mathscr{H}_0$, is then given by

$$l(k,i) = \frac{1}{2}\frac{d^2(k,i)}{J(k,i)} \qquad i \in \{1, \cdots, w\} \tag{3.27}$$

where $J(k,i)$ is the Kullback-Leibler divergence and $d(k,i)$ is the signature correlation of hypothesis $\mathscr{H}_i^k \in S_{\mathscr{H}}^k$, see § 3.1.1 for the derivation. The Kullback-Leibler divergence is a measure of the "distance" between the hypotheses $\mathscr{H}_i^k$ and $\mathscr{H}_0$ in $S_{\mathscr{H}}^k$ and is calculated recursively as follows

$$J(l,i) = J(l-1,i) + \rho^T(l,i)\mathbf{V}^{-1}(l)\rho(k,i) \qquad l \in \{k_i^\star + 1, \ldots, k\} \tag{3.28a}$$

$$J(k_i^\star, i) = 0 \tag{3.28b}$$

The signature correlation is interpreted as a least squares estimate of the value of the abrupt change, assuming that $\mathscr{H}_i^k$ is true and that no prior information about the value of the abrupt change is available, cf. [85]. It is recursively calculated as follows

$$d(l,i) = d(l-1,i) + \rho^T(l,i)\mathbf{V}^{-1}(l)\gamma(l) \qquad l \in \{k_i^\star + 1, \dots, k\} \tag{3.29a}$$

$$d(k_i^\star, i) = 0 \tag{3.29b}$$

3.2.5 The GLR Test

The GLR test establishes the validity of the hypotheses. The test is performed in two stages. First, the index, $i^\star(k)$, of the hypothesis maximizing the log-likelihood ratios is determined

$$i^\star(k) = \arg \max_{i \in \{1,\cdots,w\}} \{l(k,i)\} \tag{3.30}$$

Next, the validity of the most likely hypothesis, $\mathscr{H}_{i^\star}^k$, is assessed by comparing the maximized log-likelihood ratio with the value of a pre-selected threshold h

$$l(k, i^\star(k)) \underset{\mathscr{H}_{i^\star}^k}{\overset{\mathscr{H}_0}{\lesseqgtr}} h \tag{3.31}$$

and the detection indicator $\mathcal{E}(k)$ is set accordingly

$$\mathcal{E}(k) = \begin{cases} 0 & \mathscr{H}_0 \text{ is true} \\ 1 & \mathscr{H}_{i^\star}^k \text{ is true} \end{cases} \tag{3.32}$$

The value of h is selected as a function of the predefined probability of false alarm, denoted α, and is calculated from the tail of the distribution of the log-likelihood ratios. As the log-likelihood ratios are proportional to the square of the Gaussian random variable γ, see Eq. (3.27), the log-likelihood ratios have a χ^2 distribution. Furthermore, this χ^2 distribution has one degree of freedom only, cf. [10], p. 242. Hence, the value of h satisfies

$$\alpha = \int_h^\infty \chi^2(u)\,\mathrm{d}u \tag{3.33}$$

The Bounded GLR Test

When an upper bound in the magnitude of the abrupt change is known a priori, the GLR test can incorporate this additional information by modifying Eq. (3.30) as follows, see Ref. [10], p. 53,

$$i^{\star}(k) = \arg \max_{i \in \{1,\dots,w\}} \{ l(k,i) \mid |\hat{z}\,(k,i)| < z_{\mathrm{ML}}^{\max} \} \tag{3.34}$$

where $\hat{z}\,(k,i)$ is the hypothesis-matched estimate of the abrupt change and $z_{\mathrm{ML}}^{\max}$ is an upper bound on the magnitude of this estimate. The value of $z_{\mathrm{ML}}^{\max}$ should be larger than the a priori known upper bound, to allow for the presence of estimation errors in $\hat{z}\,(k,i)$. The estimate $\hat{z}\,(k,i)$ is given by

$$\hat{z}\,(k,i) \triangleq a^{\mathscr{H}_0}(k) + \hat{\nu}(k,i) f_i(k,k_i^{\star}) \tag{3.35}$$

In Eq. (3.35), the scaling factor, $\hat{\nu}(k,i)$, matches the shape employed by hypothesis $\mathscr{H}_i^k$ with the estimate of z and is calculated as the ratio

$$\hat{\nu}(k,i) = \frac{d(k,i)}{J(k,i)} \tag{3.36}$$

3.2.6 The ML Estimates

The GLR detector provides the ML estimate, $\hat{k}^{\star}$, of the onset time of the abrupt change, and the ML estimate, $\hat{z}_{\mathrm{ML}}$, of the value of the abrupt change. The ML estimate $\hat{k}^{\star}$ is given by

$$\hat{k}^{\star}(k) = \begin{cases} \hat{k}_0^{\star}(k) & \mathcal{E}(k) = 0 \\ k_{i^{\star}}^{\star}(k) & \mathcal{E}(k) = 1 \end{cases} \tag{3.37}$$

where $\hat{k}_0^{\star}$ is the ML estimate of the time instant of the last confirmed abrupt change

$$\hat{k}_0^{\star}(k) = \hat{k}_0^{\star}(k-1) \qquad \hat{k}_0^{\star}(0) = 0 \tag{3.38}$$

The value of $\hat{k}_0^\star(k-1)$ is updated by the re-initialization module described in the next subsection. The ML estimate $\hat{z}_{\mathrm{ML}}$ is given by

$$\hat{z}_{\mathrm{ML}}(k) = \begin{cases} a^{\mathscr{H}_0}(k) & \mathcal{E}(k) = 0 \\ a^{\mathscr{H}_0}(k) + \hat{\nu}\big(k, i^\star(k)\big) f_{i^\star}(k, k_{i^\star}^\star) & \mathcal{E}(k) = 1 \end{cases} \tag{3.39}$$

3.2.7 The Re-initialization Procedure

The purpose of the re-initialization of the detector is to allow for the detection of more than one abrupt change and to provide the GLR detector with the ability to eventually compensate for the unknown realization of z before an abrupt change. The time instant of this re-initialization is application dependent. In fault detection applications, for which no accurate isolation of the change is required, the re-initialization is usually carried out immediately after the detection of an abrupt change. In target tracking applications, the re-initialization is delayed to allow for a more accurate isolation of the target maneuver characteristics. Hence, in this work, a re-initialization of the GLR detector, indicated by $\mathcal{E}^R(k) = 1$, is performed whenever both an abrupt change is detected and the ML estimate of the time instant of the change is located at the lower end of the maximal sliding window, that is

$$\mathcal{E}^R(k) = \begin{cases} 1 & \{\mathcal{E}(k) = 1\} \wedge \{\hat{k}^\star = k - w^\star\} \\ 0 & \text{otherwise} \end{cases} \tag{3.40}$$

The re-initialization is carried out by modifying the hypothesis $\mathscr{H}_0$ so that it encapsulates the history of the process z prior to the lower end of the effective sliding window and by discarding the previously collected measurements, cf. [30, 85]. Such a re-initialization is performed as follows.

1. The reference Kalman filter is matched to the hypothesis $\mathscr{H}_{i^\star}^k$ by setting

$$a_{\text{new}}^{\mathscr{H}_0}(l) = a_{\text{old}}^{\mathscr{H}_0}(l) + \hat{\nu}(k, i^\star(k)) f_{i^\star}(l, k_{i^\star}^\star) \qquad l = k, \cdots \tag{3.41a}$$

$$\hat{x}\,(k|k)_{\text{new}}^{\mathscr{H}_0} = \hat{x}\,(k|k)_{\text{old}}^{\mathscr{H}_0} + \hat{\nu}(k, i^\star(k)) \Upsilon(k, i^\star(k)) \tag{3.41b}$$

$$\mathbf{P}(k|k)_{\text{new}}^{\mathscr{H}_0} = \mathbf{P}(k|k)_{\text{old}}^{\mathscr{H}_0} + \Upsilon(k, i^\star(k)) J^{-1}(k, i^\star(k)) \Upsilon^T(k, i^\star(k)) \tag{3.41c}$$

where

$$\Upsilon(k, i^\star(k)) \triangleq (\mathbf{I} - \mathbf{K}(k)\mathbf{H}(k))\Gamma(k, i^\star(k)) \tag{3.41d}$$

and $(\cdot)_{\text{old}}$ and $(\cdot)_{\text{new}}$ denote variables before and after re-initialization, respectively, and $(\cdot)^{\mathscr{H}_0}$ denotes variables employed by the reference Kalman filter.

2. The likelihood ratios are reset to zero by discarding the previously collected information

$$\Gamma(k, i) = 0, \quad d(k, i) = 0, \quad J(k, i) = 0 \qquad i \in \{1, \ldots, w\} \tag{3.42}$$

3. The information about the time instant of a confirmed abrupt change is preserved within $\hat{k}_0^\star$

$$\hat{k}_0^\star(k) = k^\star(k) \tag{3.43}$$

3.3 A Novel Adaptive-$\mathscr{H}_0$ GLR Detector

The novel implementation of the GLR detector of the previous section is based on the underlying assumption that the estimated realization $a^{\mathscr{H}_0}$ is indeed the true realization of the process z before the onset of the abrupt change and employs a re-initialization procedure to compensate for the unknown realization of z before an abrupt change. However, the re-initialization degrades the conditioning of the hypotheses as a re-initialization discards the collected measurements.

This section presents a novel GLR detector, named the adaptive-$\mathscr{H}_0$ GLR detector, which allows to compensate for the unknown realization of z before an abrupt change *without discarding the collected measurements.* By preserving the collected measurements, a more accurate estimate of the process z can be achieved and the reliability of the detector is improved. The adaptive-$\mathscr{H}_0$ GLR detector enables the reference acceleration for hypothesis $\mathscr{H}_0$ to be adapted on-line by introducing an additional and novel procedure for adaptation. The flowchart of the adaptive-$\mathscr{H}_0$ GLR detector is shown in Fig. 3.3. Compared to the implementation of GLR detector in § 3.2, the adaptive-$\mathscr{H}_0$ GLR detector has one more component termed "$\mathscr{H}_0$-adaptation". Four other components of the previous implementation of the GLR detector are also modified or augmented: the set of hypotheses $S^k_{\mathscr{H}}$, the GLR test, the ML estimates, and the re-initialization procedure. The calculations of the normalized signatures and of the log-likelihood ratios are similar to those of the GLR detector in § 3.2, however, in the new algorithm they employ the augmented set of hypotheses.

3.3.1 The Augmented Set of Hypotheses

The original set of hypotheses [Eqs. (3.21)] is now augmented with hypotheses whose purpose is to describe admissible shapes for a mismatch between the true realization of the process z and the realization assumed for $a^{\mathscr{H}_0}$. These additional hypotheses

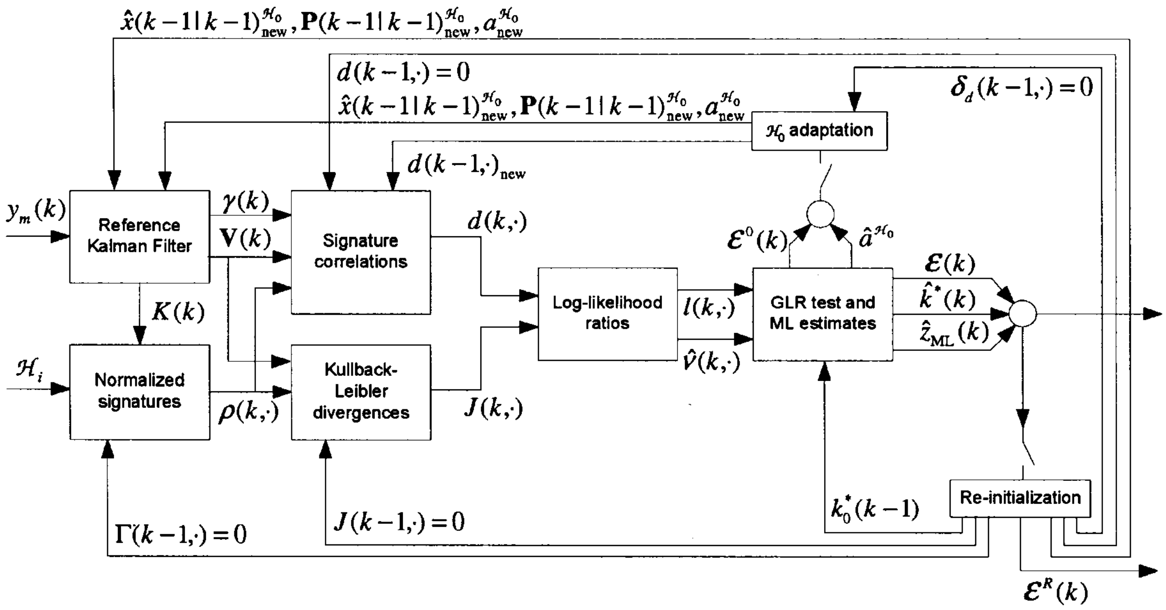

Figure 3.3: Schematic flow diagram of the adaptive-$\mathscr{H}_0$ GLR detector.

are analogs of $\mathscr{H}_0$ in the sense that they assume the absence of abrupt changes within the maximal sliding window. For simplicity of the exposition, only a single such additional hypothesis is considered here. Let $(\cdot)_\zeta$ designate quantities associated with this additional hypothesis, $\mathscr{H}_\zeta$, defined as

$$\mathscr{H}_\zeta: \quad z(l) = a^{\mathscr{H}_0}(l) + \nu_\zeta f_\zeta(l, k_0^\star) \qquad l \in \{k_0^\star, \dots, k\} \tag{3.44}$$

where $f_\zeta(\cdot, k_0^\star)$ is the shape assumed for the mismatch and ν_ζ is the intensity of the mismatch. The augmented set of hypotheses becomes $S^k_{\mathscr{H}} = \{\mathscr{H}_0, \mathscr{H}_\zeta, \mathscr{H}_1^k, \dots, \mathscr{H}_w^k\}$.

3.3.2 The Modified GLR Test

The GLR test now has the double task of: 1) establishing the validity of the hypotheses, as before, and 2) distinguishing between the event of an abrupt change in the process z and the event of a mismatch in the realization $a^{\mathscr{H}_0}$. The task of establishing the validity of the hypotheses is carried out as in § 3.2, but the index $i^\star$ is now determined according to

$$i^{\star}(k) = \arg \max_{i \in \{\zeta, 1, \ldots, w\}} \{\beta(i) l(k,i) \mid |\hat{z}\,(k,i)| < z_{\mathrm{ML}}^{\max}\} \tag{3.45}$$

where the factor β is selected such that $\beta(i) = 1$ for $i \in \{1, \cdots, w\}$ and $\beta(\zeta) \geq 1$. The purpose of the factor β is to enable the algorithm to favor the selection of the hypothesis $\mathscr{H}_{\zeta}$ whenever the available information is not sufficient for the task of distinguishing between the onset of an abrupt change and a mismatch in $a^{\mathscr{H}_0}$. The validity of the most likely hypothesis, $\mathscr{H}_{i^\star}^{k}$, is assessed by comparing the maximized log-likelihood ratio with the value of a pre-selected threshold h

$$l(k, i^{\star}(k)) \underset{\mathscr{H}_{i^\star}^{k}}{\overset{\mathscr{H}_0}{\lesseqgtr}} h \tag{3.46}$$

and the value of the detection indicator $\mathcal{E}(k)$ is set by Eq. (3.32), similarly to the new GLR detector of § 3.2.

The additional task, of deciding about the type of the event, is carried out by introducing a complementary binary variable, $\mathcal{E}^0$, whose value is set according to the rule

$$\mathcal{E}^0(k) = \begin{cases} 0 & \{\mathscr{H}_{i^\star}^{k} \text{ is true}\} \wedge \{i^{\star}(k) \neq \zeta\} \\ 1 & \{\mathscr{H}_{i^\star}^{k} \text{ is true}\} \wedge \{i^{\star}(k) = \zeta\} \end{cases} \tag{3.47}$$

In Eq. (3.47), $\mathcal{E}^0(k) = 0$ indicates the event of an abrupt change in the process z, whereas $\mathcal{E}^0(k) = 1$ indicates the event of a mismatch in the reference realization $a^{\mathscr{H}_0}$.

3.3.3 The Modified ML Estimates

The interpretation of the ML estimates provided by the detector depends on the type of event detected in the previous stage. In the event of an abrupt change ($\mathcal{E}^0(k) = 0$), there are two ML estimates: an estimate of the onset time instant and an estimate of the realization of the abrupt change. These two ML estimates are calculated as in the § 3.2 using Eqs. (3.37) and (3.39), respectively. In the event of a mismatch ($\mathcal{E}^0(k) = 1$), there is only one ML estimate, which is the value of the mismatch. There is no estimate of the onset time of the mismatch in this case because the onset time instant of the realization $a^{\mathscr{H}_0}$ is already known. The ML estimate, $\hat{a}^{\mathscr{H}_0}$, of the reference realization is given by

$$\hat{a}^{\mathscr{H}_0}(l) = a^{\mathscr{H}_0}(l) + \hat{\nu}(k,\zeta)f_\zeta(l,k_0^\star) \qquad l = k_0^\star, \cdots \tag{3.48}$$

3.3.4 The Adaptation of Hypothesis $\mathscr{H}_0$

An adaptation of hypothesis $\mathscr{H}_0$ is performed whenever an error in the reference realization employed by the hypothesis $\mathscr{H}_0$ is detected, i.e., whenever $\mathcal{E}^0(k) = 1$. Let $a^{\mathscr{H}_0}_{\text{new}}$ denote the reference realization employed by the hypothesis $\mathscr{H}_0$ after adaptation. The adaptation is

$$a^{\mathscr{H}_0}_{\text{new}} = \hat{a}^{\mathscr{H}_0}, \qquad \text{whenever } \mathcal{E}^0(k) = 1 \tag{3.49}$$

For consistency with the newly adapted reference realization, the reference Kalman filter and the likelihood ratios, which were calculated with respect to the erroneous reference realization, are corrected by employing Prop. 3.3.1.

Proposition 3.3.1 *Let the $\mathscr{H}_0$ hypothesis be adapted on-line and let $(\mathscr{H}_0)_{\text{old}}$ and $(\mathscr{H}_0)_{\text{new}}$ denote the hypotheses before and after adaptation, respectively. The outputs of the Kalman filter matched to the $(\mathscr{H}_0)_{\text{new}}$ hypothesis can be calculated in terms of the outputs of a Kalman filter matched to the $(\mathscr{H}_0)_{\text{old}}$ hypothesis as follows*

$$\hat{x}(k|k)^{\mathscr{H}_0}_{\text{new}} = \hat{x}(k|k)^{\mathscr{H}_0}_{\text{old}} + \hat{\nu}(k,\zeta)\Upsilon(k,\zeta) \tag{3.50a}$$

$$\mathbf{P}(k|k)^{\mathscr{H}_0}_{\text{new}} = \mathbf{P}(k|k)^{\mathscr{H}_0}_{\text{old}} + \Upsilon(k,\zeta)J^{-1}(k,\zeta)\Upsilon^T(k,\zeta) \tag{3.50b}$$

where the subscripts $(\cdot)_{old}$ and $(\cdot)_{new}$ denote variables before and after adaptation. Similarly, the likelihood ratios calculated with a reference Kalman filter matched to *the* $(\mathscr{H}_0)_{\text{new}}$ *hypothesis can be calculated in terms of the likelihood ratios calculated with a reference Kalman filter matched to the* $(\mathscr{H}_0)_{\text{old}}$ *hypothesis by correcting the signature correlations, d, as follows*

$$d(k,i)_{\text{new}} = d(k,i)_{\text{old}} - \hat{\nu}(k,\zeta)\delta_d(k,i) \qquad i \in \{\zeta, 1, \cdots, w\} \tag{3.51}$$

where $\delta_d(k,i)$ *is obtained from the recursion*

$$\delta_d(l,i) = \delta_d(l-1,i) + \rho^T(l,i)\mathbf{V}^{-1}(l)\rho(l,\zeta) \qquad l \in \{k_i^\star + 1, \cdots, k\} \tag{3.52a}$$

$$\delta_d(k_i^\star, i) = 0 \tag{3.52b}$$

Proof: Equation (3.49) corrects the realization $a^{\mathscr{H}_0}$, employed by the reference Kalman filter, by adopting the ML estimate of the realization of the process z. This modification of $a^{\mathscr{H}_0}$ requires a corresponding correction of the state estimate and the associated estimation error covariance (previously calculated by the reference Kalman filter). These corrections are provided by Eqs. (3.50a) and (3.50b), respectively, see Ref. [16]. The adaptation of the $a^{\mathscr{H}_0}$ realization does not require the correction of the normalized signatures and the Kullback-Leibler divergences because they are not functions of $a^{\mathscr{H}_0}$. However, the signature correlations are functions of $a^{\mathscr{H}_0}$, so they need to be corrected. The signature correlation correction, stated in Eq. (3.51), is proven next.

Let $a^{\mathscr{H}_0}_{\text{new}}$ be the reference realization, adapted using hypothesis $\mathscr{H}_\zeta$, and let $a^{\mathscr{H}_0}_{\text{old}}$ be the reference realization before the adaptation. Let $d(k,i)_{\text{old}}$ be the signature correlation calculated using $a^{\mathscr{H}_0}_{\text{old}}$ and let $d(k,i)_{\text{new}}$ be the signature correlation calculated using $a^{\mathscr{H}_0}_{\text{new}}$. These signature correlations are, according to Eq. (3.29a)

$$d(k,i)_{\text{new}} = d(k-1,i)_{\text{new}} + \rho^T(k,i)\mathbf{V}^{-1}(k)\gamma_{\text{new}}(k) \tag{3.53}$$

$$d(k,i)_{\text{old}} = d(k-1,i)_{\text{old}} + \rho^T(k,i)\mathbf{V}^{-1}(k)\gamma_{\text{old}}(k) \tag{3.54}$$

where γ_{new} and γ_{old} are the residuals of reference Kalman filters employing $a^{\mathscr{H}_0}_{\text{new}}$ or

$a_{\text{old}}^{\mathscr{H}_0}$, respectively. The distributions of the residuals γ_{new} and γ_{old} are

$$\gamma(k)_{\text{new}} \sim \mathcal{N}\big(b(k), \mathbf{V}(k)\big) \tag{3.55}$$

$$\gamma(k)_{\text{old}} \sim \mathcal{N}\big(b(k) + \hat{\nu}(k,\zeta)_{\text{old}}\rho(k,\zeta), \mathbf{V}(k)\big) \tag{3.56}$$

where b is some bias, $\rho(k,\zeta)$ is the normalized signature of hypothesis $\mathscr{H}_\zeta$, see Eq. (3.25), and $\hat{\nu}(k,\zeta)_{\text{old}}$ is the scaling factor associated with $\mathscr{H}_\zeta$ when $a_{\text{old}}^{\mathscr{H}_0}$ is employed, see Eq. (3.36). Whenever the realization $a_{\text{new}}^{\mathscr{H}_0}$ matches the true realization of the process z, the bias b is identically zero, see Ref. [10], p. 240. Whenever the realization $a_{\text{new}}^{\mathscr{H}_0}$ does not match the true realization of the process z, the bias b is non-zero and, by virtue of linearity, it is the same in both Eqs. (3.55) and (3.56). Hence, using Eqs. (3.55) and (3.56) in Eqs. (3.53) and (3.54), the following key relation is obtained

$$d(k,i)_{\text{new}} - d(k,i)_{\text{old}} = d(k-1,i)_{\text{new}} - d(k-1,i)_{\text{old}} - \hat{\nu}(k,\zeta)_{\text{old}}\left(\rho^T(k,i)\mathbf{V}^{-1}(k)\rho(k,\zeta)\right) \tag{3.57}$$

From the above relation and by observing that $d(k_i^\star,i)_{\text{new}} = d(k_i^\star,i)_{\text{old}} = 0$, it follows that the relation between the signature correlations can be rewritten as

$$d(k,i)_{\text{new}} = d(k,i)_{\text{old}} - \hat{\nu}(k,\zeta)_{\text{old}}\delta_d(k,i) \tag{3.58a}$$

where

$$\delta_d(k,i) \triangleq \sum_{j=k_i^\star}^{k} \rho^T(j,i)\mathbf{V}^{-1}(j)\rho(j,\zeta) \tag{3.58b}$$

The normalized correction term, $\delta_d(k,i)$, can be interpreted as a correlation between the normalized signatures of the hypotheses $\mathscr{H}_i^k$ and $\mathscr{H}_\zeta$. Rewriting Eq. (3.58b) in a recursive form finally yields Eqs. (3.52). ∎

Finally, the re-initialization procedure is carried out similarly to the re-initialization in § 3.2, with the addition that the $\mathscr{H}_0$ adaptation module must also be re-initialized, whenever $\mathcal{E}^R(k) = 1$, by setting

$$\delta_d(k,i) = 0 \qquad i \in \{\zeta, 1, \ldots, w\} \tag{3.59}$$

However, this realization is here necessary only if more than one abrupt change has to be diagnozed.

Chapter 4

Two Novel State Estimators for Maneuvering Targets

CONTINUOUS-time dynamical systems subject to structural changes occurring at discrete points in time are conveniently represented as hybrid systems which are combinations of continuous-time systems and discrete-event systems. The major challenge in state estimation for such systems arises from the presence of two types of uncertainties: the measurement uncertainty and the uncertainty about the current structure of the system. The last type of uncertainty arises when a continuous-time system is subject to an abrupt structural change with only partially known characteristics. Optimal state estimation in stochastic linear hybrid systems, i.e. hybrid systems subject to *random* discrete events is, in general, computationally intractable as it often fails to translate into a finite recursive state estimation scheme, cf. [47].

The jump-Markov linear system (2.1) is a stochastic hybrid system. The optimal Gaussian sum estimator for jump-Markov system is a NP-complete problem involving an exponentially growing tree of models; it cannot be implemented in real time, cf. [52]. Hence, practical, suboptimal, Gaussian sum estimators have to rely on certain model management techniques to keep the number of models limited, thus allowing the computational scheme to remain finite. Among these estimators, the most notable is the IMM estimator which employs a limited bank of models together with a technique of merging models to account for transitions between the models, cf. [13, 14]. The IMM estimator employs a bank of fixed and a priori selected models. With reference to estimation in stochastic hybrid systems, it was suggested that the introduction of a variable bank of models into a multiple model scheme could offer improvements over the IMM, cf. [52]. Until now, few attempts in this direction were made, cf. [45, 53, 54].

This chapter presents two novel multiple model estimators which employ an adaptive and variable bank of models. Both estimators generate a finite bank of models by pruning on-line a full tree of models. The pruning removes the unlikely models and yields a computationally finite estimation scheme. The pruning of the models is carried out in two steps. First, parametric families of models describing the unknown input are selected from a-priori information. Next, the bank of models is constructed by selecting on-line the most likely models from within the parametric families. The selection of the most likely models, along with their a posteriori probabilities and model-matched estimates, is achieved by employing a GLR algorithm. The state estimate is then calculated as a probabilistic mixture of the model-matched estimates. Both estimators are recursive and their computational requirements increase linearly with the number of models.

The first novel multiple model estimator is referred to as the multiple reference GLR (MR-GLR) estimator. The MR-GLR estimator employs two banks of models. The first bank describes the realization of the unknown input before an abrupt change (the "reference" realizations). This first bank is fixed and is neither variable nor adaptive. The second bank describes the realization of the unknown input after an abrupt change. The models in the second bank are variable and adaptive. The other ingredients are a cumulative sum (CUSUM) algorithm (cf. [10]), a GLR algorithm (see § 3), and a novel mapping scheme whose task is to calculate the likelihood ratios conditioned on different reference realizations. The CUSUM algorithm calculates the likelihood ratios between models, like the GLR algorithm does, however the CUSUM algorithm requires a bank of fixed (non-adaptive) models. Hence, the CUSUM algorithm is employed only with the fixed models contained in the first bank. For the adaptive models in the second bank, the calculation of the likelihood ratios is more complicated as the likelihood ratios of the models after the abrupt change (the second bank) are inherently conditioned on the models before the change (the first bank). These likelihood ratios are calculated as follows. First, the likelihood ratios conditioned on one of the reference realizations are calculated using the GLR algorithm. The GLR algorithm yields the likelihood ratios for the models in the second bank *but conditioned only on a single model in the first bank.* Next, the likelihood ratios conditioned on the remaining reference realizations are calculated by employing the novel mapping scheme which relates the first likelihood ratios with the remaining ones.

The second multiple model estimator is referred to as the adaptive multiple reference GLR (AMR-GLR) estimator. The AMR-GLR estimator is also provided with two banks of models. However, the first bank, containing models of the unknown input before the abrupt change, is now made adaptive. A GLR algorithm calculates the likelihood ratios in the first bank. The AMR-GLR estimator employs ideas from the adaptive-$\mathscr{H}_0$ GLR algorithm, presented in § 3, to calculate the likelihood ratios between the models in the second bank. However, these likelihood ratios are conditioned on only one of the reference models in the first bank. Whenever there is more than one model in the first bank, a mapping scheme is employed to yield the likelihood ratios of the remaining reference models from the one calculated by the adaptive-$\mathscr{H}_0$ GLR algorithm. As compared to the MR-GLR estimator, the AMR-GLR estimator requires less a-priori information and/or a smaller number of models in the first bank.

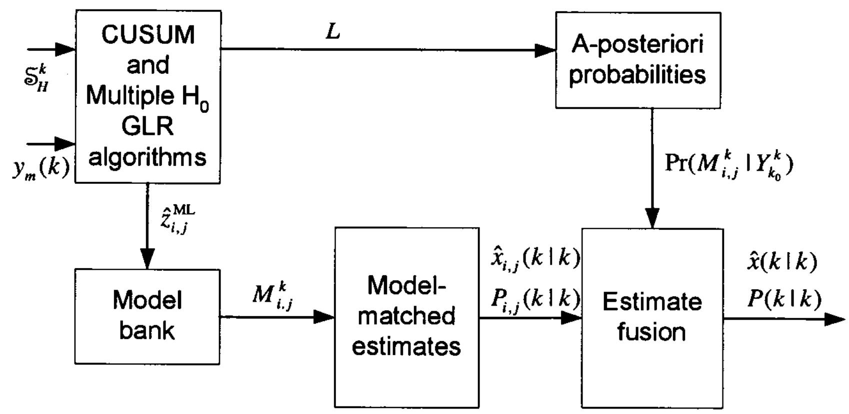

Figure 4.1: MR-GLR estimator.

4.1 The MR-GLR Estimator

The flowchart of the MR-GLR estimator is shown in Figure 4.1 and can be summarized in six steps performed repeatedly: (1) formation of a generalized set of hypotheses, (2) CUSUM and multiple reference GLR computations, (3) formation of the model banks, (4) model-matched state estimation, (5) calculation of the a posteriori probabilities of the models, and (6) estimate fusion. In the model banks, the first bank, which describes z before an abrupt change, contains q models and the second bank contains w models.

4.1.1 A Generalized Set of Hypotheses

The generalized set of hypotheses, $\mathfrak{S}_H^k$, contains hypotheses describing the history of the unknown input z over the time interval $[k_0, k]$, where k_0 denotes the time instant of initialization of the algorithm. The generalized set $\mathfrak{S}_H^k$ is partitioned into subsets of hypotheses, i.e., $\mathfrak{S}_j^k = \{S_1^k, \cdots, S_q^k\}$ which are given by $S_j^k = \{\mathscr{H}_{0,j}, \mathscr{H}_1^k, \cdots, \mathscr{H}_w^k\}$, $j \in \{1, \cdots, q\}$. Each subset of hypotheses contains a single reference hypothesis $\mathscr{H}_{0,j}$ which assumes a specific realization, $\bar{z}_j$, for the process z. The remaining w hypotheses in the subset S_j^k are parametric families of realizations describing an additive abrupt change in the process z. The abrupt change hypotheses $\mathscr{H}_i^k$ are characterized by a time instant $k_i^\star$ for an abrupt change in z and by a dynamic profile of the abrupt change. These dynamic profiles are additive with respect to the realization assumed by $\mathscr{H}_{0,j}$. The subsets S_j^k differ only by the reference realization assumed by $\mathscr{H}_{0,j}$; i.e., for all the subsets, the additive dynamic profiles employed by the abrupt change hypotheses $\mathscr{H}_i^k$, $i \in \{1, \cdots, w\}$, are the same.

4.1.2 The CUSUM Algorithm

A standard CUSUM algorithm calculates recursively the likelihood ratios, $L(\mathscr{H}_{0,j})$, between the reference hypotheses in $\mathfrak{S}_H^k$

$$L(\mathscr{H}_{0,j}) \triangleq \frac{\mathrm{p}\left(\mathcal{Y}_{k_0}^k \middle| \mathscr{H}_{0,j}\right)}{\mathrm{p}\left(\mathcal{Y}_{k_0}^k \middle| \mathscr{H}_{0,1}\right)} \qquad j \in \{2, \cdots, q\} \tag{4.1}$$

See Ref. [10] for details on the CUSUM algorithm.

4.1.3 The Multiple Reference GLR Algorithm

The multiple reference GLR algorithm employs the GLR algorithm with the addition of a mapping scheme for the likelihood ratios. The mapping scheme employs the likelihood ratios calculated by the GLR algorithm (which are obtained with respect to only one reference realization) and maps them to likelihood ratios for other reference realizations. The algorithm functions in two steps. First, the GLR algorithm is implemented by employing the hypotheses contained in the subset S_1^k and, thus, it employs the reference $\mathscr{H}_{0,1}$. For each of the abrupt change hypotheses $\mathscr{H}_i^k$ in S_1^k, the GLR algorithm yields the maximum likelihood estimate of z after the change, $\hat{z}_{i,1}^{\mathrm{ML}}$, and the generalized likelihood ratio of each hypotheses, denoted by $L(\mathscr{H}_i^k, \hat{z}_{i,1}^{\mathrm{ML}})$

$$\hat{z}_{i,1}^{\mathrm{ML}} \triangleq \bar{z}_1 + \arg\max_{\tilde{z}} \mathrm{p}\left(\mathcal{Y}_{k_0}^k \middle| \mathscr{H}_i^k, \tilde{z}, \bar{z}_1\right) \qquad i \in \{1, \cdots, w\} \tag{4.2}$$

$$L(\mathscr{H}_i^k, \hat{z}_{i,1}^{\mathrm{ML}}) \triangleq \frac{\mathrm{p}\left(\mathcal{Y}_{k_0}^k \middle| \mathscr{H}_i^k, \hat{z}_{i,1}^{\mathrm{ML}}, \bar{z}_1\right)}{\mathrm{p}\left(\mathcal{Y}_{k_0}^k \middle| \mathscr{H}_{0,1}, \bar{z}_1\right)} \tag{4.3}$$

In the above, the sum $\bar{z}_1 + \tilde{z}$ is a realization of the process z after an abrupt change. The calculation of Eqs (4.2) and (4.3) is described in § 3, it involves the use of hypotheses-matched signatures, signature correlations, Kullback-Leibler divergences, scaling factors, and state estimate differences.

Next, the values of $\hat{z}_{i,j}^{\mathrm{ML}}$ and $L(\mathscr{H}_i^k, \hat{z}_{i,j}^{\mathrm{ML}})$ are calculated with respect to the other subsets S_j^k, $j \in \{2, \cdots, q\}$, by mapping $\hat{z}_{i,1}^{\mathrm{ML}}$ and $L(\mathscr{H}_i^k, \hat{z}_{i,1}^{\mathrm{ML}})$ into S_j^k. To carry out the mapping, it must be noted that, in the GLR calculations, only the signature correlations and the scaling factors are modified by the mapping $S_1^k \Longrightarrow S_j^k$, $j \in \{2, \cdots, q\}$. Moreover, the scaling factors depend on S_j^k only because they are functions of the signature correlations. Hence, to perform the mapping $S_1^k \Longrightarrow S_j^k$ on Eqs. (4.2) and (4.3), the only requirement is the existence of an mapping between the signature correlations.

Proposition 4.1.1 *Consider the bank of reference realizations, $\{\mathscr{H}_{0,1}, \cdots, \mathscr{H}_{0,q}\}$. Each hypothesis $\mathscr{H}_{0,j}$ assumes a different reference realization $\bar{z}_j$. Let the relative realizations $\bar{z}_j^{\mathrm{rel}}$ be given by $\bar{z}_j^{\mathrm{rel}} \triangleq \bar{z}_j - \bar{z}_1$, $j \in \{2, \cdots, q\}$. Let $\bar{\rho}_j^k$ be the signature of the relative realization $\bar{z}_j^{\mathrm{rel}}$. Let $d_{i,j}^k$ denote the signature correlation of hypothesis $\mathscr{H}_i^k \in S_j^k$. Then, the mapping $d_{i,1}^k \Longrightarrow d_{i,j}^k$ is carried out as follows*

$$d_{i,j}^k = d_{i,1}^k - \delta_{i,j}^k \qquad i \in \{1, \cdots, w\},\ j \in \{2, \cdots, q\} \tag{4.4}$$

where the correction $\delta_{i,j}^k$ is recursively calculated using

$$\delta_{i,j}^k = \delta_{i,j}^{k-1} + \rho_i^{k^T} \mathbf{V}^{-1}(k) \bar{\rho}_j^k \tag{4.5}$$

In the above, $\mathbf{V}$ is the covariance of the residuals generated by the reference Kalman filter (matched to $\mathscr{H}_{0,1}$) as employed by the GLR algorithm.

Proof: The proof of Eqs (4.4) and (4.5) is the same as the proof concerning the adaptation of hypothesis $\mathscr{H}_0$ presented in § 3. ∎

Remark. The Proposition 4.1.1 allows a single GLR procedure to be used with several reference hypotheses. Alternatively, but such an approach would be numerically less efficient, several GLR algorithms can be implemented in parallel, one for each subset S_H^k.

4.1.4 The Banks of Models

The banks of models describe several possible realizations of z over the time interval $[k_0, k]$. At each time instant k, a model, $M_{i,j}^k$, is associated with the reference hypothesis $\mathscr{H}_{0,j}$ and with an abrupt change hypothesis $\mathscr{H}_i^k \in S_j^k$ as follows

$$M_{0,j}^k : \bar{z}_j(l) \tag{4.6a}$$

$$M_{i,j}^k : \bar{z}_j(l)\left[\mathbf{1}(k_0) - \mathbf{1}(k_i^\star)\right] + \hat{z}_{i,j}^{\mathrm{ML}}(l)\mathbf{1}(k_i^\star) \tag{4.6b}$$

where $i \in \{1, \cdots, w\}$, $j \in \{1, \cdots, q\}$, and $l \in \{k_0, \cdots, k\}$. The symbol $\mathbf{1}(s)$ denotes the unit step function at time instant s and $k_i^\star$ is the time instant of the abrupt change assumed by $\mathscr{H}_i^k$. The adaptation of the models through the parameters $\hat{z}_{i,j}^{\mathrm{ML}}$ is very important as it effectively allows to restrict the number of models used in the sense that for each parametric family of models considered, i.e., for each hypotheses in each subset S_j^k, a single model is incorporated into the model bank.

4.1.5 The Model-Matched Estimates

The model-matched state estimate, $\hat{x}_{i,j}(k|k)$, is obtained by assuming that the model $M_{i,j}^k$ is true

$$\hat{x}_{i,j}(k|k) \triangleq E\left(x \,\middle|\, M_{i,j}^k, \mathcal{Y}_{k_0}^k\right) \tag{4.7}$$

The model-matched estimate $\hat{x}_{0,1}(k|k)$ and its covariance $\mathbf{P}_{0,1}(k|k)$ are calculated by the reference Kalman filter of the GLR algorithm. The remaining $\hat{x}_{i,j}(k|k)$ and $\mathbf{P}_{i,j}(k|k)$ are calculated using outputs of the GLR algorithm

$$\hat{x}_{0,j}(k|k) = \hat{x}_{0,1}(k|k) + \bar{\Upsilon}_j^k \qquad i \in \{2, \cdots, q\} \tag{4.8a}$$

$$\hat{x}_{i,j}(k|k) = \hat{x}_{0,j}(k|k) + \hat{\nu}_{i,j}^k \Upsilon_i^k \qquad i \in \{1, \cdots, w\} \tag{4.8b}$$

$$\mathbf{P}_{i,j}(k|k) = \mathbf{P}_{0,1}(k|k) + \Upsilon_i^k {J_i^k}^{-1} {\Upsilon_i^k}^T \tag{4.8c}$$

where $\hat{\nu}_{i,j}^k$ is the scaling factor associated with hypothesis $\mathscr{H}_i^k \in S_j^k$ and $\bar{\Upsilon}_j^k$ is the state estimate difference between $\mathscr{H}_{0,1}$ and $\mathscr{H}_{0,j}$ as calculated by the CUSUM algorithm.

4.1.6 The A Posteriori Probabilities of the Models

The a posteriori probability of each model, $\Pr\left(M_{i,j}^k \,|\mathcal{Y}_{k_0}^k\right)$, is calculated from the likelihood ratios of the models.

Proposition 4.1.2 *Let* $\Pr\left(M_{i,j}^k\right)$ *be the unconditional probability of model* $M_{i,j}^k$. *Define the likelihood ratio* $L\left(M_{i,j}^k\right)$ *as:* $L\left(M_{i,j}^k\right) \triangleq \frac{\mathrm{p}(\mathcal{Y}_{k_0}^k|M_{i,j}^k)}{\mathrm{p}(\mathcal{Y}_{k_0}^k|M_{0,1}^k)}$. *Then, the a posteriori probability of each model is*

$$\Pr\left(M_{i,j}^k \,|\mathcal{Y}_{k_0}^k\right) = \frac{L\left(M_{i,j}^k\right)\Pr\left(M_{i,j}^k\right)}{\sum\limits_{v=0}^{w}\sum\limits_{s=1}^{q} L\left(M_{v,s}^k\right)\Pr\left(M_{v,s}^k\right)} \tag{4.9}$$

where

$$L(M_{0,1}^k) = 1 \tag{4.10a}$$

$$L(M_{0,j}^k) = L\left(\mathscr{H}_{0,j}\right) \qquad j \in \{2, \cdots, q\} \tag{4.10b}$$

$$L(M_{i,j}^k) = L\left(\mathscr{H}_i^k, \hat{z}_{i,j}^{\mathrm{ML}}\right) L\left(M_{0,j}^k\right) \qquad i \in \{1, \cdots, w\},\ j \in \{1, \cdots, q\} \tag{4.10c}$$

Proof: The conditional a posteriori probability of model M_i^k is, according to the

Bayes' rule

$$\Pr(M_{i,j}^k|\mathcal{Y}_{k0}^k) = \frac{\mathrm{p}(\mathcal{Y}_{k0}^k|M_{i,j}^k)\Pr(M_{i,j}^k)}{\sum_{v=0}^{w}\sum_{s=1}^{q}\mathrm{p}(\mathcal{Y}_{k0}^k|M_{v,s}^k)\Pr(M_{v,s}^k)} = \frac{L\left(M_{i,j}^k\right)\Pr\left(M_{i,j}^k\right)}{\sum_{v=0}^{w}\sum_{s=1}^{q}L\left(M_{v,s}^k\right)\Pr\left(M_{v,s}^k\right)} \tag{4.11}$$

The validity of Eqs (4.10) requires that the models employ the same assumptions as the hypotheses and their associated maximum likelihood estimates, as stated in Eq. (4.6b). From this one-to-one association between the model $M_{i,j}^k$ and the hypothesis $\mathscr{H}_{i,j}^k$, the CUSUM algorithm provides the likelihood ratios needed in (4.10b) and the multiple reference GLR algorithm provides the likelihood ratios required to solve Eq. (4.10c). ∎

4.1.7 The Estimate Fusion

The minimum mean square state estimate, $\hat{x}(k|k)$, and its covariance matrix, $\mathbf{P}(k|k)$, is expressed as a probabilistic mixture using the law of total probability

$$\hat{x}(k|k) \triangleq E\left(x\left|\mathcal{Y}_{k0}^k\right.\right) = \sum_{i=0}^{w}\sum_{j=1}^{q}\hat{x}_{i,j}(k|k)\Pr\left(M_{i,j}^k\left|\mathcal{Y}_{k0}^k\right.\right) \tag{4.12a}$$

$$\mathbf{P}(k|k) = \sum_{i=0}^{w}\sum_{j=1}^{q}\Pr\left(M_{i,j}^k\left|\mathcal{Y}_{k0}^k\right.\right) \times \Big\{\mathbf{P}_{i,j}(k|k) + \left[\hat{x}_{i,j}(k|k) - \hat{x}(k|k)\right]\left[\hat{x}_{i,j}(k|k) - \hat{x}(k|k)\right]^T\Big\} \tag{4.12b}$$

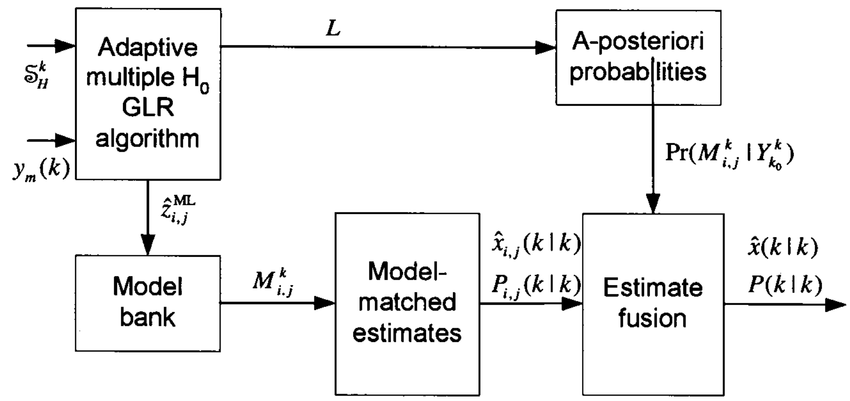

Figure 4.2: AMR-GLR estimator.

4.2 The AMR-GLR Estimator

The flowchart for the AMR-GLR estimator is shown in Figure 4.2 and it can be summarized in six repetitive steps: (1) formation of a generalized set of hypotheses, (2) adaptive multiple reference GLR computations, (3) formation of the model bank, (4) model-matched state estimation, (5) calculation of the a posteriori probabilities of the models, and (6) estimate fusion. As compared with the MR-GLR estimator, the AMR-GLR estimator differs in terms of the generalized set of hypotheses, the GLR algorithm, the bank of models, and the a posteriori probability computations. Also, the AMR-GLR does not employ a CUSUM algorithm.

4.2.1 A Generalized Set of Hypotheses

The generalized set of hypotheses, $\mathfrak{S}_H^k$, is defined similarly to § 4.1.1. The reference hypotheses $\mathscr{H}_{0,j}$ now assume a parametric family of reference realizations, characterized by a dynamic profile f_j, instead of a fixed realization $\bar{z}_j$. The generalized set of hypotheses also contains an additional subset of hypotheses, S_0^k, given by $S_0^k = \{\mathscr{H}_{0,0}, \mathscr{H}_{0,1}, \cdots, \mathscr{H}_{0,q}, \mathscr{H}_1^k, \cdots, \mathscr{H}_w^k\}$, where $\mathscr{H}_{0,0}$ is a non-adaptive reference hypothesis with the following realization for the process z: $z(l) = 0$, $l \in \{k_0, \cdots, k\}$.

At time instant k, each reference hypothesis $\mathscr{H}_{0,j}$, $j \in \{1, \cdots, w\}$, is equipped with an adaptive reference realization, $\hat{z}_{0,j}^{k-1}$, which is a member of the parametric family defined by the profile f_j. The prior reference realization $\hat{z}_{0,j}^{k-1}$ will be possibly adapted at time instant k by the action of the procedure in the following section § 4.2.2.

4.2.2 The Adaptive Multiple Reference GLR Algorithm

The adaptive multiple reference GLR algorithm employs ideas from the adaptive-$\mathscr{H}_0$ GLR algorithm with the addition of a mapping scheme to calculate the likelihood ratios of the hypotheses for several references. As opposed to the multiple reference GLR algorithm in § 4.1.3, the novelty and computational advantage of the adaptive multiple reference GLR algorithm resides in the estimation of realizations for the process z both *before and after* the abrupt change on-line. The estimated realizations lie in parametric families of realizations; each parametric family describing the process z either before or after the abrupt change. The calculations of the adaptive multiple reference GLR algorithm are carried out in four steps described below.

Step 1. The Likelihood Ratios in Set S_0^k

The calculation of the generalized likelihood ratios by a GLR algorithm involve the computation of signature correlations as an intermediate step, see § 3.2.4. Consider the following generalized likelihood ratios between the hypotheses in S_0^k and the non-adaptive reference hypothesis $\mathscr{H}_{0,0}$ calculated using the GLR algorithm of § 3.2.

$$L(\mathscr{H}_i^k, \hat{z}_{i,0}^{\mathrm{ML}}, \mathscr{H}_{0,0}) \triangleq \frac{\mathrm{p}\left(\mathcal{Y}_{k_0}^k \middle| \mathscr{H}_i^k, \hat{z}_{i,0}^{\mathrm{ML}}\right)}{\mathrm{p}\left(\mathcal{Y}_{k_0}^k \middle| \mathscr{H}_{0,0}\right)} \tag{4.13a}$$

$$L(\mathscr{H}_{0,j}, \hat{z}_{0,j}^{\mathrm{ML}}, \mathscr{H}_{0,0}) \triangleq \frac{\mathrm{p}\left(\mathcal{Y}_{k_0}^k \middle| \mathscr{H}_{0,j}, \hat{z}_{0,j}^{\mathrm{ML}}\right)}{\mathrm{p}\left(\mathcal{Y}_{k_0}^k \middle| \mathscr{H}_{0,0}\right)} \tag{4.13b}$$

For use in the following steps, let $d^k_{i,0}$, $i \in \{1, \cdots, w\}$, denote the signature correlations involved in the calculation of Eq. (4.13a). The calculation of the maximum likelihood estimates $\hat{z}^{\mathrm{ML}}_{i,0}$ and $\hat{z}^{\mathrm{ML}}_{0,j}$ from the signature correlations is described in § 3. The generalized likelihood ratios in Eq. (4.13b) are employed later in the section § 4.2.5 to calculate the a posteriori probabilities of the models.

Step 2. The Likelihood Ratios in Set S^k_j with the Prior Reference

The following generalized likelihood ratios of the abrupt change hypotheses in each set S^k_j, $j \in \{1, \cdots, q\}$, are calculated

$$L(\mathscr{H}^k_i, \hat{z}^{\mathrm{ML}}_{i,j}, \hat{z}^{k-1}_{0,j}) \triangleq \frac{\mathrm{p}\left(\mathcal{Y}^k_{k_0} \middle| \mathscr{H}^k_i, \hat{z}^{\mathrm{ML}}_{i,j}\right)}{\mathrm{p}\left(\mathcal{Y}^k_{k_0} \middle| \mathscr{H}_{0,j}, \hat{z}^{k-1}_{0,j}\right)} \tag{4.14}$$

where $\mathscr{H}_{0,j}$ is the reference hypothesis in S^k_j and $\hat{z}^{k-1}_{0,j}$ is the prior reference realization adapted at time instant $k-1$. The calculation of the generalized likelihood ratios in Eq. (4.14) is carried out by mean of the signature correlations, see § 3.2.4. The signature correlations associated with the likelihood ratios in Eq. (4.14), and denoted $d^k_{i,j}$, $i \in \{1, \cdots, w\}$, are calculated by a suitable mapping of the signature correlations $d^k_{i,0}$ associated with the likelihood ratios in Eq. (4.13a). The likelihood ratios in Eqs. (4.13a) and (4.14) do not employ the same reference realization. The mapping of the signature correlations to a different reference realization is obtained by employing Prop. 4.1.1 as follows

$$d^k_{i,j} = d^k_{i,0} - \nu^{k-1}_{0,j}\delta^k_{i,j} \tag{4.15}$$

where the scaling factor $\nu^{k-1}_{0,j}$ is the parameter relating the adapted reference realization $\hat{z}^{k-1}_{0,j}$ to the dynamic profile $f_j \in \mathscr{H}_{0,j}$, i.e., the value of the scaling factor is such that $\hat{z}^{k-1}_{0,j} = \nu^{k-1}_{0,j} f_j$, and the correction $\delta^k_{i,j}$ is calculated recursively using

$$\delta^k_{i,j} = \delta^{k-1}_{i,j} + {\rho^k_i}^T \mathbf{V}^{-1}(k) \rho^k_{0,j} \tag{4.16}$$

where $\rho_{0,j}^k$ is the innovation signature of the dynamic profile $f_j \in \mathscr{H}_{0,j}$, see § 3.2.3, and $\mathbf{V}$ is the residual covariance of the Kalman filter employed by the GLR algorithm, see § 3.2.2.

Step 3. The Adaptation of the Reference Hypotheses

The current estimate of the reference realization, $\hat{z}_{0,j}^k$, associated with the reference hypothesis $\mathscr{H}_{0,j}$ is calculated by applying the adaptation procedure of the adaptive-$\mathscr{H}_0$ algorithm, see § 3.3.4, to each subset S_j^k. The adaptation procedure applies a modified GLR test, see § 3.3.2, to each subset S_j^k. and employs the generalized likelihood ratios calculated in Eq. (4.14). The modified GLR test sets the value of the binary indicator $\mathcal{E}^0$ where the value $\mathcal{E}^0(k) = 1$ indicates a mismatch. Whenever the modified GLR test indicates a mismatch in the reference realization $\hat{z}_{0,j}^{k-1}$ of subset S_j^k, the reference is adapted as follows

$$\hat{z}_{0,j}^k = \begin{cases} \hat{z}_{0,j}^{\mathrm{ML}} & \text{when } \mathcal{E}^0(k) = 1 \\ \hat{z}_{0,j}^{k-1} & \text{otherwise} \end{cases} \tag{4.17}$$

Step 4. The Likelihood Ratios in Set S_j^k with the Adapted Reference

Finally, the generalized likelihood ratios matched to the current adapted references $\hat{z}_{0,j}^k$, $j \in \{0, \cdots, j\}$, are calculated for each subset S_j^k

$$L(\mathscr{H}_i^k, \hat{z}_{i,j}^{\mathrm{ML}}, \hat{z}_{0,j}^k) \triangleq \frac{\mathrm{p}\left(\mathcal{Y}_{k_0}^k \,\middle|\, \mathscr{H}_i^k, \hat{z}_{i,j}^{\mathrm{ML}}\right)}{\mathrm{p}\left(\mathcal{Y}_{k_0}^k \,\middle|\, \mathscr{H}_{0,j}, \hat{z}_{0,j}^k\right)} \tag{4.18}$$

These generalized likelihood ratios are calculated as in step 2 except that the current adapted references are used instead of the prior ones.

4.2.3 The Bank of Models

The bank of models describes several possible realizations of z over the time interval $[k_0, k]$. The bank of models of the AMR-GLR estimator is similar to the bank of models of MR-GLR estimator in § 4.1.4 except that in the AMR-GLR estimator the reference realizations are estimated on-line. At each time instant k, a model, $M^k_{i,j}$, is associated with the hypothesis $\mathscr{H}_{0,j}$ and with $\mathscr{H}^k_i \in S^k_j$ as follows

$$M^k_{0,j} : \hat{z}^k_{0,j}(l) \tag{4.19a}$$

$$M^k_{i,j} : \hat{z}^k_{0,j}(l)\left[\mathbf{1}(k_0) - \mathbf{1}(k^\star_i)\right] + \hat{z}^{\mathrm{ML}}_{i,j}(l)\mathbf{1}(k^\star_i) \tag{4.19b}$$

where $i \in \{1, \cdots, w\}$, $j \in \{1, \cdots, q\}$, and $l \in \{k_0, \cdots, k\}$.

4.2.4 The Model-Matched Estimates

The model-matched state estimate, $\hat{x}_{i,j}(k|k)$, is calculated under the assumption that the model $M^k_{i,j}$ is true

$$\hat{x}_{i,j}(k|k) \triangleq E\left(x \,\middle|\, M^k_{i,j}, \mathcal{Y}^k_{k_0}\right) \tag{4.20}$$

The reference Kalman filter of the GLR algorithm in § 4.2.2 delivers the model-matched estimate $\hat{x}_{0,0}(k|k)$ and its covariance $\mathbf{P}_{0,0}(k|k)$. The remaining $\hat{x}_{i,j}(k|k)$ and $\mathbf{P}_{i,j}(k|k)$ are calculated using the outputs from the GLR algorithm

$$\hat{x}_{0,j}(k|k) = \hat{x}_{0,0}(k|k) + \hat{\nu}^k_{0,j}\bar{\Upsilon}^k_j, \qquad j \in \{1, \cdots, q\} \tag{4.21a}$$

$$\hat{x}_{i,j}(k|k) = \hat{x}_{0,j}(k|k) + \hat{\nu}^k_{i,j}\Upsilon^k_i, \qquad i \in \{1, \cdots, w\} \tag{4.21b}$$

$$\mathbf{P}_{0,j}(k|k) = \mathbf{P}_{0,0}(k|k) + \bar{\Upsilon}^k_j\, \bar{J}^{k^{-1}}_j\, \bar{\Upsilon}^{k^T}_j \tag{4.21c}$$

$$\mathbf{P}_{i,j}(k|k) = \mathbf{P}_{0,j}(k|k) + \Upsilon^k_i J^{k^{-1}}_i \Upsilon^{k^T}_i \tag{4.21d}$$

where $\bar{J}^k_j$, $\bar{\Upsilon}^k_j$, $\hat{\nu}^k_{0,j}$ are the Kullback-Leibler divergence, the normalized state estimate difference, and the scaling factor, respectively, associated with the reference hypothesis $\mathscr{H}_{0,j}$; see § 3 for details.

4.2.5 The A Posteriori Probabilities of the Models

The a posteriori probabilities are calculated from the likelihoods of the models.

Proposition 4.2.1 *Let $\Lambda(M_{i,j}^k)$ be the likelihood of the model $M_{i,j}^k$, i.e., $\Lambda(M_{i,j}^k) \triangleq \mathrm{p}\left(\mathcal{Y}_{k_0}^k \middle| M_{i,j}^k\right)$. Let γ be the residual of the reference Kalman filter matched to the hypothesis $\mathscr{H}_{0,0}$ and the associated model $M_{0,0}^k$. The a posteriori probability of each model is*

$$\Pr\left(M_{i,j}^k \middle| \mathcal{Y}_{k_0}^k\right) = \frac{\Lambda\left(M_{i,j}^k\right) \Pr\left(M_{i,j}^k\right)}{\sum_{s=1}^{w} \sum_{v=0}^{q} \Lambda\left(M_{s,v}^k\right) \Pr\left(M_{s,v}^k\right)} \tag{4.22}$$

with

$$\Lambda(M_{i,j}^k) = L\left(\mathscr{H}_i^k, \hat{z}_{i,j}^{\mathrm{ML}}, \hat{z}_{0,j}^k\right) \Lambda\left(M_{0,j}^k\right) \tag{4.23a}$$

$$\Lambda(M_{0,j}^k) = \begin{cases} L\left(\mathscr{H}_{0,j}, \hat{z}_{0,j}^{\mathrm{ML}}, \mathscr{H}_{0,0}\right) \Lambda\left(M_{0,0}^k\right) & \text{if } \hat{z}_{0,j}^k = \hat{z}_{0,j}^{\mathrm{ML}} \\ \frac{1}{2\pi} \frac{e^{-\frac{1}{2}\gamma_j^T(k)\mathbf{V}^{-1}(k)\gamma_j(k)}}{\|\mathbf{V}(k)\|^{\frac{1}{2}}} \Lambda(M_{0,j}^{k-1}) & \text{otherwise} \end{cases} \tag{4.23b}$$

$$\Lambda(M_{0,0}^k) = \mathrm{p}\left(y_m(k) \middle| M_{0,0}^k\right) \Lambda(M_{0,0}^{k-1}) \tag{4.23c}$$

where

$$\gamma_j(k) = \gamma(k) - \nu_{0,j}^k \rho_{0,j}^k \tag{4.24a}$$

$$\mathrm{p}\left(y_m(k) \middle| M_{0,0}^k\right) = \frac{1}{2\pi} \frac{e^{-\frac{1}{2}\gamma^T(k)\mathbf{V}^{-1}(k)\gamma(k)}}{\|\mathbf{V}(k)\|^{\frac{1}{2}}} \tag{4.24b}$$

and where γ_j is the residuals of a reference Kalman filter matched to the reference hypothesis $\mathscr{H}_{0,j}$.

Proof: By the definition of the models in § 4.2.3, the likelihood of model $M_{i,j}^k$ is equal to the likelihood of the hypotheses: $\Lambda(M_{i,j}^k) = \mathrm{p}\left(\mathcal{Y}_{k_0}^k | \mathscr{H}_i^k, \hat{z}_{i,j}^{\mathrm{ML}}, \hat{z}_{0,j}^k\right)$ and $\Lambda(M_{0,j}^k) = \mathrm{p}\left(\mathcal{Y}_{k_0}^k | \mathscr{H}_{0,j}, \hat{z}_{0,j}^k\right)$. Hence, Eq. (4.23a) follows from the definition of $L\left(\mathscr{H}_i^k, \hat{z}_{i,j}^{\mathrm{ML}}, \hat{z}_{0,j}^k\right)$, see Eq. 4.18.

In Eq. (4.23b), the expression selected depends on the possible adaptation of the reference hypothesis $\mathscr{H}_{0,j}$. Whenever the reference hypothesis is adapted, i.e., whenever $\hat{z}^k_{0,j} = \hat{z}^{\mathrm{ML}}_{0,j}$, the likelihood of the reference model $M^k_{0,j}$ follows from the definition of $L(\mathscr{H}_{0,j}, \hat{z}^{\mathrm{ML}}_{0,j}, \mathscr{H}_{0,0})$ in Eq. (4.13b). Whenever the reference hypothesis is not adapted, the likelihood is calculated recursively using the total probability theorem. By the independent Gaussian noise assumption in Eq. (2.1), the total probability theorem yields the recursive expression (4.23b) for the likelihood of the model $M^k_{0,j}$.

In Eq. (4.24a), $\nu^k_{0,j}\rho^k_{0,j}$ is the signature of the reference $\mathscr{H}_{0,j}$ in the residuals of the reference Kalman filter matched to $\mathscr{H}_{0,0}$, see § 3. By linearity, it follows that the residuals of a reference Kalman filter matched to $\mathscr{H}_{0,j}$ are given by Eq. (4.24a). The Eq. (4.24b) delivers the marginal likelihood of the model and it follows from the assumption of independent Gaussian noises in Eq. (2.1). The same assumption permits to express the likelihood of the model in the recursive form given by Eq. (4.23c). ∎

4.2.6 The Estimate Fusion

The minimum mean square state estimate, $\hat{x}\,(k|k)$, and its covariance matrix, $\mathbf{P}(k|k)$, are probabilistic mixtures calculated as for the MR-GLR estimator

$$\hat{x}\,(k|k) \triangleq E\left(x \left|\mathcal{Y}^k_{k_0}\right.\right) = \sum_{i=0}^{w}\sum_{j=1}^{q} \hat{x}_{\,i,j}\,(k|k)\,\Pr\left(M^k_{i,j} \left|\mathcal{Y}^k_{k_0}\right.\right) \tag{4.25a}$$

$$\mathbf{P}(k|k) = \sum_{i=0}^{w}\sum_{j=1}^{q} \Pr\left(M^k_{i,j} \left|\mathcal{Y}^k_{k_0}\right.\right) \times \Big\{\mathbf{P}_{i,j}(k|k) + \left[\hat{x}_{\,i,j}(k|k) - \hat{x}\,(k|k)\right]\left[\hat{x}_{\,i,j}(k|k) - \hat{x}\,(k|k)\right]^T\Big\} \tag{4.25b}$$

Chapter 5

Novel Terminal Guidance Schemes

THE pursuit-evasion engagement between two non-cooperative agents (the pursuer and the evader) requires the development of control strategies for both agents. The task of defining and implementing the pursuer's strategy is the duty of the guidance system which usually consist of many components. The seeker and estimator measure the target signal and extract the information required by the guidance law, respectively. The control system (autopilot) then translates the output from the guidance law into control actuator commands which effect a change to the vehicle motion. What is most often termed "guidance" is the combination of the estimator with a guidance policy or guidance law, cf. [77].

The guidance problem can be separated into two phases: the midcourse phase and the terminal phase, cf. [36]. The midcourse phase occurs after the launch phase of the pursuer and before the terminal phase. The terminal phase is initiated once the target is acquired by the sensors carried on-board the pursuer. The pursuer's solution to the terminal guidance problem is the so-called terminal guidance law and this solution is employed during the last time instants of the engagement.

The terminal guidance laws are usually derived using deterministic optimal control techniques, cf. [90], or game theoretic approaches, cf. [65, 67]. In most cases, the resulting terminal guidance law takes the form of a function whose argument is the ballistic miss. The various guidance laws then differ in terms of the type of function involved and in the terms of the formula employed to calculate the ballistic miss. For simplicity, the guidance law derived from these techniques usually neglect the interactions with the estimator. A notable exception is the game theoretic DGL/C law which approximates the interaction with the estimator by assuming a time delay on the available information about the evader's acceleration, cf. [67, 68]. However, the value of the time delay has to be selected a priori and this time delay is only an approximation of the true interaction between the guidance law and the estimator. As a result of this interaction, the optimal controller, is in general, a function of the whole pdf of the filtered state, cf. [86]. Practical optimal solutions to the stochastic control problem are only available for a few special cases, most notably the class of LQG problems. Consequently, sub-optimal strategies are of significant interest. The strategies for stochastic control can be conveniently divided into two broad classes: the conventional feedback control algorithms and the fully dual closed-loop control algorithms, cf. [4].

The conventional feedback control strategies depend on the information that is currently available but ignore the possibility that future measurements will become available. However, information about the future behavior of the system (via the system model and system noise statistics) may be employed. This type of strategy precludes any active probing, i.e., deliberately modifying the trajectory of the pursuer to improve the observability of the system.

The fully dual closed-loop control strategies (dual control) make use of the current information and take at least some account of the fact that future measurements will be available. These type of strategies may employ active probing by the controller to improve observability.

Perfect interception of a maneuvering tactical ballistic missile (BM) is an open problem whose difficulty arises from imperfect information about the evader's acceleration and from the fact that the maneuverability of the pursuer is often only marginally larger than that of the evader, cf. [66]. This chapter introduces two new feedback control techniques capable of exploiting more of the available information than the usual optimal control and game theoretic approaches. Such capability is of paramount importance in the imperfect information environment characterizing the interception problem of a BM. The two new techniques are: a novel formula to predict the ballistic miss, and a novel integrated estimator-guidance scheme. In addition, the chapter presents a novel discretization technique for continuous-time, nonlinear, and unbounded control commands and for bounded bang-bang control commands. The last is of practical interest as continuous-time bang-bang guidance laws are efficient against a highly maneuverable target, but are difficult to implement in discrete-time, as required in a realistic setting.

The new predictor of the ballistic miss (also known as the zero effort miss) employs a bank of adaptive semi-Markov models to represent the *future* evasive maneuvers. The ballistic miss is calculated as a probabilistic mixture of the models. The mixture is a function of both future and past evasive maneuvers. As compared to Markovian predictions, the semi-Markov predictor requires more a-priori information than the usuals Markovian predictors, but provides for a more accurate modeling of the behavioral pattern of an evasive target. This new prediction of the ballistic miss is then employed as the argument of a terminal guidance law.

The new integrated estimator-guidance scheme employs banks of state estimators and guidance laws together with a governor to improve the homing accuracy against a maneuvering evader. Guidance schemes employing a bank of guidance law have been presented before, see Ref. [63]. The novelty here lies in the introduction of a governor that assesses on-line the uncertainty of the state estimate and selects a guidance law from the provided bank according to the specifics of the identified uncertainty. The employed state estimator is suboptimal and the governor also modifies it on-line to further improve the accuracy of the state estimate.

5.1 A Semi-Markov Predictor for the Zero Effort Miss

The zero effort miss (ZEM) at time t is defined as the miss distance if the pursuer applies a zero command policy over the time interval $[t, t_f]$ and the target performs the expected maneuvers. In the context of a pursuit-evasion engagement, the exact value of the ZEM is not available because its calculation requires exact information about both the current state of the target and the target future trajectory. However, a conditional mean estimate of the ZEM can be calculated as an approximation of the ZEM. The calculation of the estimated ZEM requires the current state estimate of the system and the expectation about the target's future acceleration command. The latter is usually assumed or calculated to be zero, i.e.: $E\left(z(l)|\mathcal{Y}_{k_0}^k\right) = 0,\ l > t$, where t denotes the current time.

In applications to target tracking, it has been demonstrated that multiple model approaches are highly efficient techniques for state estimation, cf. [7]. In the same context, it was also suggested that semi-Markov models can more closely match the observed behavioral patterns of a maneuvering target than the commonly used Markovian models, cf. [17] and references therein.

This section presents a new predictor for the zero effort miss which employs a Bayesian multiple model approach (applied to prediction rather than to state estimation) in conjunction with a bank of semi-Markov models to describe the predicted process. The semi-Markov modeling of the motion of the target stems from the assumption that the transition probabilities between the levels of the target acceleration depend on the sojourn time of the maneuver and this implies that in general $E\left(z(l)|\mathcal{Y}_{k_0}^k\right) \neq 0$, a.e. $l > t$. Furthermore, the bank of models is made variable and adaptive by employing a GLR type adaptive algorithm to calculate the maximum likelihood realizations for the future evasive maneuvers and the a-posteriori probability of each model. The adaptive-$\mathscr{H}_0$ GLR algorithm is selected for this task. The GLR algorithm requires making several hypotheses about the onset time of an evasive maneuver and about the type of maneuver expected.

5.1.1 A Bayesian Multiple Model Zero Effort Miss

At any time instant k, the ZEM corresponds to the value $x_1(t_f)$ subject to $u(l) = 0,\ k\Delta \leq l \leq t_f$, and is defined by:

$$\mathrm{ZEM}(k) = \mathbf{D}\left(\mathbf{\Phi}(t_f, k\Delta)x(k) + \int_t^{t_f} \mathbf{\Phi}(t_f, l)\mathbf{B}_2(l)z(l)\,\mathrm{d}l\right) \tag{5.1a}$$

$$\mathbf{D}^T \triangleq \begin{bmatrix} 1 & 0 & \cdots & 0 \end{bmatrix} \tag{5.1b}$$

where $\mathbf{\Phi}$ is the transition matrix, Δ is the sampling time interval of the continuous-time system, and $t = k\Delta$.

The ZEM, as given by Eq. (5.1), cannot be calculated explicitly because the values of x and z are not available. Thus, the ZEM must be estimated. A new formula to calculate the conditional expectation in Eq. (5.1) using a Bayesian multiple model approach is introduced in Proposition 5.1.1.

Proposition 5.1.1 *Let z be a random process with an unknown pdf. Consider a finite set of random processes, z_i, $i \in \{0, \cdots, w\}$, defined in the time interval $[t, t_f]$ whose pdfs are known. Assume that the random process z matches a member of this finite set of random processes (in the sense that it has the same pdf as one of the z_i),* *i.e.,*

$$\mathrm{p}\left(z(l)\right) = \mathrm{p}\left(z_i(l)\right), \qquad l \in [t, t_f] \tag{5.2}$$

for some i, $i \in \{0, \dots, w\}$. Then, the conditional expectation of the ZEM *can be calculated as follows:*

$$E\left(\mathrm{ZEM}(k)|\mathcal{Y}_{k_0}^{k}\right) = \mathbf{D}\boldsymbol{\Phi}(t_f, t)\hat{x}(k) + \hat{\Theta}(k) \tag{5.3a}$$

with

$$\hat{x}(k) \triangleq E\left(x|\mathcal{Y}_{k_0}^{k}\right) \tag{5.3b}$$

$$\hat{\Theta}(k) \triangleq \sum_{i=0}^{w} \mathbf{D}\left(\int_{t}^{t_f} \boldsymbol{\Phi}(t_f, l)\mathbf{B}_2(l)\hat{z}_i(l)\,\mathrm{d}l\right) \mathrm{Pr}\left(\hat{z}_i|z_i, \mathcal{Y}_{k_0}^{k}\right) \tag{5.3c}$$

$$\hat{z}_i(l) \triangleq E\left(z_i(l)|\mathcal{Y}_{k_0}^{k}\right) \tag{5.3d}$$

where $\mathrm{Pr}\left(\hat{z}_i|z_i, \mathcal{Y}_{k_0}^{k}\right)$ *is the a-posteriori probability of $\hat{z}_i$ and $t = k\Delta$.*

Proof: Applying the conditional expectation operator to (5.1) and using the properties of the expectation operator yields

$$E\left(\mathrm{ZEM}(k)|\mathcal{Y}_{k_0}^{k}\right) = \mathbf{D}\boldsymbol{\Phi}(t_f, t)E\left(x(k)|\mathcal{Y}_{k_0}^{k}\right) + \mathbf{D}\int_{t}^{t_f} \boldsymbol{\Phi}(t_f, l)\mathbf{B}_2(l)E\left(z(l)|\mathcal{Y}_{k_0}^{k}\right)\,\mathrm{d}l \tag{5.4}$$

By the law of total probability, the conditional expectation of the future of the process z, $E\left(z(l)|\mathcal{Y}_{k_0}^{k}\right)$, $l \in (t, t_f]$, can be written as a probabilistic mixture

$$E\left(z(l)|\mathcal{Y}_{k_0}^{k}\right) = \sum_{i=0}^{w} \hat{z}_i(l)\mathrm{Pr}\left(\hat{z}_i|z_i, \mathcal{Y}_{k_0}^{k}\right) \tag{5.5}$$

where the realization $\hat{z}_i$ is defined by Eq. (5.3d). The equation (5.3) now follows by substituting Eq. (5.5) into Eq. (5.4). ∎

5.1.2 Adaptive Semi-Markov Acceleration Model

The computation of Eqs (5.3c) and (5.3d) requires stating a set of models, in the form of a set of random processes z_i, $i \in \{0, \cdots, w\}$, that adequately describe the future behavior of the process z. The conditional expectations and a-posteriori probabilities of each random process z_i are then calculated. To this end, let each random process z_i be defined as follows:

1. The stochastic process z_i is a piecewise constant process whose value changes at random time instants.
2. The *last* abrupt change in the value of process z_i occurs at time instant $k_i^\star \in [k_0, k]$.
3. At time instant k, the value of the process z_i is denoted $\hat{z}_i^{\mathrm{C}}$, i.e., $z_i(k) = \hat{z}_i^{\mathrm{C}}(k)$.
4. The *future* value of the process z_i satisfies $z_i(l) \in \{-\hat{z}_i^{\mathrm{C}}(k), \hat{z}_i^{\mathrm{C}}(k)\}$, $l \in (t, t_f]$, and the value of z_i changes at most once in the time interval $l \in (t, t_f]$.
5. The time instant of a switch in the value of z_i is random and is selected according to a Poisson distribution with a variable rate, α_i. This variable rate is a function of the sojourn time between switches and is given by

$$\alpha_i(l) = \lambda \frac{\delta_i}{\delta_l}, \qquad \delta_i \triangleq l - k_i^\star \Delta, \;\; \delta_l \triangleq l - t, \;\; l \in (t, t_f] \tag{5.6}$$

   where δ_i is the sojourn time and λ is a positive, non-zero, constant Poisson parameter.

Each random process model z_i is characterized by a different model-matched value for both $\hat{z}_i^{\mathrm{C}}(k)$ and $k_i^\star$. The conditioning of the intensity of the Poisson process on the sojourn time between the switches generates a semi-Markov process, cf. [17].

Proposition 5.1.2 *The conditional expectation in the interval of the random switching process $z_i(l)$, $l \in (t, t_f]$, conditioned on the σ-algebra $\mathcal{Y}_{k_0}^k$ and characterized by the Poisson distributed random switches of rate as given by Eq.* (5.6) *is*

$$\hat{z}_i(l) = \hat{z}_i^{\mathrm{C}}(k)\left(2e^{-\lambda(l-k_i^{\star}\Delta)} - 1\right), \qquad l \in (t, t_f],\ \ t = k\Delta \tag{5.7}$$

Proof: In the absence of measurements in the interval $(t, t_f]$, the conditional expectation of the random process $z_i(l)$, $l \in (t, t_f]$, conditioned on the σ-algebra $\mathcal{Y}_{k_0}^k$ is equivalent to the unconditional expectation of z_i and is given

$$\hat{z}_i(l) = \hat{z}_i^{\mathrm{C}}(k)\mathrm{P}_i^1(l) - \hat{z}_i^{\mathrm{C}}(k)\mathrm{P}_i^2(l) \tag{5.8a}$$

$$\mathrm{P}_i^1(l) \triangleq \Pr\left(z_i(l) = \hat{z}_i^{\mathrm{C}}(k)\,|\delta_i\right) \tag{5.8b}$$

$$\mathrm{P}_i^2(l) \triangleq \Pr\left(z_i(l) = -\hat{z}_i^{\mathrm{C}}(k)\,|\delta_i\right) \tag{5.8c}$$

From the Poisson distribution of the switches, the rate of the Poisson process given by Eq. (5.6), and the assumption of at most one switch in the interval $(t, t_f]$, the transition probabilities are given by, cf. [50]

$$\Pr\left(z_i(l) = \hat{z}_i^{\mathrm{C}}(k)\,|\,\delta_i\right) = e^{-\lambda\delta_i} \tag{5.9a}$$

$$\Pr\left(z_i(l) = -\hat{z}_i^{\mathrm{C}}(k)\,|\delta_i\right) = 1 - e^{-\lambda\delta_i} \tag{5.9b}$$

Thus, using Eq. (5.9) in Eq. (5.8), the expectation $\hat{z}_i$ is calculated as

$$\hat{z}_i(l) = \hat{z}_i^{\mathrm{C}}(k)\left(2e^{-\lambda(l-k_i^{\star}\Delta)} - 1\right), \qquad t \in (t, t_f] \tag{5.10}$$

∎

The set of semi-Markov models is further modified (adaptively) by conditioning the value of $\hat{z}_i^{\mathrm{C}}$ on the measurements. The value of $\hat{z}_i^{\mathrm{C}}$ and the associated a posteriori probability $\Pr\left(\hat{z}_i|z_i, \mathcal{Y}_{k_0}^k\right)$ are calculated by employing an adaptive-$\mathscr{H}_0$ GLR algorithm, see below.

5.1.3 Estimate $\hat{z}_i^{\mathrm{C}}$ and the a Posteriori Probabilities

An adaptive-$\mathscr{H}_0$ GLR algorithm is equipped with a set of hypotheses whose members comprise: a "no change" hypothesis, $\mathscr{H}_0$, and w hypotheses $\mathscr{H}_i^k$, $i \in \{1, \cdots, w\}$, describing abrupt changes. Each hypothesis $\mathscr{H}_i^k$ assumes that the process z is subject to an abrupt change at instant $k_i^\star$ and that the value of the process z is constant in the interval $[k_i^\star, k]$. The GLR algorithm then calculates the maximum likelihood estimate of the process z with respect to each hypothesis

$$\hat{z}_i^{\mathrm{ML}} \triangleq \arg\max_z \mathrm{p}\left(\mathcal{Y}_{k_0}^k | \mathscr{H}_i^k, z\right) \tag{5.11}$$

In order to employ a GLR algorithm to calculate the a posteriori probabilities of the random processes z_i, $i \in \{0, \cdots, w\}$, it is necessary to associate the hypothesis $\mathscr{H}_i^k$ with the random process z_i. This association is achieved by employing the same value $k_i^\star$ for both the random process z_i and the hypothesis $\mathscr{H}_i^k$ and by setting

$$\hat{z}_i^{\mathrm{C}}(k) = \hat{z}_i^{\mathrm{ML}}(k) \tag{5.12}$$

The association also requires that the value of the reference realization, $\bar{z}$, employed by the GLR algorithm is the true realization of z before the true switch instant $k^\star$, i.e., $\bar{z}(l) = z(l)$, $l \in [k_0, k^\star)$. The a posteriori probabilities of the random process models are then provided by Prop. 5.1.3.

Proposition 5.1.3 *Let hypothesis $\mathscr{H}_i^k$ assume that the random process z is piecewise constant and that the value of z has last changed at time instant $k_i^\star$, $k_i^\star < k$. Let $L\left(\mathcal{Y}_{k_0}^k | \mathscr{H}_i^k\right)$ be the generalized likelihood ratio of hypothesis $\mathscr{H}_i^k$*

$$L\left(\mathcal{Y}_{k_0}^k | \mathscr{H}_i^k\right) = \frac{\mathrm{p}\left(\mathcal{Y}_{k_0}^k | \hat{z}_i^{\mathrm{ML}}, \mathscr{H}_i^k\right)}{\mathrm{p}\left(\mathcal{Y}_{k_0}^k | \bar{z}_0, \mathscr{H}_0\right)} \tag{5.13}$$

where $\bar{z}_0$ is the reference realization employed by the hypothesis $\mathscr{H}_0$.

Let z_i be a random process defined as in § 5.1.2 and let Eq. (5.12) *hold. Let the minimum magnitude for an abrupt change in the value of the process z be $\nu_{\min}$. Then,* *the probability that a switch occurred,* P_s*, is calculated as:*

$$\mathrm{P}_s = \sum_{i=1}^{w} \iota(i) \frac{L\left(\mathcal{Y}_{k_0}^k | \mathscr{H}_i^k\right) \Pr\left(\hat{z}_i^{\mathrm{ML}}, \mathscr{H}_i^k\right)}{L\left(\mathcal{Y}_{k_0}^k | \mathscr{H}_0\right) \Pr\left(\hat{z}_j^{\mathrm{ML}}, \mathscr{H}_0\right) + \sum_{j=1}^{w} L\left(\mathcal{Y}_{k_0}^k | \mathscr{H}_j^k\right) \Pr\left(\hat{z}_j^{\mathrm{ML}}, \mathscr{H}_j^k\right)} \tag{5.14a}$$

$$\iota(i) \triangleq \begin{cases} 1 & \text{when } |\hat{z}_i^{\mathrm{ML}}(k) - \hat{z}_0(k)| > \nu_{\min} \\ 0 & \text{otherwise} \end{cases} \tag{5.14b}$$

where $\Pr\left(\hat{z}_i^{\mathrm{ML}}, \mathscr{H}_i^k\right)$ *is the unconditional probability of the realization* $\hat{z}_j^{\mathrm{ML}}$ *associated with hypothesis* $\mathscr{H}_i^k$*.*

The a posteriori probability of each expectation $\hat{z}_i(l)$*,* $l \in (t, t_f]$*, conditioned on the* σ*-algebra* $\mathcal{Y}_{k_0}^k$ *is given by*

$$\Pr\left(\hat{z}_0(l) | z_0, \mathcal{Y}_{k_0}^k\right) = 1 - \mathrm{P}_s \tag{5.15a}$$

$$\Pr\left(\hat{z}_i(l) | z_i, \mathcal{Y}_{k_0}^k\right) = \frac{\iota(i) L\left(\mathcal{Y}_{k_0}^k | \mathscr{H}_i^k\right) \Pr\left(\hat{z}_i^{\mathrm{ML}}, \mathscr{H}_i^k\right)}{\sum_{j=1}^{w} \iota(j) L\left(\mathcal{Y}_{k_0}^k | \mathscr{H}_j^k\right) \Pr\left(\hat{z}_j^{\mathrm{ML}}, \mathscr{H}_j^k\right)} \mathrm{P}_s \tag{5.15b}$$

Proof: The a posteriori probability of the maximum likelihood realization of hypothesis $\mathscr{H}_i^k$, i.e., $\Pr\left(\hat{z}_i^{\mathrm{ML}}(k) | \mathscr{H}_i^k, \mathcal{Y}_{k_0}^k\right)$, is calculated, using the Bayes' rule, as

$$\Pr\left(\hat{z}_i^{\mathrm{ML}}(k) | \mathscr{H}_i^k, \mathcal{Y}_{k_0}^k\right) = \frac{L\left(\mathcal{Y}_{k_0}^k | \mathscr{H}_i^k\right) \Pr\left(\hat{z}_i^{\mathrm{ML}}, \mathscr{H}_i^k\right)}{L\left(\mathcal{Y}_{k_0}^k | \mathscr{H}_0\right) \Pr\left(\hat{z}_j^{\mathrm{ML}}, \mathscr{H}_0\right) + \sum_{j=1}^{w} L\left(\mathcal{Y}_{k_0}^k | \mathscr{H}_j^k\right) \Pr\left(\hat{z}_j^{\mathrm{ML}}, \mathscr{H}_j^k\right)} \tag{5.16}$$

The a posteriori probability of the random process $z_i(l)$, $l \in (t, t_f]$, is obtained by calculating the a posteriori probability, P_s, that a change to the value $\hat{z}_i^{\mathrm{C}}$ occurred at the time instant $k_i^\star$, i.e., that $z(k_i^\star) = \hat{z}_i^{\mathrm{C}}(k)$. The a posteriori probability P_s can be calculated from the a posteriori probability of the hypotheses in Eq. (5.16) whenever the random processes are defined according to § 5.1.2 and also by assuming that Eq. (5.12) holds. The a posteriori probability P_s is calculated as the summation of the a posteriori probability of all the abrupt change hypotheses for whose the maximum likelihood estimate of the change meets or exceeds a minimum magnitude,

$\nu_{\min}$, for the change

$$\mathrm{P}_s = \sum_{1}^{w} \iota(i) \Pr\left(\hat{z}_i^{\mathrm{ML}}(k) | \mathscr{H}_i^k, \mathcal{Y}_{k_0}^k\right) \tag{5.17}$$

where ι is given by Eq. (5.14b). As discussed in the literature, see p. 57 in Ref. [10], a minimum magnitude, $\nu_{\min}$, for the change must be employed to distinguish between an abrupt change hypothesis indicating a jump and an abrupt change hypothesis indicating no jump. This need is due to the fundamental nature of the generalized likelihood ratios which permits for a "jump" of zero magnitude at $k_i^\star$.

Similarly, the a posteriori probability that no change occurred, i.e., $(1 - \mathrm{P}_s)$, is given by the summation of the a posteriori probability of the no change hypothesis with the a posteriori probability of all the abrupt change hypotheses failing to meet the minimum magnitude for the change

$$1 - \mathrm{P}_s = \Pr\left(\hat{z}_0^{\mathrm{ML}}(k) | \mathscr{H}_0, \mathcal{Y}_{k_0}^k\right) + \sum_{1}^{w} (1 - \iota(i)) \Pr\left(\hat{z}_i^{\mathrm{ML}}(k) | \mathscr{H}_i^k, \mathcal{Y}_{k_0}^k\right) \tag{5.18}$$

Hence, the a posteriori probability of the random process $z_0(l)$, $l \in (t, t_f]$, associated with the no change hypothesis $\mathscr{H}_0$, is given by Eq. (5.15a). Consequently, the a posteriori probability of the random process $z_i(l)$, $l \in (t, t_f]$, associated with the abrupt change hypothesis $\mathscr{H}_i^k$, $i \in \{1, \cdots, w\}$, is given by Eq. (5.15b). ∎

Remark In Prop. 5.1.3, the values of the unconditional probabilities $\Pr\left(\hat{z}_i^{\mathrm{ML}}, \mathscr{H}_i^k\right)$, $i = 0, \ldots, w$, are determined from the a priori information about the process z. If no a priori information is available, then the unconditional probabilities should be selected equiprobable, i.e., $\Pr\left(\hat{z}_i^{\mathrm{ML}}, \mathscr{H}_i^k\right) = \frac{1}{w+1}$. If it is known a priori that the process z can takes only two values, i.e., $z \in \{-a, a\}$, than the unconditional probabilities can be represented by a bi-modal distribution, for example: $\Pr\left(\hat{z}_i^{\mathrm{ML}}, \mathscr{H}_i^k\right) = \frac{1}{\mathfrak{N}}\left(e^{-(\hat{z}_i^{\mathrm{ML}} - a)^2/\sigma_+^2} + e^{-(\hat{z}_i^{\mathrm{ML}} + a)^2/\sigma_-^2}\right)$ where $\mathfrak{N}$ is a normalizing constant and σ_+ and σ_- are the standard deviations of the two modes.

5.1.4 An Example

Let the predicted ZEM associated with the system matrices in Eqs. (2.13) be calculated by employing the predictor in Prop. 5.1.1 and by using the semi-Markov models of § 5.1.2. Let also the elements of the estimated state vector be: $E\left(x(k)|\mathcal{Y}_{k_0}^k\right) = \left[\begin{array}{cccc} \hat{x}_1(k) & \hat{x}_2(k) & \hat{x}_3(k) & \hat{x}_4(k) \end{array}\right]^T$. Then, the predicted ZEM is calculated as

$$E\left(\text{ZEM}(k)|\mathcal{Y}_{k_0}^k\right) = \mathbf{D}\boldsymbol{\Phi}(t_f, t)\hat{x}(k) + \hat{\Theta}(k) \tag{5.19}$$

where

$$\mathbf{D}\boldsymbol{\Phi}(t_f, t)\hat{x}(k) = \hat{x}_1(k) + \hat{x}_2(k)t_{go} + \hat{x}_3(k)\tau_E\Phi(k, \tau_E) - \hat{x}_4(k)\tau_P\Phi(k, \tau_P) \tag{5.20a}$$

with

$$\Phi(l, \beta) \triangleq t_f - l\Delta - \beta\left(1 - e^{-(t_f - l\Delta)/\beta}\right), \qquad \beta \in \{\tau_P, \tau_E\} \tag{5.20b}$$

The prediction $\hat{\Theta}(k)$ is calculated by employing Prop. 5.1.2 and Eq. (5.12) in Eq. (5.3c) and by making use of Prop. 5.1.3 as follows

$$\hat{\Theta}(k) = \sum_{i=0}^{w} \left(2\xi_2(k, k_i^\star) - \xi_1(k)\right)\hat{z}_i^{\text{ML}}(k)\Pr\left(\hat{z}_i(l)|z_i, \mathcal{Y}_{k_0}^k\right) \tag{5.21a}$$

where

$$\xi_1(k) \triangleq \frac{t_{go}^2}{2} - \tau_E\Phi(k, \tau_E) \tag{5.21b}$$

$$\xi_2(k, k_i^\star) \triangleq \begin{cases} \lambda^{-1}e^{-\lambda(t - t_i^\star)}\Phi\left(k, \lambda^{-1}\right), & \text{when } \lambda^{-1} = \tau_E \\ \lambda^{-1}e^{-\lambda(t - t_i^\star)} \times \frac{\lambda^{-1}\Phi\left(k, \lambda^{-1}\right) - \tau_E\Phi(k, \tau_E)}{\lambda^{-1} - \tau_E}, & \text{otherwise} \end{cases} \tag{5.21c}$$

In the above, the factor $\Phi\left(k, \lambda^{-1}\right)$ is calculated as in (5.20b) with $\beta = \lambda^{-1}$ and $t_i^\star = k_i^\star\Delta$.

5.2 Decision Directed Adaptive Estimation and Guidance

The Eqs. (2.1) and (2.4) define a finite horizon, non-Gaussian, stochastic dual control problem with bounded inputs and a terminal cost function. The estimation and control tasks are in general not separable for such problems, cf. [86]. In the quest to find a solution to this type of problems, it is worthwhile recalling that a *partial* separation theorem holds for Gaussian and non-Gaussian discrete-time linear systems with hard constraints on the control and under mild regularity assumptions concerning the conditional distributions involved. This partial separation theorem, see Theorem 1 in Striebel [78], requires that:

(1) at any given time k, all the past values of the controls, u_i, and of the outputs, y_i, for $i = (1, ..., k)$, are accessible through direct measurements, and

(2) the cost function involves only $(x(k), u_i)$, $k = T_f$, $i = (1, ..., T_f - 1)$ as its arguments, where $x(k)$ denotes the state of the system at time instant k and T_f denotes a fixed time horizon.

The partial separation theorem guarantees that the conditional distribution of the state, as derived in the process of optimal filtering, does not depend on the optimal control and the cost function involved. The partial separation theorem hence works "one way": the optimal estimator can be derived independently from the optimal controller, but the optimal controller must then be obtained as a function of the pdf of the filtered state, cf. [86].

The decision directed adaptive estimation and guidance scheme is an attempt to deliver a finite dimensional and recursive sub-optimal solution to the stochastic dual control problem on the basis of the partial separation theorem. The proposed adaptive scheme solves the filtering problem and the guidance problem semi-separately in

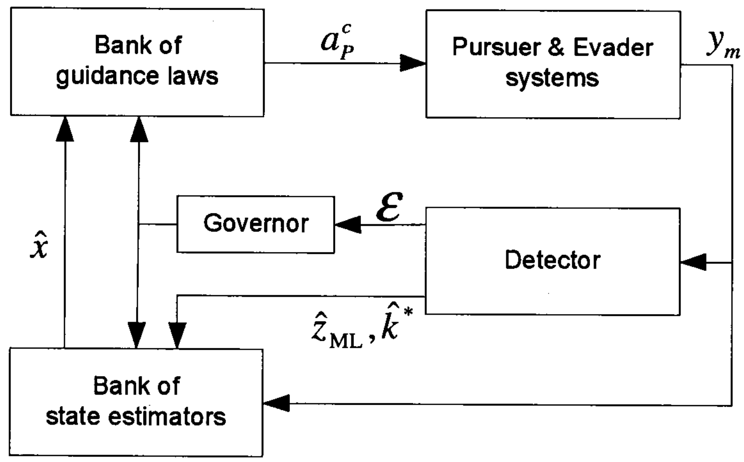

Figure 5.1: Decision directed adaptive estimation and guidance scheme.

that the solution of the filtering problem is obtained first while its error characteristics are next used in the design of the guidance law. More precisely, the behavior of the conditional pdf is partitioned into "modes" characterizing the type of uncertainties affecting the conditional pdf. Decision theory is then employed to identify on-line the mode of uncertainty and to adapt the controller accordingly. Furthermore, a sub-optimal, but computationally feasible, adaptive state estimator is employed (the optimal nonlinear filters for jump-diffusion processes are generally infinite dimensional, cf. [47]). Analogous adaptive sub-optimal approaches to state estimation have been proposed before in the context of target tracking, cf. [30, 58].

The decision directed adaptive estimation and guidance scheme requires the following components: a maneuver detector, a bank of state estimators, a bank of guidance laws, and an on-line governor. The resulting integrated estimation and guidance approach is adaptive and hierarchical, see Figure 5.1 which explains its structure. The functions performed by this scheme are described as follows. At each time instant, the on-line governor selects a state estimator and a guidance law from the respective banks. This selection is based on the current level of uncertainty about the system which is assessed on the basis of the output values from a maneuver detector and the available prior information about the expected number of evasive maneuvers. The task of the maneuver detector is to deliver a decision concerning the event of an abrupt change in the commanded acceleration of the evader and also an estimate of the characteristics of such an abrupt change. An abrupt change is a change occurring instantaneously or over a single sampling time interval. The output signals from the maneuver detector are:

- an estimate of the onset time of the evasive maneuver, $\hat{k}^{\star}$,
- an estimate of the evader's commanded acceleration during the evasive maneuver, $\hat{z}_{\mathrm{ML}}$, and
- the state of a binary indicator $\mathcal{E}$; while an abrupt change is detected, $\mathcal{E}(k) = 1$, otherwise $\mathcal{E}(k) = 0$.

An example implementation of the decision directed adaptive estimation and guidance scheme is described below. This example assumes that a single evasive maneuver is expected and it employs an adaptive-$\mathscr{H}_0$ GLR algorithm for maneuver detection, a Kalman filter with shaping filters for state estimation, and a bank of game theoretic guidance laws.

5.2.1 A Maneuver Detector

An adaptive-$\mathscr{H}_0$ GLR detector is selected to address the task of maneuver detection. The GLR detector employs a set of hypotheses, $\{\mathscr{H}_0, \mathscr{H}_i^k, i = 1, \cdots, w\}$, about the unknown evasive maneuver and recursively calculates the following generalized likelihood ratio, $L(\mathscr{H}_i^k, \mathscr{H}_0)$, for each of the hypotheses

$$L\left(\mathscr{H}_i^k, \mathscr{H}_0\right) \triangleq \frac{\mathrm{p}\left(\mathcal{Y}_{k_0}^k \middle| \mathscr{H}_i^k\right)}{\mathrm{p}\left(\mathcal{Y}_{k_0}^k \middle| \mathscr{H}_0\right)} \tag{5.22}$$

where $\mathcal{Y}_{k_0}^k$ is the σ-algebra generated by the measurements. A positive decision concerning the onset of a maneuver is rendered whenever the maximum likelihood ratio in Eq. (5.22) exceeds the value of a threshold and the maximum likelihood estimate $\hat{k}^\star$ and $\hat{z}_{\mathrm{ML}}$ are delivered; see § 3 for more details.

5.2.2 A Bank of State Estimators

For simplicity, the bank of state estimators contains two members, referred to as E_0 and E_1. Both estimators have the same general form which is that of a Kalman filter enhanced by a shaping filter. The shaping filter is used as a finite dimensional linear approximation to the input random process z;[1] it is employed by augmenting the system with a Wiener process acceleration model (Ref. [7], p. 264)

$$dz \approx dw_a, \qquad dw_a \sim \mathcal{N}(0, Q_{\mathrm{a}}) \tag{5.23}$$

where dw_a is a stochastic process with a zero-mean Gaussian distribution and with covariance Q_{a}; Q_{a} is referred to as the jerk process covariance. The approximation (5.23) preserves the autocorrelation function of the random process z whenever a single evasive maneuver is expected [33] and tracks a piecewise constant input provided that the value of Q_{a} is chosen to be sufficiently large [55]. However, it is known that the introduction of the jerk process in the estimation degrades the rejection of the Gaussian noises in the original system.

The estimators E_0 and E_1 employ different values for the jerk process covariance; these covariances are denoted Q_{a1} and Q_{a2}, respectively. In this application, the values of Q_{a1} and Q_{a2} are chosen as follows

$$Q_{\mathrm{a1}} = 4\frac{\left(z^{\max}\right)^2}{t_f} \tag{5.24a}$$

$$Q_{\mathrm{a2}} = \frac{4}{25}\frac{\left(z^{\max}\right)^2}{t_f} \tag{5.24b}$$

[1] The detector provides an estimate, $\hat{z}_{\mathrm{ML}}$, of the process z but a shaping filter is used to independently estimate z because the value of $\hat{z}_{\mathrm{ML}}$ is affected by the detection delay and by possible false detections.

The larger covariance, $Q_{\mathrm{a}1}$, is obtained following the formula recommended by Ref. [89] for terminal guidance applications against a maneuvering target. The smaller covariance, $Q_{\mathrm{a}2}$, is a heuristic trade-off between:

(a) optimal Gaussian noise rejection (for which $Q_{\mathrm{a}2}$ should be set to zero), and

(b) providing the filter with a sufficiently broad bandwidth to compensate for errors in the estimates $\hat{k}^{\star}$ and $\hat{z}_{\mathrm{ML}}$ (for which $Q_{\mathrm{a}2}$ must be sufficiently large).

The estimator E_0 is designed to be employed at time instants where the uncertainty in the system is dominated by the uncertainty about the unknown evasive maneuver. The estimator E_1 is suitable for times when the evasive maneuver is already detected and estimated (the uncertainty in the system is then dominated by the Gaussian noise processes).

5.2.3 A Bank of Guidance Laws

The bank of guidance laws is, for simplicity, also limited to two members referred to as DGL/C and DGL/1, respectively. Both guidance laws assume first order dynamics for both the pursuer and the evader and the availability of full state observation. These laws were derived in Refs [65, 67] as an optimal solution to either a perfect information or delayed information deterministic zero-sum pursuit-evasion game (the Appendix A outlines the solution procedure)

$$\tilde{J} = \inf_{a_P^{\mathrm{c}} \in \mathcal{A}_P^{\mathrm{c}}} \sup_{a_E^{\mathrm{c}} \in \mathcal{A}_E^{\mathrm{c}}} |x_1(t_f)|, \qquad \begin{array}{l} \mathcal{A}_P^{\mathrm{c}} \triangleq \left\{ a_P^{\mathrm{c}} \in \mathcal{P} \,\middle|\, |a_P^{\mathrm{c}}(t)| \leq (a_P^{\mathrm{c}})^{\max} \;\; a.e. \;\; t \in [0, t_f] \right\} \\ \mathcal{A}_E^{\mathrm{c}} \triangleq \left\{ a_E^{\mathrm{c}} \in \mathcal{P} \,\middle|\, |a_E^{\mathrm{c}}(t)| \leq (a_E^{\mathrm{c}})^{\max} \;\; a.e. \;\; t \in [0, t_f] \right\} \end{array} \tag{5.25}$$

In the above, $\tilde{J}$ is the cost of the game, $x_1(t_f)$ is the miss distance, $\mathcal{P}$ denotes the family of piecewise-continuous functions, while $\mathcal{A}_P^{\mathrm{c}}$ and $\mathcal{A}_E^{\mathrm{c}}$ represent the feasible sets for the pursuer and evader strategies, respectively. Since the game theoretic formulation is deterministic, the random process z in Eq. (2.1a) is replaced by the deterministic variable a_E^c. The constants $(a_P^c)^{\max}$ and $(a_E^c)^{\max}$ provide hard bounds on the commanded accelerations. The deterministic problem in Eq. (5.25) is viewed as an approximation to the control part of the original dual stochastic control problem in Eqs. (2.1). In the continuous-time setting of Eq. (5.25), the DGL/C and DGL/1 laws both take the same form (see the Appendix A)

$$a_P^c(t) = (a_P^c)^{\max} \operatorname{sign}(\mathrm{ZEM}(t)) \tag{5.26}$$

where ZEM is the zero effort miss distance, i.e., the miss distance when the pursuer applies a zero acceleration policy (i.e., $a_P^c(\cdot) = 0$) over the time interval $[t, t_f]$. The DGL/C and DGL/1 guidance laws differ in the way in which the ZEM is calculated. The DGL/C law calculates the ZEM explicitly taking into account a delay in the estimate of the acceleration of the evader, while the DGL/1 law assumes no such delay. Whenever the evasive maneuver is highly uncertain, the DGL/C law achieves a smaller miss distance than the DGL/1 law. Otherwise, the DGL/1 law achieves the smallest miss distance, see the discussion in Ref. [71].

5.2.4 A Governor

An on-line governor employs the value of the indicator variable $\mathcal{E}$ to select a state estimator and a guidance law from the respective banks. This selection is motivated by the assumption of a single evasive maneuver and takes account of an inherent delay in the estimation of the evader's commanded acceleration. Whenever $\mathcal{E}(k) = 0$, the value of the actual evader's commanded acceleration is uncertain since a recent, but yet undetected, evasive maneuver might still have taken place. The current estimate of the evader's commanded acceleration is considered reliable whenever $\mathcal{E}(k) = 1$ because the already detected single evasive maneuver is included in such an estimate. The governor thus employs an on-line decision rule which selects both the state estimator, E_i, $i \in \{0, 1\}$, and the guidance law, DGL/j, $j \in \{C, 1\}$, relative to the level of uncertainty about the current evader's commanded acceleration. The decision rule is hence stated as

$$(E_i, \mathrm{DGL}/j) = \begin{cases} (E_0, \mathrm{DGL/C}) & \text{for } \mathcal{E}(k) = 0 \\ (E_1,\ \mathrm{DGL}/1) & \text{for } \mathcal{E}(k) = 1 \end{cases} \tag{5.27}$$

5.2.5 The Re-Initialization of the State Estimator

The sub-optimal Kalman filters employed in the bank of state estimators can be re-initialized to improve the accuracy of the state estimate. Such re-initialization is achieved here by exploiting the information contained in the detector's estimates $\hat{z}_{\mathrm{ML}}$ and $\hat{k}^{\star}$. The re-initialization is employed when the detector updates its current estimates, which takes place only in two situations: when an evasive maneuver is detected at time instant k (whenever $\mathcal{E}(k) = 1$) and in the event of a false detection of a maneuver that is indicated by the sequence of events: $\{\mathcal{E}(k-1) = 1, \mathcal{E}(k) = 0\}$.[2]

The re-initialization of the state estimator at time instant k requires correcting the value of the state estimate $\hat{x}(k-1|k-1)$ and its covariance $\mathbf{P}(k-1|k-1)$. The re-initialization of the state estimator can be carried out in various ways; the simplest approach is to re-use the previous estimate without corrections. However, the drawback of this approach is that it ignores any new information about the evasive maneuver delivered by the detector such as the value of the current estimates $\hat{z}_{\mathrm{ML}}$ and $\hat{k}^{\star}$. Another approach is to reset the state estimate to be equal to $\hat{z}_{\mathrm{ML}}$ over the entire time interval $[\hat{k}^{\star}, k]$. This particular approach can, however, degrade the state estimate due to the errors in $\hat{z}_{\mathrm{ML}}$ and $\hat{k}^{\star}$. What seems to be a reasonable trade-off between the two extreme approaches is the following. Rather than imposing the estimate history to be that of $\hat{z}_{\mathrm{ML}}$ over the entire time interval $[\hat{k}^{\star}, k]$, it is preferable to constrain the state estimate only at *a single time instant* by requiring that $\hat{x}(l|l)$ and

[2] If more than one evasive maneuver is expected, the definition of a false detection is more complicated, see § 3.

$\hat{z}_{\mathrm{ML}}(k)$ coincide at $l = \hat{k}^\star$. In this way, the subsequent state estimates in the interval $[\hat{k}^\star, k]$ are let to converge to $\hat{z}_{\mathrm{ML}}$ under the action of the Kalman filter whenever the value of $\hat{z}_{\mathrm{ML}}$ is correct or else the Kalman filter has the liberty to compensate for any error that might arise.

To define this procedure more precisely, the re-initialized state estimate and covariance are calculated in at most two steps.

1. If a correction of the state estimate $\delta\hat{x}(k-2)_{\mathrm{old}}$ was already made at time $k-1$, this correction is removed by restoring the previous sequence of estimates

$$\hat{x}(k-1|k-1)_{\mathrm{ori}} = \hat{x}(k-1|k-1)_{\mathrm{old}} - \Xi(k-1)\delta\hat{x}(k-2)_{\mathrm{old}} \tag{5.28a}$$
$$\Xi(k-1) \triangleq \left(\mathbf{I} - \tilde{\mathbf{K}}(k-1)\tilde{\mathbf{H}}\right)\tilde{\mathbf{F}} \tag{5.28b}$$

   where the subscripts $(\cdot)_{\mathrm{ori}}$ and $(\cdot)_{\mathrm{old}}$ denote the state estimate without and with the correction at $k-1$, respectively, $\tilde{\mathbf{K}}$ is the Kalman gain, and $\tilde{\mathbf{H}}$ and $\tilde{\mathbf{F}}$ are the measurement and discrete state transition matrices used by the estimators.[3]

2. The corrected state estimate, $\hat{x}(k-1|k-1)_{\mathrm{new}}$, is calculated using the updated values of both $\hat{z}_{\mathrm{ML}}$ and $\hat{k}^\star$. Let $\delta\hat{z}$ be the difference between the estimates rendered by the detector and by the state estimator for the process z at the time instant $\hat{k}^\star$, i.e., $\delta\hat{z} \triangleq \hat{z}_{\mathrm{ML}}(k) - \hat{z}(k^\star|k^\star)_{\mathrm{ori}}$. Then,

$$\hat{x}(k-1|k-1)_{\mathrm{new}} = \hat{x}(k-1|k-1)_{\mathrm{ori}} + \delta\hat{x}(k-1)_{\mathrm{new}} \tag{5.29}$$

   where the correction term $\delta\hat{x}(k-1)_{\mathrm{new}}$ is obtained from

$$\delta\hat{x}(l)_{\mathrm{new}} = \Xi(l)\,\delta\hat{x}(l-1)_{\mathrm{new}}, \qquad l = \hat{k}^\star(k)+1,\cdots,k-1 \tag{5.30a}$$
$$\delta\hat{x}(\hat{k}^\star)_{\mathrm{new}} = \begin{bmatrix} 0 & \cdots & 0 & \delta\hat{z} \end{bmatrix}^T \tag{5.30b}$$

   The proof of Eqs. (5.29) and (5.30) is provided in Prop. 5.2.1.

[3]The system matrices of the state estimators contain a shaping filter. Hence, they differ from the system matrices in Eqs (2.1).

For simplicity, the covariance of the re-initialized state estimate is updated by

$$\mathbf{P}_{\text{new}}(k-1|k-1) = \mathbf{P}_{\text{old}}(k-1|k-1) \tag{5.31}$$

Proposition 5.2.1 *Consider a Kalman filter with system matrices $\tilde{F}$, $\tilde{G}$, and $\tilde{H}$ and let $\hat{x}(\cdot,\cdot)$ be its state estimate. Suppose that at time instant k, it is desired to force the past state estimate $\hat{x}(k^\star,k^\star)$, $k^\star < k$, to adopt the value $\hat{x}(k^\star|k^\star)_{\text{new}}$. Let $\delta\hat{x}(k^\star|k^\star)$ denote the difference*

$$\delta\hat{x}(k^\star|k^\star) \triangleq \hat{x}(k^\star|k^\star)_{\text{new}} - \hat{x}(k^\star|k^\star)_{\text{old}} \qquad k^\star < k \tag{5.32}$$

Then, the current state estimate consistent with the modified history of $\hat{x}(\cdot,\cdot)$ is

$$\hat{x}(k|k)_{\text{new}} = \hat{x}(k|k)_{\text{old}} + \delta\hat{x}(k|k) \tag{5.33}$$

$$\delta\hat{x}(l|l) = \Xi(l)\delta\hat{x}(l-1|l-1), \qquad l = k^\star+1,\cdots,k \tag{5.34}$$

where the subscripts $(\cdot)_{\text{old}}$ and $(\cdot)_{\text{new}}$ denote the variables before and after modification of the estimate history, respectively.

Proof: By linearity, the difference $\delta\hat{x}(k^\star|k^\star)$ is propagated forward in time using the Kalman filter

$$\hat{x}(l+1|l) = \tilde{\mathbf{F}}\hat{x}(l|l) + \tilde{\mathbf{G}}u(l) \tag{5.35a}$$

$$\hat{x}(l|l) = \hat{x}(l|l-1) + \tilde{\mathbf{K}}(l)\left(y_m(l) - \tilde{\mathbf{H}}\hat{x}(l|l-1)\right) \tag{5.35b}$$

Repetitive applications of filter (5.35) to Eq. (5.32) yields

$$\delta\hat{x}(k|k) = \left(\prod_{i=0}^{k-k^\star-1} \Xi(k-i)\right)\delta\hat{x}(k^\star|k^\star) \tag{5.36}$$

The equation (5.36) re-written in a recursive form is

$$\delta\hat{x}(l|l) = \Xi(l)\delta\hat{x}(l-1|l-1), \qquad l = k^\star+1,\cdots,k \tag{5.37}$$

Thus, by propagating and by reversing Eq. (5.32) and by employing Eq. (5.37), the current state estimate consistent with the modification of $\hat{x}(k^\star|k^\star)$ is

$$\hat{x}(k|k)_{\text{new}} = \hat{x}(k|k)_{\text{old}} + \delta\hat{x}(k|k) \tag{5.38}$$

$\blacksquare$

5.3 A Discretization Scheme for a Class of Control Commands

A discretization scheme for a class of nonlinear control laws is presented below. The technique delivers discretized control laws that correspond to the respective continuous-time laws. An example discretization of the continuous-time DGL/0, DGL/1, and DGL/C guidance laws is presented.

Lemma 5.3.1 *Let A be a linear bounded operator $A : \mathbb{R}^{i_u} \longrightarrow \mathbb{R}^{i_n}$. Let $\mathscr{R}(A)$ be the range of the operator A. Then, the following relation holds*

$$\mathscr{R}(A) = \mathscr{R}(AA^*) \tag{5.39}$$

Proof: Step 1. Proof that $\mathscr{R}(A) \supset \mathscr{R}(AA^*)$.
Consider $y \in \mathscr{R}(AA^*)$. Then,

$$\exists v \in \mathbb{R}^{i_u} \qquad AA^*v = y \tag{5.40}$$

Let $x \triangleq A^*v$. Then,

$$Ax = y \tag{5.41}$$

Hence, $y \in \mathscr{R}(A)$.

Step 2. Proof that $\mathscr{R}(A) \subset \mathscr{R}(AA^*)$.
Consider $y \in \mathscr{R}(A)$. Then,

$$\exists x \in \mathbb{R}^{i_n} \qquad Ax = y \tag{5.42}$$

By the Orthogonal Projection Theorem, x has a unique decomposition

$$x = x_1 + x_2, \qquad x_1 \in \mathscr{N}(A),\ x_2 \in \mathscr{N}^{\perp}(A) \tag{5.43}$$

Then,

$$Ax = A(x_1 + x_2) = Ax_2 = y \tag{5.44}$$

Since A operates between Hilbert spaces, $\mathscr{N}^{\perp}(A) = \mathscr{R}(A^*)$. It follows that $x_2 \in \mathscr{R}(A^*)$. Hence,

$$\exists v \in \mathbb{R}^{i_u} \qquad A^* v = x_2 \tag{5.45}$$

Therefore

$$Ax_2 = AA^* v = y \tag{5.46}$$

Thus, $y \in \mathscr{R}(AA^*)$.

From steps 1 and 2, it follows that $\mathscr{R}(A) = \mathscr{R}(AA^*)$. ∎

Proposition 5.3.2 *Consider a deterministic system with linear dynamics of the form*

$$\dot{x}(t) = \mathbf{A}(t)x(t) + \mathbf{B}_1(t)u(t) + \mathbf{B}_2(t)a(t), \qquad t \in [t_1, t_2] \tag{5.47}$$

where $x(t) \in \mathbb{R}^{i_n}$, $u(t) \in \mathbb{R}^{i_u}$, and $a(t) \in \mathbb{R}^{i_a}$. Suppose that $\mathbf{A}$, $\mathbf{B}_1$, and $\mathbf{B}_2$ are continuous matrix functions of time. Suppose that the transition matrix for this system is $\Phi(\cdot,\cdot)$. Let u and a be the control and deterministic disturbance vector functions, respectively. Let $y(t) \triangleq g(t|x(t)) \in \mathbb{R}^{i_g}$, $t \in [t_1, t_2]$, be the system output. Further, suppose that g is restricted to the following class

$$g(t|x(t)) \triangleq \mathfrak{G}(t)x(t) \tag{5.48}$$

where $\mathfrak{G}$ is a given $i_g \times i_n$ time-varying matrix.

Define an output controllability operator $\mathfrak{D} : \mathbb{R}^{i_u} \longrightarrow \mathbb{R}^{i_g}$

$$\mathfrak{D} \triangleq \mathfrak{G}(t_2)\mathfrak{O}_1 \tag{5.49a}$$

$$\mathfrak{O}_1 \triangleq \int_{t_1}^{t_2} \Phi(t_2, \tau)\mathbf{B}_1(\tau)\,\mathrm{d}\tau \tag{5.49b}$$

Let $x(t; u, x_1, t_1)$ denote the trajectory of the system emanating from initial condition x_1 at t_1 and due to the control action u.

For any fixed initial condition x_1 and for any given control function $u(t) \in \mathbb{R}^{i_u}$, $t \in [t_1, t_2]$, there exists a constant control $u_d \in \mathbb{R}^{i_u}$ such that

$$g(t_2, x(t_2; u, x_1, t_1)) = g(t_2, x(t_2; u_d, x_1, t_1)) \tag{5.50}$$

if and only if

$$\mathfrak{C} \in \mathscr{R}(\mathfrak{D}) \tag{5.51a}$$

with

$$\mathfrak{C} \triangleq \mathfrak{G}(t_2)\mathfrak{A}_1 \tag{5.51b}$$

$$\mathfrak{A}_1 \triangleq \int_{t_1}^{t_2} \Phi(t_2, \tau)\mathbf{B}_1(\tau)u(\tau)\,\mathrm{d}\tau \tag{5.51c}$$

The constant control u_d (of minimum norm) is given by

$$u_d = \mathfrak{D}^* z \tag{5.52a}$$

where z is any solution of

$$\mathfrak{D}\mathfrak{D}^* z = \mathfrak{C} \tag{5.52b}$$

In case $\mathfrak{D}\mathfrak{D}^*$ is invertible, u_d is given by the usual pseudo-inverse

$$u_d = \mathfrak{D}^* \left(\mathfrak{D}\mathfrak{D}^*\right)^{-1} \mathfrak{C} \tag{5.52c}$$

Proof: For brevity of notation, let $x(t) \triangleq x(t; u, x_1, t_1)$ and $x_d(t) \triangleq x(t; u_d, x_1, t_1)$. Under the action of respective control functions, the states x and x_d at time instant t_2 are given by

$$x(t_2) = \Phi(t_2, t_1)x(t_1) + \int_{t_1}^{t_2} \Phi(t_2, \tau)\mathbf{B}_1(\tau)u(\tau)\,\mathrm{d}\tau + \int_{t_1}^{t_2} \Phi(t_2, \tau)\mathbf{B}_2(\tau)a(\tau)\,\mathrm{d}\tau \tag{5.53a}$$

$$x_d(t_2) = \Phi(t_2, t_1)x(t_1) + \left(\int_{t_1}^{t_2} \Phi(t_2, \tau)\mathbf{B}_1(\tau)\,\mathrm{d}\tau\right) u_d + \int_{t_1}^{t_2} \Phi(t_2, \tau)\mathbf{B}_2(\tau)a(\tau)\,\mathrm{d}\tau \tag{5.53b}$$

In short,

$$x(t_2) = x^0(t_2) + \mathfrak{A}_1 + \mathfrak{A}_2 \tag{5.54a}$$

$$x_d(t_2) = x^0(t_2) + \mathfrak{O}_1 u_d + \mathfrak{A}_2 \tag{5.54b}$$

where

$$x^0(t_2) \triangleq \Phi(t_2, t_1)x(t_1) \tag{5.54c}$$

$$\mathfrak{A}_2 \triangleq \int_{t_1}^{t_2} \Phi(t_2, \tau)\mathbf{B}_2(\tau)a(\tau)\, \mathrm{d}\tau \tag{5.54d}$$

and $\mathfrak{O}_1$ and $\mathfrak{A}_1$ are given by Eqs. (5.49b) and (5.51c), respectively. Then,

$$g(t_2, x(t_2)) - g(t_2, x_d(t_2)) = \mathfrak{G}(t_2)x(t_2) - \mathfrak{G}(t_2)x_2(t_2) \tag{5.55a}$$

$$= \mathfrak{D}u_d - \mathfrak{C} \tag{5.55b}$$

where $\mathfrak{D}$ and $\mathfrak{C}$ are given by Eqs. (5.49a) and (5.51b), respectively. By virtue of assumption (5.51a), it follows that

$$\inf_{u_d} \left|\left|g(t_2, x(t_2)) - g(t_2, x_d(t_2))\right|\right| = \min_{u_d} \left|\left|\mathfrak{D}u_d - \mathfrak{C}\right|\right| = 0 \tag{5.56}$$

Since $\mathscr{R}(\mathfrak{D}) = \mathscr{R}(\mathfrak{D}\mathfrak{D}^*)$ by Lemma 5.3.1, then u_d is given by Eq. (5.52a) because

$$\mathfrak{D}u_d = \mathfrak{D}\mathfrak{D}^* z = \mathfrak{C} \tag{5.57}$$

Clearly, if $\mathfrak{D}\mathfrak{D}^*$ is invertible, u_d is given by Eq. (5.52c), the usual Moore-Penrose pseudo-inverse, as readily follows from the Orthogonal Projection Theorem. ∎

Corollary 5.3.3 *Under the assumptions of Prop. 5.3.2, suppose that the control input $u \in \mathbb{R}^{i_u}$ is bringing the system output y to zero at time t_2, i.e.,*

$$y(t_2) = g(t_2, x(t_2; u, x_1, t_1)) = 0 \tag{5.58}$$

Then, the "equivalent" dead-beat constant control input u_d exists if and only if $\mathfrak{C} \in \mathscr{R}(\mathfrak{D})$, see Eq. (5.51)*, and is given by*

$$u_d = \mathfrak{D}^* z \tag{5.59a}$$

where z is any solution of

$$\mathfrak{D}\mathfrak{D}^* z = -\mathfrak{G}(t_2)\left(x^0(t_2) + \mathfrak{A}_2\right) \tag{5.59b}$$

with x^0 and $\mathfrak{A}_2$ given by Eqs. (5.54c) *and* (5.54d), *respectively. In case $\mathfrak{D}\mathfrak{D}^*$ is invertible, u_d is given by*

$$u_d = -\mathfrak{D}^*\left(\mathfrak{D}\mathfrak{D}^*\right)^{-1}\mathfrak{G}(t_2)\left(x^0(t_2) + \mathfrak{A}_2\right) \tag{5.59c}$$

Proof: By employing Eq. (5.54a), the value of the function $g(t_2, x(t_2))$ is given by

$$g(t_2, x(t_2)) = \mathfrak{G}(t_2)x^0(t_2) + \mathfrak{G}(t_2)\mathfrak{A}_1 + \mathfrak{G}(t_2)\mathfrak{A}_2 \tag{5.60a}$$

$$= \mathfrak{G}(t_2)x^0(t_2) + \mathfrak{C} + \mathfrak{G}(t_2)\mathfrak{A}_2 \tag{5.60b}$$

By virtue of the assumption (5.58), it follows that

$$0 = \mathfrak{G}(t_2)x^0(t_2) + \mathfrak{C} + \mathfrak{G}(t_2)\mathfrak{A}_2 \tag{5.61}$$

Hence,

$$\mathfrak{C} = -\mathfrak{G}(t_2)\left(x^0(t_2) + \mathfrak{A}_2\right) \tag{5.62}$$

The Eq. (5.59) follows by employing Eq. (5.62) in Prop. 5.3.2 if $\mathfrak{C} \in \mathscr{R}(\mathfrak{D})$. ∎

Theorem 5.3.4 *Consider the system given in Prop. 5.3.2 with the additional assumption that it is a single input single output system, i.e., $u \in \mathcal{L}^2, [t_1, t_2]$, and $y(t) \in \mathbb{R}^1$. Additionally, suppose that the control input u must stay bounded by a fixed constant $u^{\max}$*

$$|u(t)| \leq u^{\max}, \qquad t \in [t_1, t_2] \tag{5.63}$$

Define the function $\mathfrak{P}(t) : [t_1, t_2] \longrightarrow \mathcal{L}^2 \times \mathbb{R}^1$ and the constants $\mathfrak{T}$ and $\mathfrak{Z}$ by

$$\mathfrak{P}(t) \triangleq \mathfrak{G}(t_2)\Phi(t_2, t)\mathbf{B}_1(t) \tag{5.64}$$

$$\mathfrak{T} \triangleq \mathfrak{G}(t_2)x^0(t_2) + \mathfrak{G}(t_2)\mathfrak{A}_2 \tag{5.65}$$

$$\mathfrak{Z} \triangleq \int_{t_1}^{t_2} \mathfrak{P}(\tau)\,\mathrm{d}\tau \tag{5.66}$$

where x^0 *and* $\mathfrak{A}_2$ *are defined in Eqs.* (5.54c) *and* (5.54d), *respectively. Suppose* $\mathfrak{P}$ *is not identically zero and does not change sign.*

Under these conditions, for any initial condition x_1

$$\inf_{u\in\mathcal{A}_u} \left|g(t_2, x(t_2; u, x_1, t_1))\right| = \min_{u_d\in\mathcal{A}_d} \left|g(t_2, x(t_2; u_d, x_1, t_1))\right| \tag{5.67a}$$

$$\mathcal{A}_u \triangleq \left\{u \in \mathcal{L}^2 \middle| \, |u(t)| \le u^{\max},\ t \in [t_1, t_2]\right\} \tag{5.67b}$$

$$\mathcal{A}_d \triangleq \left\{u_d \in \mathbb{R}^1 \middle| \, |u_d| \le u^{\max},\ t \in [t_1, t_2]\right\} \tag{5.67c}$$

Furthermore, the minimum in the right hand side of Eq. (5.67) *is achieved by*

$$u_d = \begin{cases} -\mathfrak{T}/3, & \textit{whenever } |\mathfrak{T}/3| \le u^{\max} \\ -u^{\max}\operatorname{sign}\big(\mathfrak{T}\mathfrak{P}(t_1)\big), & \textit{otherwise} \end{cases} \tag{5.68}$$

Proof: Adopt the same short hand notation as given in Eq. (5.53).

Case 1.: Suppose that

$$\inf_{u\in\mathcal{A}_u} \left|g(t_2|x(t_2))\right| = c \neq 0 \tag{5.69}$$

By Eq. (5.60b), it follows that

$$c = \inf_{u\in\mathcal{A}_u} |\mathfrak{T} + \mathfrak{C}| \tag{5.70}$$

where only $\mathfrak{C}$ is a function of the control signal u and is given by Eq. (5.51b). Since $\mathfrak{C} \in \mathbb{R}^1$ and $\mathfrak{T} \in \mathbb{R}^1$, the assumption that $c \neq 0$ implies that

$$c = \min\{r_1, r_2\} \tag{5.71a}$$

$$r_1 \triangleq |\mathfrak{T} + \mathfrak{C}^{\max}|, \qquad \mathfrak{C}^{\max} \triangleq \sup_{u\in\mathcal{A}_u} \mathfrak{C} \tag{5.71b}$$

$$r_2 \triangleq |\mathfrak{T} + \mathfrak{C}^{\min}|, \qquad \mathfrak{C}^{\min} \triangleq \inf_{u\in\mathcal{A}_u} \mathfrak{C} \tag{5.71c}$$

By employing Eq. (5.51), it follows that $\mathfrak{C}^{\max}$ is given by

$$\mathfrak{C}^{\max} = \sup_{u\in\mathcal{A}_u} \left(\mathfrak{G}(t_2) \int_{t_1}^{t_2} \Phi(t_2, \tau)\mathbf{B}_1(\tau)u(\tau)\,\mathrm{d}\tau \right) \tag{5.72}$$

As $\mathfrak{G}$ is a linear operator, then

$$\mathfrak{C}^{\max} = \sup_{u \in \mathcal{A}_u} \int_{t_1}^{t_2} \mathfrak{G}(t_2)\Phi(t_2,\tau)\mathbf{B}_1(\tau)u(\tau)\,\mathrm{d}\tau \tag{5.73a}$$

$$= \sup_{u \in \mathcal{A}_u} \int_{t_1}^{t_2} \mathfrak{P}(\tau)u(\tau)\,\mathrm{d}\tau \tag{5.73b}$$

where $\mathfrak{P}$ is given by Eq. (5.64). By virtue of the assumption that $\mathfrak{P}$ does not change sign, it follows that

$$\mathfrak{C}^{\max} = \begin{cases} \left(\int_{t_1}^{t_2} \mathfrak{P}(\tau)\,\mathrm{d}\tau\right) u^{\max}, & \text{if } \mathfrak{P}(t_1) \geq 0 \\ -\left(\int_{t_1}^{t_2} \mathfrak{P}(\tau)\,\mathrm{d}\tau\right) u^{\max}, & \text{otherwise} \end{cases} \tag{5.74}$$

Similarly,

$$\mathfrak{C}^{\min} = \begin{cases} -\left(\int_{t_1}^{t_2} \mathfrak{P}(\tau)\,\mathrm{d}\tau\right) u^{\max}, & \text{if } \mathfrak{P}(t_1) \geq 0 \\ \left(\int_{t_1}^{t_2} \mathfrak{P}(\tau)\,\mathrm{d}\tau\right) u^{\max}, & \text{otherwise} \end{cases} \tag{5.75}$$

Thus,

$$c = \begin{cases} \mathfrak{T} - u^{\max} \int_{t_1}^{t_2} \mathfrak{P}(\tau)\,\mathrm{d}\tau, & \text{if } \big(\mathfrak{T}\mathfrak{P}(t_1)\big) \geq 0 \\ \mathfrak{T} + u^{\max} \int_{t_1}^{t_2} \mathfrak{P}(\tau)\,\mathrm{d}\tau, & \text{otherwise} \end{cases} \tag{5.76}$$

and that c is achieved by a control $u \in \mathcal{L}^2, [t_1, t_2]$, which is in fact constant so that u_d in Eq. (5.67) is given by

$$u_d = -u^{\max}\mathrm{sign}\big(\mathfrak{T}\mathfrak{P}(t_1)\big), \tag{5.77}$$

The above is easily seen by considering the four following cases

$$\begin{aligned} &\text{if } \mathfrak{T} \geq 0, \text{ then } c = |\mathfrak{T} + \mathfrak{C}^{\min}| \Longrightarrow \begin{cases} u(t) = -u^{\max}, t \in [t_1, t_2], & \text{if } \mathfrak{P}(t_1) \geq 0 \\ u(t) = u^{\max}, t \in [t_1, t_2], & \text{if } \mathfrak{P}(t_1) < 0 \end{cases} \\ &\text{if } \mathfrak{T} < 0, \text{ then } c = |\mathfrak{T} + \mathfrak{C}^{\max}| \Longrightarrow \begin{cases} u(t) = u^{\max}, t \in [t_1, t_2], & \text{if } \mathfrak{P}(t_1) \geq 0 \\ u(t) = -u^{\max}, t \in [t_1, t_2], & \text{if } \mathfrak{P}(t_1) < 0 \end{cases} \end{aligned} \tag{5.78}$$

Case 2. Suppose that

$$\inf_{u \in \mathcal{A}_u} \big| g(t_2 | x(t_2)) \big| = 0 \tag{5.79}$$

By virtue of assumptions (5.67) and (5.79), it follows that

$$0 = \inf_{u \in \mathcal{A}_u} \big| g(t_2 | x(t_2; u, x_1, t_1)) \big| = \inf_{u \in \mathcal{A}_u} |\mathfrak{T} + \mathfrak{C}| \tag{5.80}$$

where only $\mathfrak{C}$ is a function of u. Then, there exists a sequence of control functions $u_i \in \mathcal{L}^2, [t_1, t_2]$, and such that $u_i \in \mathcal{A}_u$, $i = 1, \cdots$, which generates this infimum, meaning

$$-\mathfrak{T}_i \triangleq \int_{t_1}^{t_2} \mathfrak{P}(\tau) u_i(\tau)\, \mathrm{d}\tau \longrightarrow -\mathfrak{T} \qquad \text{as } i \longrightarrow \infty \tag{5.81}$$

For each i, let

$$u_{d,i} = -\frac{\mathfrak{T}_i}{\mathfrak{Z}} \tag{5.82}$$

Hence,

$$-\mathfrak{T}_i = u_{d,i} \mathfrak{Z} \qquad \forall i \tag{5.83}$$

and for all i

$$|u_{d,i}|\, |\mathfrak{Z}| = |u_{d,i} \mathfrak{Z}| = \left| \int_{t_1}^{t_2} \mathfrak{P}(\tau) u_i(\tau)\, \mathrm{d}\tau \right| \leq u^{\max} |\mathfrak{Z}| \tag{5.84}$$

by virtue of the facts that $u_i \in \mathbb{R}^1$, $u_{d,i} \in \mathbb{R}^1$, and $\mathfrak{P}$ does not change sign. Therefore,

$$|u_{d,i}| \leq u^{\max} \qquad \forall i \tag{5.85}$$

Since the sequence $u_{d,i}$ is bounded, it contains at least one convergent subsequence (this convergent subsequence is "of course" a sequence of zeroes when $\mathfrak{Z} = 0$). To simplify the notation, let $\{u_{d,i}\}$ denote this subsequence and let u_d be its limit.

It follows that

$$\int_{t_1}^{t_2} \mathfrak{P}(\tau) u_i(\tau)\, \mathrm{d}\tau = u_{d,i} \int_{t_1}^{t_2} \mathfrak{P}(\tau)\, \mathrm{d}\tau \longrightarrow u_d \int_{t_1}^{t_2} \mathfrak{P}(\tau)\, \mathrm{d}\tau = -\mathfrak{T} \qquad \text{as } i \longrightarrow \infty \tag{5.86}$$

and

$$|u_d| \leq u^{\max} \tag{5.87}$$

as a limit of a sequence bounded by the same number. Therefore,

$$u_d = -\frac{\mathfrak{X}}{\mathfrak{Z}} \tag{5.88}$$

and u_d delivers the minimum in Eq. (5.67).

Finally, the minimum in Eq. (5.67) is found by first computing the right hand side of Eq. (5.88) and determining if it satisfies the pre-specified bound $u^{\max}$. If this is so, then the u_d of Eq. (5.88) is indeed the minimizing control. Otherwise, the u_d of Eq. (5.77) is the minimizing control which however does not deliver $g(t_2, x(t_2)) = 0$.

∎

5.3.1 An Example: The Discretized DGL/0, DGL/1 and DGL/C Laws

The DGL guidance laws are each optimal game theoretic solutions to a continuous-time deterministic linear pursuit-evasion problem with bounded inputs. These guidance laws are of the form

$$u_i(t) = u^{\max}\operatorname{sign}\big(\mathrm{ZEM}_i(t)\big) \qquad i \in \{0, 1, C\} \tag{5.89}$$

with

$$\mathrm{ZEM}_i(t) \triangleq \mathbf{D}\Phi_i(t_f, t)x(t) \tag{5.90a}$$

$$\mathbf{D} \triangleq \begin{bmatrix} 1 & 0 & 0 & 0 \end{bmatrix} \tag{5.90b}$$

$$x^T = \begin{bmatrix} x_1 & x_2 & x_3 & x_4 \end{bmatrix} \tag{5.90c}$$

Here, u_i, $i \in \{0, 1, C\}$, are the control commands for the DGL/i laws and Φ_i are transition matrices of three different systems also of the form (5.47). The ZEM has the property that $\mathrm{ZEM}(t_f)$ is equal to the miss distance. In each of the three cases, the ZEM plays the role of the function g in the optimal control problem of Theorem 5.3.4 and $\hat{u}$, as given by Eq. (5.89), is the optimal solution. The linear systems associated with each Φ_i, $i \in \{0, 1, C\}$, differ only by the assumptions about the dynamics of the evasive maneuvers. The explicit expressions for ZEM_i are, cf. [38, 65, 67],

$$\mathrm{ZEM}_0(t) = x_1(t) + x_2(t)t_{\mathrm{go}} - x_4(t)\Omega_P(t) \tag{5.91a}$$

$$\mathrm{ZEM}_1(t) = x_1(t) + x_2(t)t_{\mathrm{go}} + x_3(t)\Omega_E(t) - x_4(t)\Omega_P(t) \tag{5.91b}$$

$$\mathrm{ZEM}_C(t) = x_1(t) + x_2(t)t_{\mathrm{go}} + x_3(t)\Omega_E(t)e^{-\Delta_l/\tau_E} - x_4(t)\Omega_P(t) \tag{5.91c}$$

where

$$\Omega_j \triangleq \tau_j\big(t_{\mathrm{go}} - \tau_j(1 - e^{-t_{\mathrm{go}}/\tau_j})\big) \qquad j \in \{E, P\} \tag{5.91d}$$

and τ_P, τ_E, and Δ_l are parameters.

In order to obtain a guidance law which is cost-equivalent to Eq. (5.89) and delivers a control command with a constant value in time intervals of a given length Δ, Theorem 5.3.4 is applied as follows.

The optimal controls u_i as given by Eq. (5.89) are clearly piecewise-continuous and bounded functions (because of the continuity of ZEM_i) and hence are members of $\mathcal{L}^2$ over any finite interval of time. In the context of Theorem 5.3.4, this optimal control is viewed as the solution to the following optimal control problem

$$\inf_{u \in \mathcal{A}_u} \mathrm{ZEM}_i(t_f) \tag{5.92}$$

where $\mathcal{A}_u$ is defined by Eq. (5.67b) and subject to the constraints provided by the dynamical model for the propagation of the ZEM_i over the interval $[0, t_f]$ which is easily obtained by differentiating Eqs. (5.91) with respect to time. Assuming that $\mathrm{ZEM}_i(t)$ lies on the optimal trajectory for the system on $[0, t_f]$, it then follows from the Bellman's principle of optimality that the control u_i restricted to any subinterval $[t, t+\Delta]$ is also optimal for the optimal control problem (5.92) over the restricted horizon $[t, t+\Delta]$. The Theorem 5.3.4 is now readily applied with $t_1 = t$ and $t_2 = t+\Delta$, provided that the functions $\mathfrak{P}_i$, corresponding to this restricted control problem, satisfy the assumptions. For the pursuit-evasion scenario used in the derivation of the DGL/1 law, i.e., for $\Phi = \Phi_1$, the formulae for $\mathfrak{P}_i$ are obtained by comparing Eqs. (2.4), (5.64), (5.90a), and (5.91). Similarly, it is found that the linear operator $\mathfrak{G}$ is given by $\mathfrak{G}(t) = \mathbf{D}\Phi_i(t_f, t)$.

Claim 5.3.5 *The function $\mathfrak{P}_i(\tau)$, $i \in \{0, 1, C\}$, $\tau \in [0, t_f]$, does not change sign.*

Proof: From the definition of $\mathfrak{P}_i$ in Eq. (5.67b), it follows that

$$\mathfrak{P}_0(\tau) = \mathfrak{P}_1(\tau) = \mathfrak{P}_C(\tau) = -t_f + \tau_P + \tau - \tau_P e^{-(t_f-\tau)/\tau_P} \tag{5.93}$$

Consider,

$$\frac{\mathrm{d}\mathfrak{P}_i}{\mathrm{d}\tau} = 1 - e^{-(t_f-\tau)/\tau_P}, \qquad i \in \{0, 1, C\} \tag{5.94}$$

Clearly, $\mathrm{d}\mathfrak{P}_i/\mathrm{d}\tau \geq 0$ for $\tau \in [0, t_f]$, and hence the function $\mathfrak{P}_i(\tau)$ is growing monotonically in the interval $[0, t_f]$. Moreover, the maximum of $\mathfrak{P}_i(\tau)$, $\tau \in [0, t_f]$, is

$$\max_{\tau\in[0,t_f]} \mathfrak{P}_i(\tau) = \mathfrak{P}_i(t_f) = 0, \qquad i \in \{0, 1, C\} \tag{5.95}$$

Thus, $\mathfrak{P}_i(\tau)$, $i \in \{0, 1, C\}$, $\tau \in [0, t_f]$, is always negative. ∎

Let $t = k\Delta$, and let $u_{d,i}$ be the control command delivered by the discretized DGL/i law, $i \in \{0, 1, C\}$, for $t \in [0, t_f]$. Then, from Eq. (5.68) it follows that

$$\hat{u}_{d,i}(k) = \begin{cases} a_i(k)/\Theta_P(k) & \text{whenever } |a_i(k)/\Theta_P(k)| \leq u^{\max} \\ u^{\max}\mathrm{sign}\big(a_i(k)\big) & \text{otherwise} \end{cases} \tag{5.96}$$

where

$$a_0(k) = \mathrm{ZEM}_0(k) + \mathfrak{N}_0(k) \tag{5.97a}$$

$$a_1(k) = \mathrm{ZEM}_1(k) + \mathfrak{N}_1(k) \tag{5.97b}$$

$$a_C(k) = \mathrm{ZEM}_C(k) + \mathfrak{N}_C(k) \tag{5.97c}$$

with

$$\Theta_P(k) = \Delta\left(t_{\mathrm{go}} - \tau_P\right) + \tau_P^2 e^{-t_{\mathrm{go}}/\tau_P}\left(e^{\Delta/\tau_P} - 1\right) - \frac{\Delta^2}{2} \tag{5.98a}$$

$$\mathfrak{N}_0(k) = \int_t^{t+\Delta} \big(t_f - \tau_E - \tau + \mathfrak{J}_0(k)\big)a(\tau)\,\mathrm{d}\tau \tag{5.98b}$$

$$\mathfrak{N}_1(k) = \int_t^{t+\Delta} \big(t_f - \tau_E - \tau + \mathfrak{J}_1(k)\big)a(\tau)\,\mathrm{d}\tau \tag{5.98c}$$

$$\mathfrak{N}_C(k) = \int_t^{t+\Delta} \Big(t_f - \tau_E - \tau + (1 - e^{-\Delta_l/\tau_E})\mathfrak{J}_0(k) + e^{-\Delta_l/\tau_E}\mathfrak{J}_1(k)\Big)a(\tau)\,\mathrm{d}\tau \tag{5.98d}$$

$$\mathfrak{J}_0(k) \triangleq e^{-(t-\tau)/\tau_E}e^{-\Delta/\tau_E}(\tau_E - t_{\mathrm{go}} + \Delta) \tag{5.98e}$$

$$\mathfrak{J}_1(k) \triangleq e^{-(t-\tau)/\tau_E}e^{-t_{\mathrm{go}}/\tau_E}\tau_E \tag{5.98f}$$

The calculation of $\mathfrak{N}_i$, $i \in \{0, 1, C\}$, requires specifying the realization of $a(\tau)$, $\tau \in [t, t + \Delta]$.

Important Remark 1.

The Claim 5.3.5, that guarantees that $\mathfrak{P}$ does not change sign over the whole engagement, is a sufficient *but not necessary* condition for application of Theorem 5.3.4. The necessary condition for application of Theorem 5.3.4 is that $\mathfrak{P}$ does not change sign over the sampling time interval.

Important Remark 2.

The Theorem 5.3.4 guarantees that there is no control strategies in $\mathcal{L}^2, [t_1, t_2]$, that achieve a smaller value of ZEM_i than that delivered by $u_{d,i}$. Since the continuous-time DGL/i law, $i \in \{0, 1, C\}$, is only a subset of the strategies in $\mathcal{L}^2, [t_1, t_2]$, it is guaranteed that the discretized control signal $u_{d,i}$ is at least as good to minimize ZEM_i as the continuous-time DGL/i law, if not better. Moreover, Theorem 5.3.4 guarantees that the control signal $u_{d,i}$ is of minimal norm.

Chapter 6

Summary of Simulation Results Involving the Novel Detection, Estimation, and Guidance Schemes

THE efficiency and superiority of the novel schemes are demonstrated by extensive simulations in application to a pursuit-evasion terminal engagement between an interceptor (the pursuer) and a maneuvering ballistic missile (the evader). The mathematical description of the engagement is presented in § 2. The simulation parameters are selected to represent the interception problem of a maneuvering ballistic missile re-entering the atmosphere after its midcourse suborbital flight. Discussions of realistic values for these parameters are found in Refs [40, 77, 79]. The control strategy employed by the evader is a bang-bang maneuver with a single switch over the time interval of the engagement. The time instant of the switch is unknown to the pursuer. The statistical performances of the algorithms are evaluated through Monte Carlo simulations. The Monte Carlo simulation repeats the pursuit-evasion scenario several times. Each repetition is characterized by a specific noise realization and a specific onset time instant for the evasive bang-bang maneuver.

Table 6.1: Simulation parameters

Parameter	Value
Initial distance	$X_0 = 20\ 000$ m
Pursuer velocity	$V_P = 2\ 300$ m/s
Evader velocity	$V_E = 2\ 700$ m/s
Pursuer maximal acceleration	$u^{\max} = 30$ g
Evader maximal acceleration	$z^{\max} = 15$ g
Pursuer time constant	$\tau_P = 0.2$ s
Evader time constant	$\tau_E = 0.2$ s
Measurement rate	$f = 100$ Hz
Measurement angular noise standard deviation	$\sigma = 0.1$ mrad
False alarm probability	$\alpha = 0.001$
Maximal magnitude of $\hat{z}_{\mathrm{ML}}$	$z_{\mathrm{ML}}^{\max} = 100$ g

6.1 Simulation Parameters

The nonlinear dynamics of the pursuit-evasion engagement is provided by Eqs. (2.7) while the linearized dynamics is given by Eqs. (2.8). In this scenario, the known input, u, is the acceleration command of the pursuer, and the unknown input subject to additive abrupt changes, z, is the evader's acceleration command. The simulation parameters, common to all simulations, are provided in Table 6.1. The value of $z^{\max}$ is unknown to the pursuer. Furthermore, the sampling time interval of the discrete-time system, Δ, is obtained from the measurement rate f as: $\Delta = 1/f$. The initial heading angles are zero, i.e., $\phi_P(0) = 0$ and $\phi_E(0) = 0$, see Fig. 2.1, and the initial evader's acceleration command is $z(0) = 15$ g. The theoretical false alarm probability, α, is employed to select the threshold, h, used in the GLR test and is computed, using Eq. (3.33), to be $h = 10.83$. The value of the bound $z_{\mathrm{ML}}^{\max}$ is selected larger than $z^{\max}$

to permit for the presence of estimation errors in $\hat{z}(k,i)$, see § 3.2.5.

To present the results, it is useful to define the time-to-go at the onset of the evader's maneuver, $\mathrm{tgo}_{\mathrm{sw}}$:

$$\mathrm{tgo}_{\mathrm{sw}} \triangleq t_f - t^\star, \qquad t^\star \triangleq k^\star \Delta \tag{6.1}$$

where $k^\star$ is the onset time instant of the evasive maneuver.

6.1.1 Parameters for the Detection Statistics

The detection statistics of the adaptive-$\mathscr{H}_0$ GLR detector are compared to those of the GLR detector. The Monte Carlo simulations employ 40 different time instants for the onset of the evader's maneuver, and a total 40 000 different noise realizations. Each repetition employs the linearized dynamics of the engagement. The following criteria are chosen for the comparison:

(i) the false alarm rate,

(ii) the rate of missed detection,

(iii) the detection delay (the average and the standard deviation), and

(iv) the error in the estimation of z (the average and the standard deviation).

The reference Kalman filter employed by the GLR algorithms requires a reference realization which is initially selected to be $a^{\mathscr{H}_0}(l) = 0,\ l \geq 0$. Hence, the reference realization $a^{\mathscr{H}_0}$ is initially mismatched with respect to $z(0)$. The reference Kalman filter uses a nonzero process noise covariance matrix, $\mathbf{Q}_k$, given by

$$\mathbf{Q}_k = \int_0^\Delta \mathbf{\Phi}(\tau)\mathbf{Q}\mathbf{\Phi}^T(\tau)\,\mathrm{d}\tau, \qquad \mathbf{Q} = \mathrm{diag}\{q_{11}, q_{22}, q_{33}, 0\} \tag{6.2}$$

where the transition matrix, $\mathbf{\Phi}$, is provided in Eq. (2.14a), and where $q_{11} = 1$ m^2, $q_{22} = 10$ m^2/s^2, and $q_{33} = 1$ m^2/s^4. The nonzero $\mathbf{Q}_k$ provides some bandwidth to compensate for the uncertainties in the isolation of the abrupt change and possible nonlinearities.

The GLR and the adaptive-$\mathscr{H}_0$ GLR detectors also require a set of hypotheses describing the normalized shape of an evasive maneuver. A constant normalized shape is employed for all the hypotheses, i.e., $f_i(l, k^\star) = 1$, $l \in [k^\star, k]$, for all i. The hypotheses differ only by the onset time instant of the evasive maneuver. All the onset time instants are contained within a temporal sliding window. The maximal width, $w^\star$, of the sliding window employed by the GLR detector $w^\star = 70$ whereas the adaptive-$\mathscr{H}_0$ GLR detector employs a maximal sliding window of width $w^\star = 400$ and an effective sliding window of width $w^\star_{\text{eff}} = 70$. Using a tuning process, the factor $\beta(\zeta)$, employed by the GLR test in the adaptive-$\mathscr{H}_0$ GLR algorithm, is set to $\beta(\zeta) = 1.05$.

Remark 1. A larger value for $w^\star$ is desirable to improve the diagnosis of the evasive maneuver. However, the GLR detector requires a smaller $w^\star$ than the adaptive-$\mathscr{H}_0$ GLR detector in order to have the ability of detecting two events during the engagement: the one event triggered by a possible mismatch between the realizations $a^{\mathscr{H}_0}$ and z, and another event triggered by the evader's maneuver. In the case of the adaptive-$\mathscr{H}_0$ GLR detector, the detection of a mismatch does not prevent the detection of the evader's maneuver. Hence, a larger maximal sliding window can be employed to improve the diagnosis of the evasive maneuver.

6.1.2 Parameters for the Estimation Statistics

The estimation statistics of the AMR-GLR estimator are compared to those of the IMM estimator since the latter is recognized to have good performance in tracking problems involving highly maneuvering targets, cf. [44]. The Monte Carlo simulations employ a single onset time instant for the evasive maneuver (i.e., $t = 2.0$ s) and 100 different noise realizations. Each repetition employs the linearized dynamics of the engagement. Five different implementations of the IMM estimators, denoted as IMM1, ..., IMM5, are compared with the AMR-GLR estimator.

The AMR-GLR estimator calculates the (unnormalized) total probability, $\Pr(M_i^k)$, as follows:[1]

$$\Pr(M_i^k) = \begin{cases} e^{-\frac{1}{2}\left(\hat{z}_0^{\mathrm{ML}}(k)-\hat{z}_{\mathscr{H}}(k)\right)^2/\sigma_a^2}, & \text{when } i=0 \\ e^{-\frac{1}{2}\left(|\hat{z}_i^{\mathrm{ML}}(k)|-|\hat{z}_{\mathscr{H}}(k)|\right)^2/\sigma_b^2}, & \text{otherwise} \end{cases} \tag{6.3}$$

where $i \in \{0, \cdots, w\}$, $\sigma_a = 10$ [g] and $\sigma_b = 2$ [g]. Contrary to the IMM estimators, the AMR-GLR estimator does not employ Markovian transition probabilities between the models.

The estimators IMM1, IMM2, IMM3, and IMM4 employ a bank of three Kalman filters equipped with a shaping filter (SF). The SF approximates the unknown evasive command acceleration by a Wiener process acceleration model (WPAM), cf. [7]. The three Kalman filters differ only by the covariance, $\mathbf{Q}_w$, of the WPAM; the three employed values in the bank of IMM1 are $\mathbf{Q}_w \in \{0, 9, 225\}$ [g^2], $\mathbf{Q}_w \in \{0, 25, 2500\}$ [g^2] for IMM2 and IMM4, and $\mathbf{Q}_w \in \{0, 25, 10000\}$ [g^2] for IMM3. The estimators IMM2 and IMM4 differ only by their Markovian transition probability matrices listed below.

The estimator IMM5 incorporates 9 Kalman filters in its bank. Each filter assumes constant acceleration levels for z which are $\{-30, -20, -10, -5, 0, 5, 10, 20, 30\}$ [g]. None of the filters match the true target's command acceleration at any time; the last is realistic since $\hat{z}^{\max}$ is unknown to the pursuer.

The elements, $\Pr(M_i^k|M_j^{k-1})$, of the Markovian transition probability matrix are

[1] The total probability in Eq. (6.3) can be unnormalized since it is only used within a ratio, see Eq. (4.22).

set to:

$$\left.\begin{array}{l}\text{IMM1}\\ \text{IMM2}\\ \text{IMM3}\end{array}\right\} \Longrightarrow \begin{cases} \Pr(M_i^k|M_i^{k-1}) = & 0.98 \\ \Pr(M_i^k|M_j^{k-1}) = & 0.01 \quad i \neq j \end{cases} \tag{6.4a}$$

$$\text{IMM4} \Longrightarrow \begin{cases} \Pr(M_i^k|M_i^{k-1}) = & 0.995 \\ \Pr(M_i^k|M_j^{k-1}) = & 0.0025 \quad i \neq j \end{cases} \tag{6.4b}$$

$$\text{IMM5} \Longrightarrow \begin{cases} \Pr(M_i^k|M_i^{k-1}) = & 0.98 \\ \Pr(M_i^k|M_j^{k-1}) = & 0.0025 \quad i \neq j \end{cases} \tag{6.4c}$$

6.1.3 Parameters for the Homing Accuracy of the Guidance Law With Semi-Markov Models

Two terminal guidance laws of the following form are considered

$$u(k) = u^{\max}\text{sign}\left(\text{ZEM}(k)\right) \tag{6.5}$$

The first guidance law calculate the ZEM using the Bayesian semi-Markov predictor given in Eqs. (5.19)-(5.21). The second guidance law is the so-called DGL/1 law and its ZEM is calculated by employing Eq. 5.91b. The Monte Carlo simulations employ 50 different time instants for the onset of the evasive maneuver and a total of 10 000 different noise realizations. Each repetition employs the linearized dynamics of the engagement. For both guidance laws, the state estimate is delivered by a Kalman filter with a WPAM shaping filter. The covariance of the WPAM is selected to be $Q_a = 225$ g^2. The two comparison criteria are: the single shot kill probability (SSKP), defined as the probability of a successful interception, and the required lethal radius, R_k, of the pursuer, see § 2.1 for details.

The semi-Markov guidance law calculates the (unnormalized) total probability of the semi-Markov models, $\Pr\left(\hat{z}_i^{\mathrm{ML}}, \mathscr{H}_i\right)$, as follows:

$$\Pr\left(\hat{z}_i^{\mathrm{ML}}, \mathscr{H}_i\right) = \begin{cases} \mathcal{N}\left(\hat{z}_i^{\mathrm{ML}}, Q_0\right), & \text{for } i = 0 \\ \mathcal{N}\left(-\hat{z}_i^{\mathrm{ML}}, Q_0\right), & \text{for } i = 1, \cdots, w \end{cases} \tag{6.6}$$

where $Q_0 = 9\ \mathrm{g}^2$. The value of the Poisson parameter employed in Eq. (5.21c) is $\lambda = 0.25$ for the semi-Markov model $\left(\hat{z}_i^{\mathrm{ML}}, \mathscr{H}_0\right)$ and is $\lambda = 0.0025$ for the other semi-Markov models.

6.1.4 Parameters for the Homing Accuracy of the Decision Directed Adaptive Guidance and Estimation Scheme

The homing accuracy of the decision directed adaptive guidance and estimation scheme is studied with two different banks of guidance laws. In the first case, the adaptive scheme employs a bank of guidance laws containing the game theoretic DGL/1 and DGL/C laws. In the second case, the bank contains the MEL and PN laws. In both cases, the homing accuracy of the adaptive scheme is compared with that of the non-adaptive laws matched with the state estimator E_0 (see § 5.2.2 for a description of estimator E_0). The equations of the DGL/1 and DGL/C laws are described in § 5.3.1 and the PN and MEL laws are given by (see chapter 8 in Ref. [90])

$$u(k) = N\frac{x_1(k) + x_2(k)t_{\mathrm{go}}}{t_{\mathrm{go}}^2} \qquad \text{PN law} \tag{6.7a}$$

$$u(k) = \frac{N'}{t_{\mathrm{go}}^2}\left[x_1 + x_2 t_{\mathrm{go}} + 0.5 x_3 t_{\mathrm{go}}^2 - x_4 \tau_P^2 (e^{-a} + a - 1)\right] \qquad \text{MEL law} \tag{6.7b}$$

with

$$N' \triangleq \frac{6a^2(e^{-a} + a - 1)}{2a^3 - 6a^2 + 6a + 3 - 12ae^{-a} - 3e^{-2a}} \tag{6.7c}$$

$$a \triangleq \frac{t_{\mathrm{go}}}{\tau_P} \tag{6.7d}$$

The navigation constant of the PN law, N, employs the value $N = 4$. The information delay, a parameter of the DGL/C law in Eq. (5.91c), is selected to have the value

$\Delta_l = 0.3$ s. The Monte Carlo simulations employ 100 different time instants for the onset of the evasive maneuver and a total of 200 000 different noise realizations. Each repetition employs the nonlinear dynamics of the engagement. The two comparison criteria are: the single shot kill probability (SSKP), defined as the probability of a successful interception, and the required lethal radius R_k of the pursuer. The decision directed adaptive guidance and estimation scheme employs a tuning process to set the value of the factor $\beta(\zeta)$ to $\beta(\zeta) = 1.00$; the factor $\beta(\zeta)$ is employed by the GLR test in the adaptive-$\mathscr{H}_0$ GLR algorithm.

6.1.5 Parameters for the Homing Accuracy of the Discretized Guidance Laws

The discretized versions of the DGL/0, DGL/1, and DGL/C laws are delivered by Eqs. (5.96)-(5.98) with the assumption that $z(\tau) = 0, \tau \in [t, t + \Delta]$. The discretized DGL laws are compared to two different sample and hold approximations of the continuous-time DGL laws. In the first sample and hold approximation, the continuous-time DGL laws update the value of the command $u(\cdot)$ at each sampling time interval Δ. In the second sample and hold approximation, the value of the command $u(\cdot)$ is updated a 1 000 times during each sampling time interval Δ, hence the command is updated at a much higher rate than in the first implementation. To update the command at a rate higher than the measurement rate, an assumption about the evader's acceleration between two sampling time is required. Here, the employed assumption is the same as for the discretized DGL laws, i.e., $z(\tau) = 0, \tau \in [t, t + \Delta]$.

The first sample and hold approximation corresponds to a straight forward application of the continuous-time DGL laws to a discrete-time setting. The second sample and hold approximation, with its higher update rate of the control command, better approximate a continuous-time system than the first simple and hold approximation;

hence, the lost of performance is decreased for the sample and hold approximation at the higher update rate.

For all the guidance laws, the state estimate is delivered by a Kalman filter with a WPAM shaping filter. The covariance of the WPAM is selected to be $Q_a = 225$ g^2. The Monte Carlo simulations employ 100 different time instants for the onset of the evasive maneuver and a total of 200 000 different noise realizations. Each repetition employs the nonlinear dynamics of the engagement. The statistical performance of the guidance laws are compared in terms of the required R_k to achieve SSKP=0.95.

6.2 The Detection Statistics

A decision test (such as the GLR test) involves risks of making two types of false decisions: rejecting the null hypothesis when it is true (type I error), and accepting the null hypothesis when it is false (type II error), see Ref. [43], p. 65. The false alarm rate (type I error) and the miss detection rate (type II error), for the GLR and the adaptive-$\mathscr{H}_0$ GLR detectors, are shown in Fig. 6.1. Here, the false alarm rate is calculated as a ratio between (a) the ensemble average of false alarms before the onset of the evasive maneuver, and (b) the number of decisions delivered before the onset (a decision is delivered at each discrete time instant). The missed detection rate is calculated by dividing the total number of engagements with at least one detection after the onset of the evasive maneuver by 1 000 (the Monte Carlo simulation employs 1000 engagements with the same onset time).

As seen from Fig. 6.1a, the adaptive-$\mathscr{H}_0$ GLR detector delivers a false alarm probability about 4 times smaller than that obtained by the GLR detector. The peak in the false alarm probability, at $\mathrm{tgo}_{\mathrm{sw}} \in [3.3, 3.8]$ s, is interpreted as follows. Whenever the onset of the evasive maneuver is close to the beginning of the engagement, the GLR detector cannot separate the event caused by a mismatch in $a^{\mathscr{H}_0}$ and the event

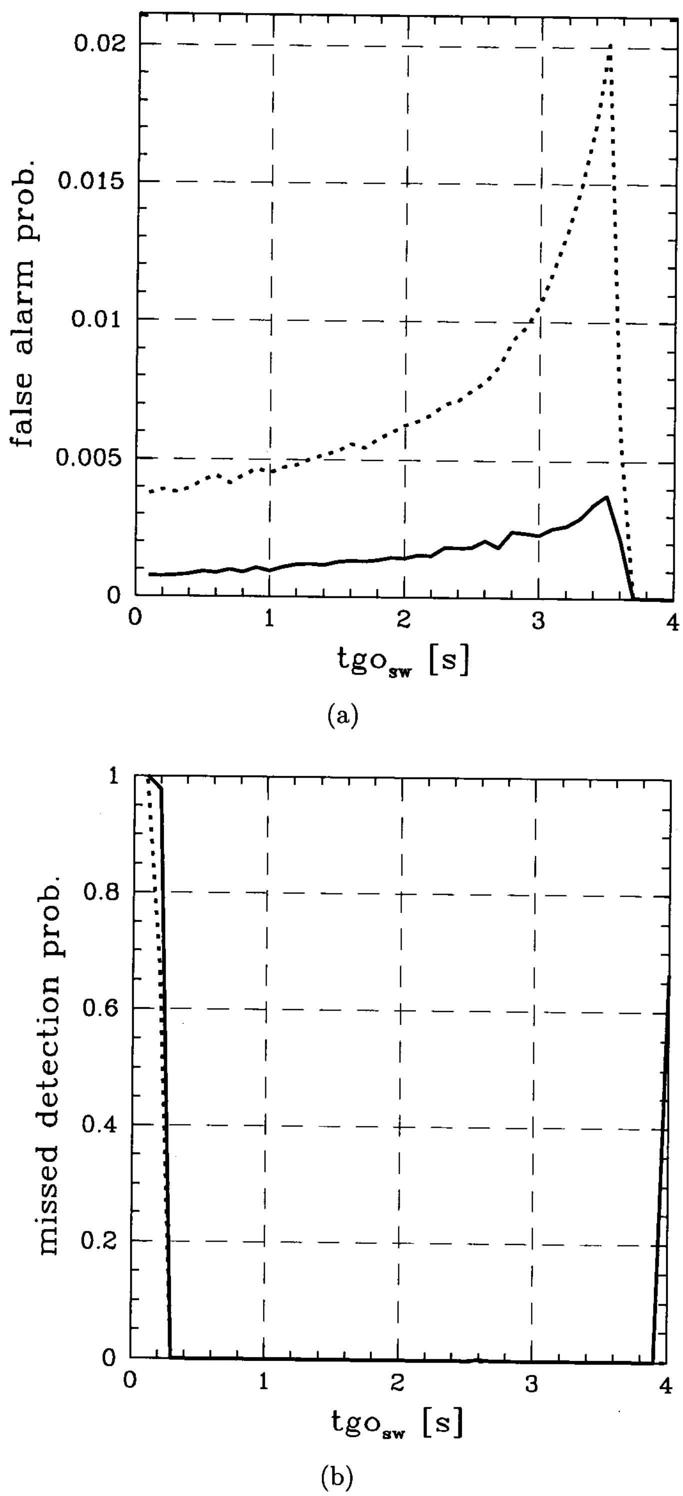

Figure 6.1: False alarm and missed detection rates. Continuous line: adaptive-$\mathscr{H}_0$ GLR detector, dotted line: GLR detector. Panels: (a) false alarm rate, (b) missed detection rate.

caused by the evasive maneuver. Because both events are present within the sliding window of the detector and since the detector has no single hypothesis that accounts for both, a larger false alarm probability results.

Figure 6.1b shows that the adaptive-$\mathscr{H}_0$ and the GLR detectors have, overall, similar missed detection probabilities. For an evasive maneuver with an onset time instant at $\mathrm{tgo}_{\mathrm{sw}} \in [0, 0.3]$ s, the detection is missed because there is not sufficient time left in the engagement to deliver a decision (see the discussion concerning the detection delays in the sequel). For an evasive maneuver with an onset time instant at $\mathrm{tgo}_{\mathrm{sw}} \in [3.9, 4.0]$ s, the adaptive-$\mathscr{H}_0$ GLR detector may miss the detection of the maneuver because the available information is not sufficient to distinguish between an alarm raised due to the onset of an evasive maneuver and that due to a mismatch in $a^{\mathscr{H}_0}$.

Due to the necessity of collecting sufficient information to deliver a statistically significant decision, there is always a time delay between the onset time of the evasive maneuver and the time instant at which this maneuver is detected. The average detection delay and its standard deviation, for the GLR and the adaptive-$\mathscr{H}_0$ GLR detectors, are shown in Fig. 6.2. The GLR and the adaptive-$\mathscr{H}_0$ GLR have similar average detection delays. The dip in the average detection delay produced by the GLR detector at $\mathrm{tgo}_{\mathrm{sw}} \in [3.5, 3.7]$ s deserves an explanation as it is not a manifestation of a superior quality of the GLR detector. Instead, it results from the GLR detector's inability to separate an event caused by a mismatched $a^{\mathscr{H}_0}$ and an event caused by the onset of an evasive maneuver. In the situation where both events are present within the sliding window, it can happen, by a fortuitous chance, that the GLR detector raises an alarm but which is actually a reaction to the initial mismatch in $a^{\mathscr{H}_0}$ rather than a reaction to the event of the onset of the maneuver. In other words, at this point, the GLR detector raises an alarm for the wrong reason; this does not happen in the case of the adaptive-$\mathscr{H}_0$ GLR detector.

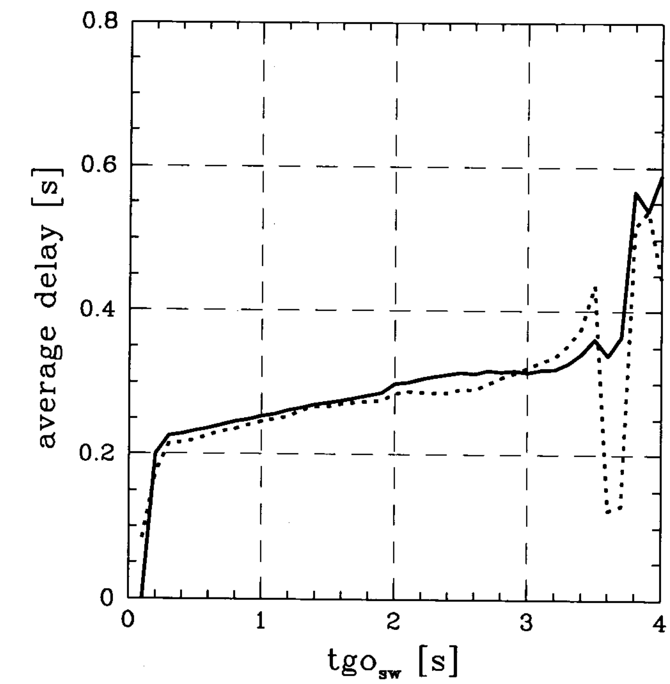

(a)

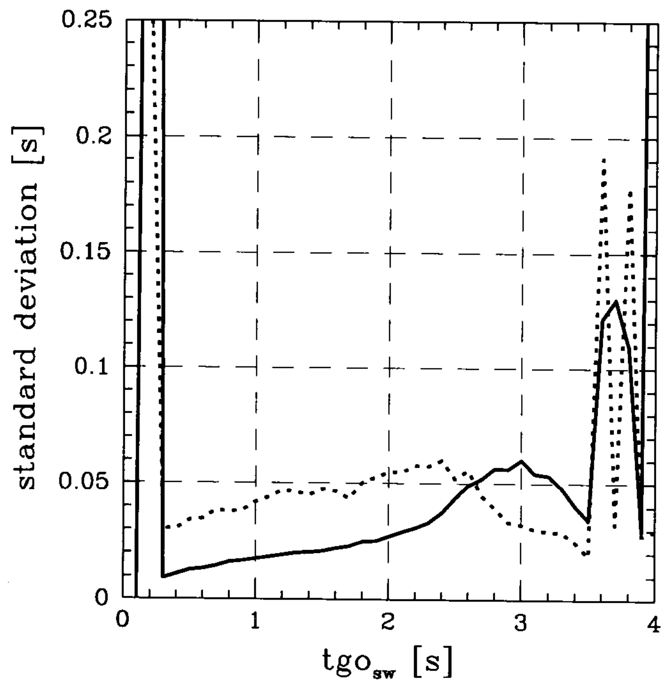

(b)

Figure 6.2: Detection delay. Continuous line: adaptive-$\mathscr{H}_0$ GLR detector, dotted line: GLR detector. Panels: (a) average detection delay, (b) standard deviation of the detection delay.

Figure 6.2b shows that the adaptive-$\mathscr{H}_0$ GLR detector exhibits a smaller standard deviation in the detection delay than the GLR detector for $\mathrm{tgo_{sw}} \in [0.2, 2.6]$ s. The standard deviation plots for the detection delays, for $\mathrm{tgo_{sw}} \in [2.7, 4]$ s, exhibit a complex behavior due to the initial mismatch in $a^{\mathscr{H}_0}$. The standard deviation of the detection delay for $\mathrm{tgo_{sw}} \in [0, 0.2]$ s is high because all detections in this interval are fortuitous in the sense that they are not triggered by the onset of the evader's maneuver but by parasitic phenomena (noises, mismatched $a^{\mathscr{H}_0}$).

The GLR detectors provide an estimate, $\hat{z}_{\mathrm{ML}}$, of the true evader's acceleration command, z. The mean and standard deviation of the estimation error, $e(k) = \hat{z}_{\mathrm{ML}}(k) - z(k)$, are shown in Figs. 6.3 and 6.4, respectively. The results are presented for six different onset times of the evader's maneuver. In all cases, the initial mismatch in $a^{\mathscr{H}_0}$ is detected and first corrected at $t_{\mathrm{go}} \approx 3.6$ s. At that point, the average error in the estimate from the GLR detector demonstrates a much larger overshoot than the one from the adaptive-$\mathscr{H}_0$ GLR detector. The pulse-like feature in the plots of Fig. 6.3 is generated by the evader's maneuver: the birth of the pulse happens at the onset of a maneuver and its left slope corresponds to the actual detection of the maneuver. The width of the pulse is associated with the detection delay. Following the detection of the maneuver, both detectors exhibit an overshoot in the average error of the estimate. This overshoot is clearly much larger using the GLR detector and is particularly pronounced for $\mathrm{tgo_{sw}} = 3.5$ s. This is attributed to a mismatch in the reference realization $a^{\mathscr{H}_0}$. The adaptive-$\mathscr{H}_0$ GLR detector avoids this pitfall due to its ability to separate the event of a mismatch and the event of the onset of the evasive maneuver. Additionally, the GLR detector delivers many false alarms (manifested as spikes in the average error) as compared to a negligible number of false alarms in the case of the adaptive-$\mathscr{H}_0$ GLR detector (no visible spikes in the average error).

The standard deviation of the estimation error in $\hat{z}_{\mathrm{ML}}$ is demonstrated to be much smaller by employing the adaptive-$\mathscr{H}_0$ GLR detector as compared to the one from the

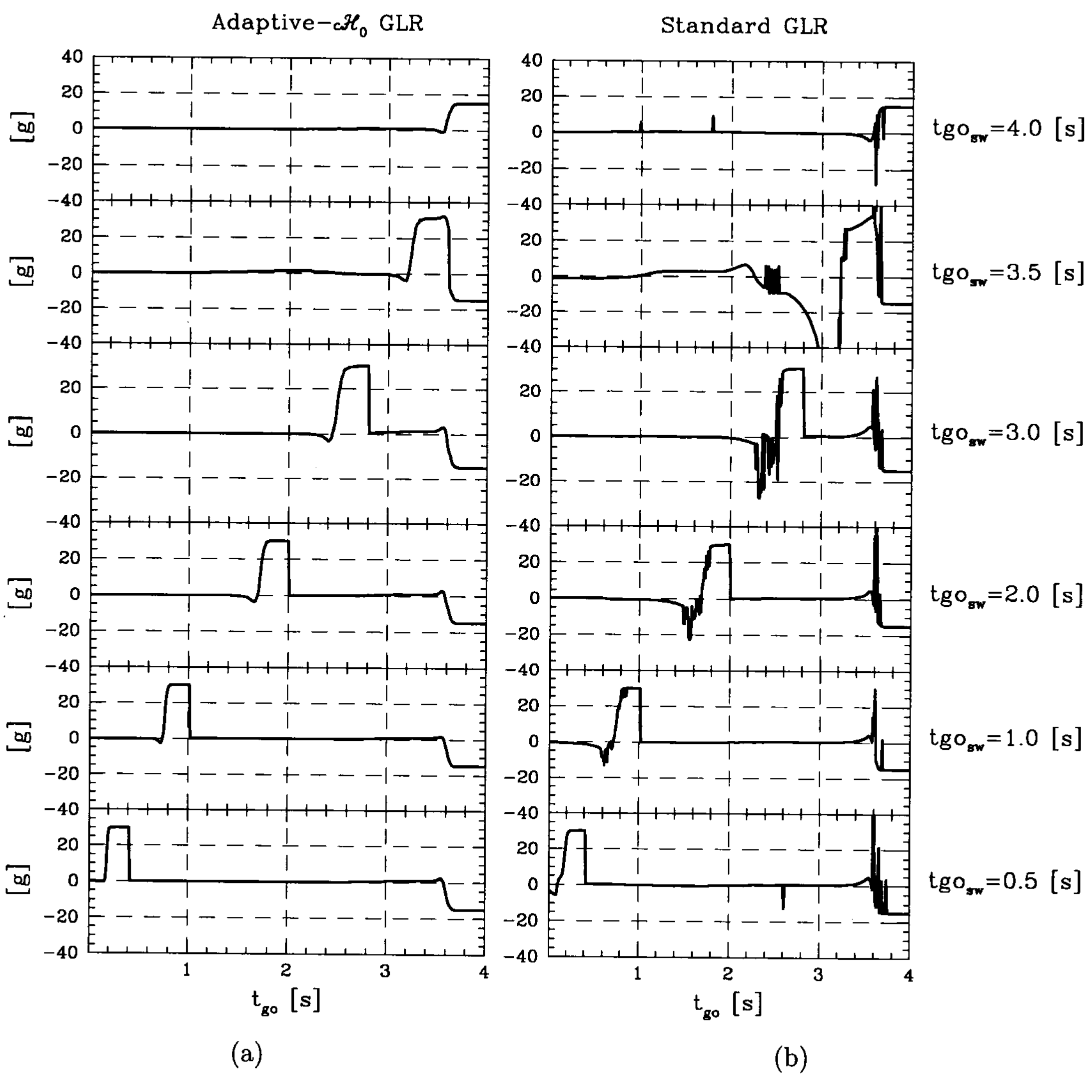

Figure 6.3: Average error of the estimate of the evader's command acceleration for several onset time instant of the bang-bang maneuver. Panels: (a) adaptive-$\mathcal{H}_0$ GLR detector, (b) GLR detector.

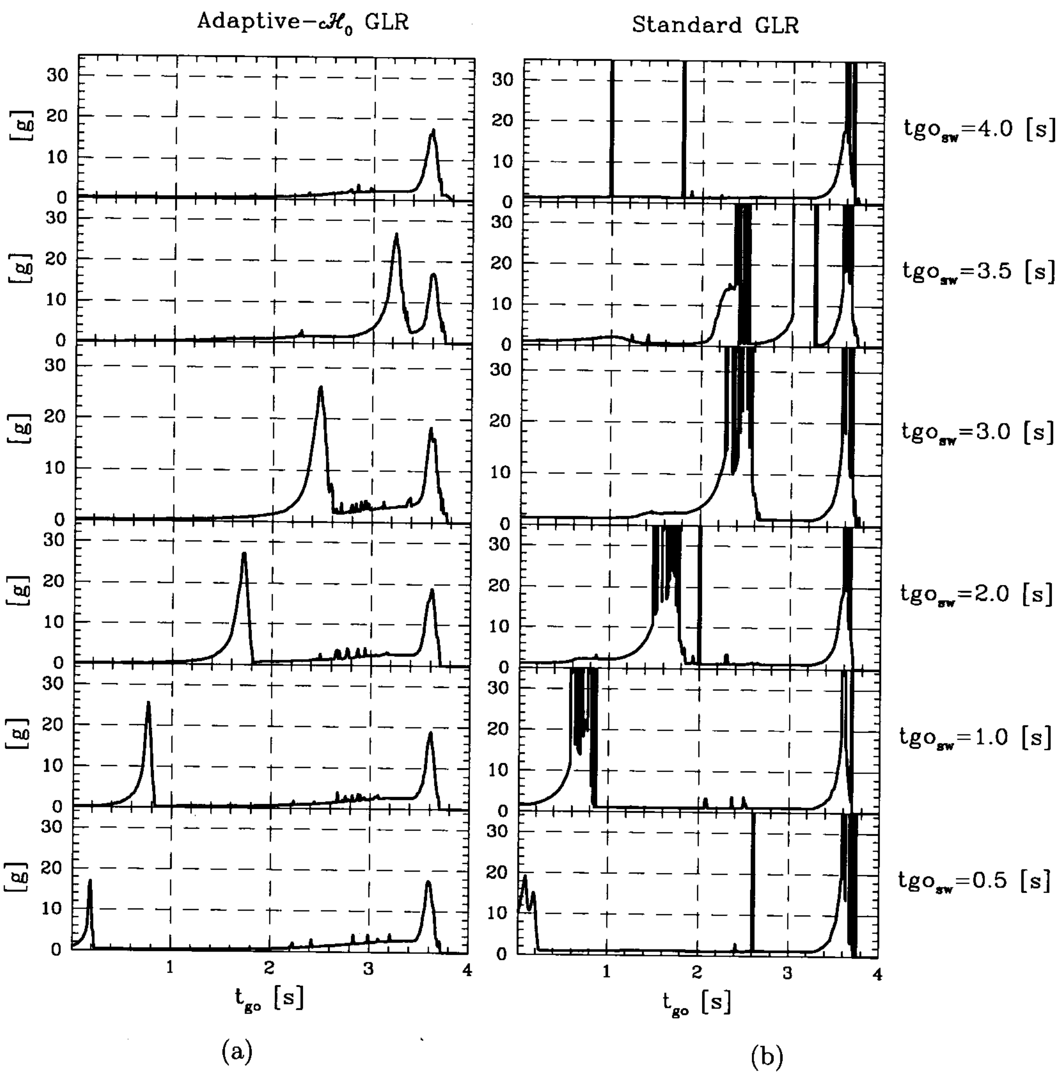

Figure 6.4: Standard deviation of the estimation error of the evader's command acceleration for several onset time instant of the bang-bang maneuver. Panels: (a) adaptive-$\mathscr{H}_0$ GLR detector, (b) GLR detector.

GLR detector, see Fig. 6.4. Moreover, the GLR detector fails to provide a consistent estimate of the evader's acceleration command; note the non-zero bias in the standard deviation plots in Fig. 6.4b. In contrast, the adaptive-$\mathscr{H}_0$ GLR detector can serve as a consistent filter.

6.3 The Estimation Statistics

The estimated evader's acceleration is depicted in Figure 6.5 for one sample noise realization (all the estimators employ the same sample noise realization). As compared with the estimates from the IMM estimators, the estimate from the AMR-GLR estimator is characterized by a better noise rejection and faster convergence after an abrupt change.

The magnitude of the average error in the estimate of the evader's acceleration is depicted in Figure 6.6a. As compared to the estimates from the IMM estimators, the estimate from the AMR-GLR estimator converges faster after an abrupt change. Specifically, the IMM1 estimator exhibits both a large average error and a slow convergence of the estimate. For the IMM2 and IMM3 estimators, increasing the covariance of the SF improves the convergence after an abrupt change, but not sufficiently to reach the rate of convergence of the AMR-GLR estimator. Further increasing the covariance of the SF at a level higher than IMM3 (not shown here) does not yield further improvements in the convergence of the estimate. As for the IMM4 estimator, it converges faster than the IMM2 estimator despite using the same bank of filters. It happens because IMM4 employs lower Markovian transition probabilities. However, the IMM4 estimator also exhibits the largest worse-case average error. The IMM5 estimator is characterized by a biased estimate. Additional simulations, not shown here, employing the IMM5 estimator with different values for its Markovian transition probabilities did not significantly improve the performance.

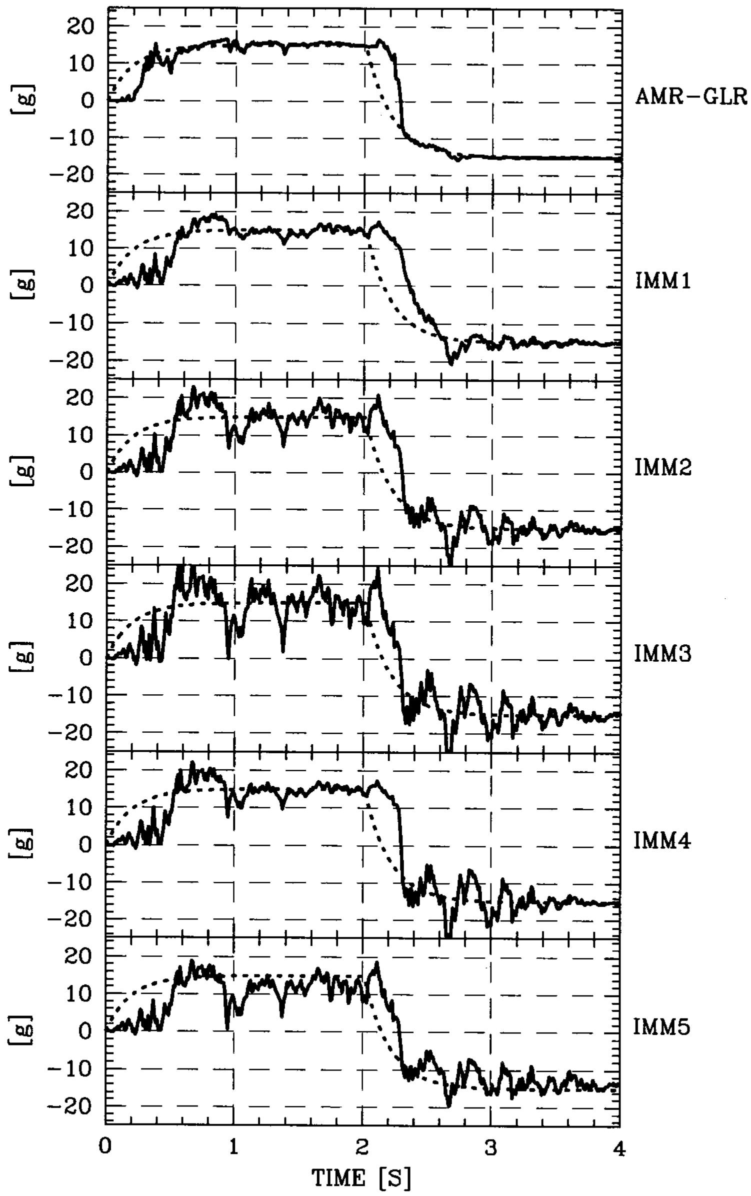

Figure 6.5: Estimation of the evader's acceleration. All the estimators employed the same noise realization. Solid line: estimated value, dashed line: true value.

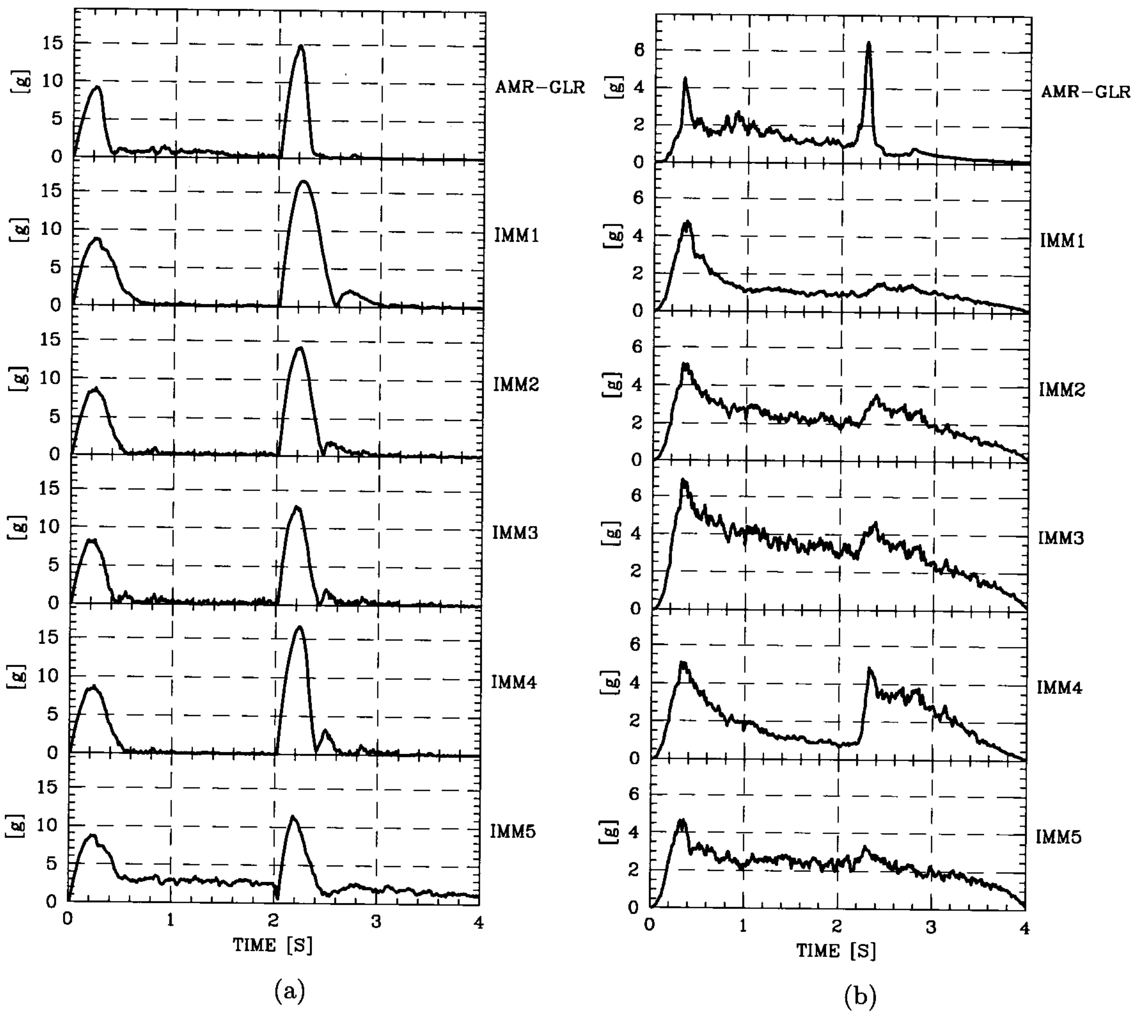

Figure 6.6: Statistics of the estimation error. The estimate is the evader's acceleration. Panels: (a) magnitude of the average estimation error, (b) standard deviation of the estimation error.

Table 6.2: Computational requirements

Estimator	time [10^{-2}s]	factor
IMM with 3 filters	28	1×
AMR-GLR with 70 hypotheses	151	5.4×
IMM with 9 filters	160	5.8×

The standard deviation (SD) in the estimate of the evader's acceleration is depicted in Figure 6.6b. The estimate from the AMR-GLR estimator exhibits a peak SD at $t \sim 2.4$ s, the last occurs in reaction to the abrupt change in the evader command acceleration. Before the peak, the AMR-GLR estimator and the IMM1 estimator yield estimates with similar SD. After the peak, the lowest SD is achieved by the AMR-GLR estimator. The IMM1 estimator exhibits a SD lower than the IMM2 and IMM3 estimators because the covariance of its SF is the lowest. The IMM4 estimator demonstrates a large SD of its estimate at the beginning of the engagement and after the peak; the low Markovian transition probabilities render the estimate sensitive to noise and model uncertainty initially and after an abrupt change. The IMM5 estimator is similar to the IMM2 estimator in terms of the SD.

To summarize the results in Figures 6.6a and 6.6b, the estimate from the AMR-GLR estimator demonstrates simultaneously fast convergence after an abrupt change and a low standard deviation. In the same situation, the IMM estimator can provide either an estimate with a fast convergence rate, or an estimate with a low standard deviation, *but not both simultaneously.*

The computational requirements of the estimators are displayed in Table 6.2. In terms of computational requirements, the AMR-GLR estimator with 70 hypotheses is similar to an IMM estimator with 9 filters. The IMM estimator with 9 filters requires five times more computational time than the IMM estimator with 3 filters. The IMM

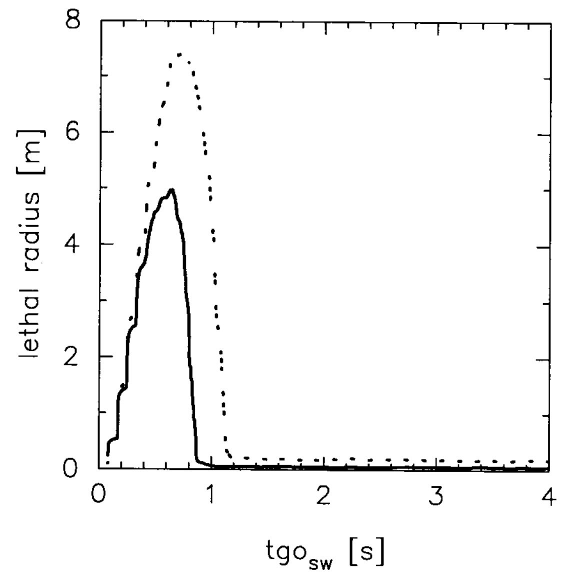

Figure 6.7: Required lethal radius to guarantee SSKP=0.95. The guidance laws are: (1) solid line - the Bayesian semi-Markov law, and (2) dotted line - the DGL/1 law.

estimator has a computational requirement increasing faster than linearly with the number of filters because its procedure for mixing initial conditions is a quadratic operation with respect to the number of filters. The computational requirements of the AMR-GLR estimator increase linearly with the number of hypotheses, cf. [84].

6.4 Homing Accuracy of the Guidance Law for Semi-Markov Processes

The minimum R_k of the pursuer, required to achieve a SSKP $= 0.95$, is shown in Fig. 6.7 as a function of tgo_{sw}. The Bayesian semi-Markov guidance law consistently achieves a smaller miss distance than the DGL/1 law and the worst-case miss distance is reduced by $\sim$ 30%. The miss distance for maneuvers occurring in the interval $tgo_{sw} \in [0.8, 1.2]$ s is essentially zero by employing the Bayesian semi-Markov law. By comparison, the DGL/1 law reaches $\sim$ 6 m in the same interval.

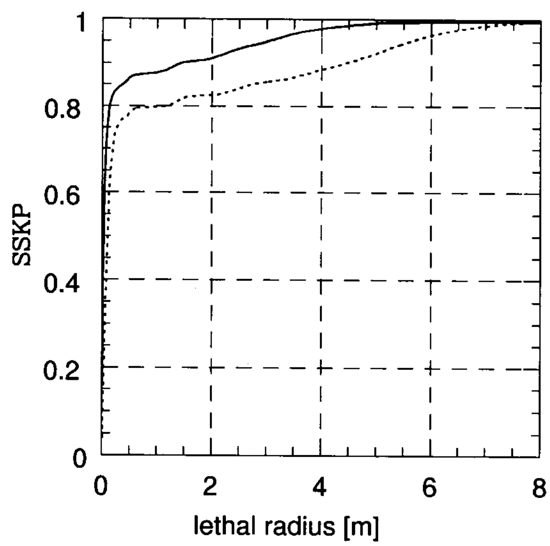

Figure 6.8: Overall SSKP versus the lethal radius. The guidance laws are: (1) solid line - the Bayesian semi-Markov law, and (2) dotted line - the DGL/1 law.

The relationship between the overall SSKP and the required R_k is shown in Figure 6.8. This overall SSKP was obtained by assuming a uniform distribution for the onset of the evasive maneuver. The results show that if, for example, a SSKP $= 0.90$ is required, then the pursuer needs the following minimum R_k: (i) $R_k \approx 2$ [m] using the Bayesian semi-Markov law, or (ii) $R_k \approx 5$ [m] using the DGL/1 law.

6.5 Homing Accuracy of the Decision Directed Adaptive Guidance and Estimation Scheme

The minimum R_k of the interceptor required to achieve a SSKP $= 0.95$ is shown in Fig. 6.9 as a function of the onset time of the evasive maneuver. The decision directed adaptive scheme requires a R_k which is always smaller or equal to that of the non-adaptive combination of E_0 with DGL/C. As compared with the non-adaptive combination of E_0 with DGL/1, the decision directed adaptive scheme requires a

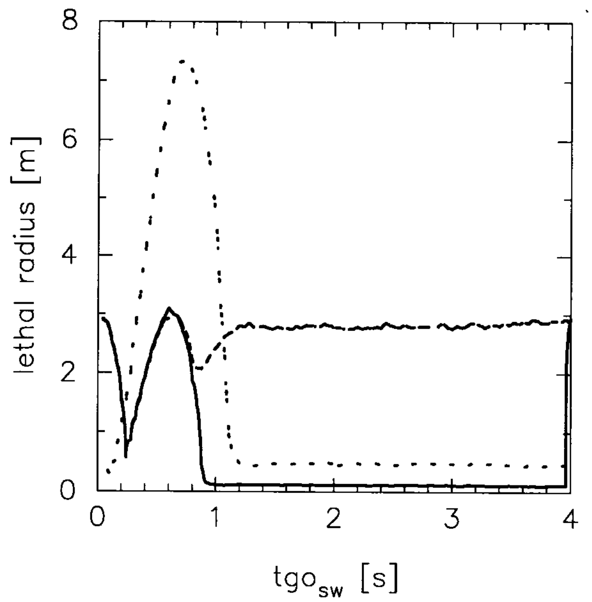

Figure 6.9: Required lethal radius of the pursuer to guarantee SSKP = 0.95. Three curves are compared: solid line - decision directed adaptive scheme, dotted line - non-adaptive E_0 filter with a pure DGL/1 law, and dashed line - non-adaptive E_0 filter with a pure DGL/C law.

smaller R_k except for $\text{tgo}_{\text{sw}} \in [0, 0.2]$ [s] and near the beginning of the engagement at $\text{tgo}_{\text{sw}} \approx 4.0$ [s].

When the onset of the maneuver is at $\text{tgo}_{\text{sw}} \in [0.9, 3.9]$ [s], the adaptive scheme has sufficient time after detection of the maneuver to both improve the state estimate (by reduction of the filter bandwidth) and to bring the trajectory of the pursuer on a collision course with the evader (by employing the DGL/1 law). The improved state estimate from the low bandwidth filter E_1 allows the adaptive scheme to achieve a smaller miss distance than that of the off-line combination of DGL/1 with a high bandwidth filter. Because a low bandwidth filter such as E_1 can only be used after a maneuver occurs, its implementation requires an on-line decision mechanism (like the governor of the adaptive scheme) to decide when to turn it on.

When the onset of the maneuver is $\text{tgo}_{\text{sw}} < 0.9$ [s], the adaptive scheme does not have sufficient time left after detection of the maneuver to bring the pursuer's trajectory on a collision course with the evader. Prior to the detection, the pursuer trajectory is set by the DGL/C law while, after detection, the trajectory is determined by the DGL/1 law. The lack of time left after detection when $tgo_{sw} < 0.9$ [s] means that the trajectory of the pursuer employing the adaptive scheme is somewhere between the trajectories set by application of pure DGL/C and DGL/1 laws.

When the onset of a maneuver is $tgo_{sw} \in [0, 0.2]$ [s], there is not enough time left in the engagement for a significant change of, either, the evader's achieved acceleration or the evader's trajectory. For this reason, the DGL/1 law works reasonably well as the interceptor trajectory as little needs to be corrected to remain on a collision course with the evader. In the same situation, the decision directed adaptive scheme does not perform as well because there is not enough time left after the onset of the maneuver for it to react to the change, i.e., to bring the interceptor's trajectory on a collision course with the evader.

When the onset of a maneuver occurs near the beginning of the engagement, i.e., at $tgo_{sw} \approx 4.0$ [s], the maneuver detector does not have sufficient information to distinguish between the onset of an evasive maneuver and the error in the initial conditions. The onset of an evasive maneuver may then go unnoticed by the detector so, the governor of the adaptive scheme fails to get activated.

The overall SSKP is obtained by assuming a uniform distribution for the onset of the evader's maneuver. The relationship between the overall SSKP and the required R_k is shown in Figure 6.10. For example, if SSKP = 0.8 is required, then the pursuer must have the following lethal radii: (i) $R_k \approx 0.2$ [m] for the decision directed adaptive scheme, (ii) $R_k \approx 0.7$ [m] for the non-adaptive combination of E_0 with DGL/1, and (iii) $R_k \approx 3.2$ [m], for the non-adaptive combination of E_0 with DGL/C.

The homing accuracy of the decision directed adaptive scheme using a different

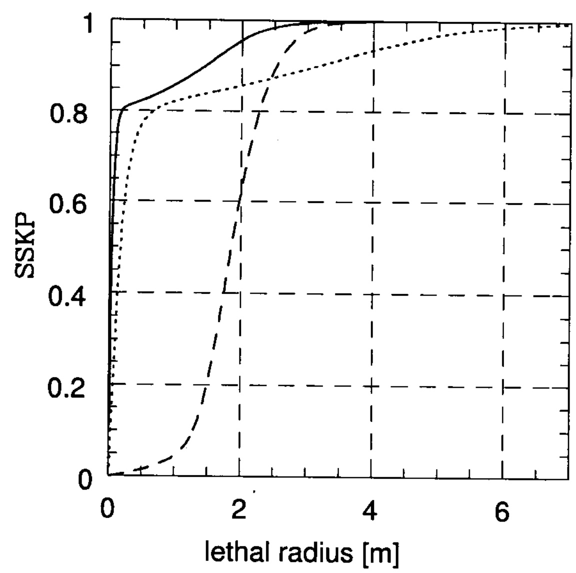

Figure 6.10: Overall SSKP versus the interceptor lethal radius. Three curves are compared: solid line - decision directed adaptive scheme, dotted line - non-adaptive Kalman filter with a pure DGL/1 law, and dashed line - non-adaptive Kalman filter with a pure DGL/C law.

bank of guidance laws is shown in Figure 6.11. The bank of guidance laws now contains the PN and MEL laws. Although the miss distance using the new bank is about 10 times higher than that of the bank containing the DGL/1 and DGL/C laws, the interpretation of the results is similar to the preceding Figures 6.9 and 6.10. It also demonstrates that the decision directed adaptive scheme works well with different families of guidance laws.

To summarize the Figures 6.9 - 6.11, the decision directed adaptive scheme achieves miss distances significantly smaller than the off-line combination of the DGL/1, DGL/C, PN, and MEL laws with an estimator.

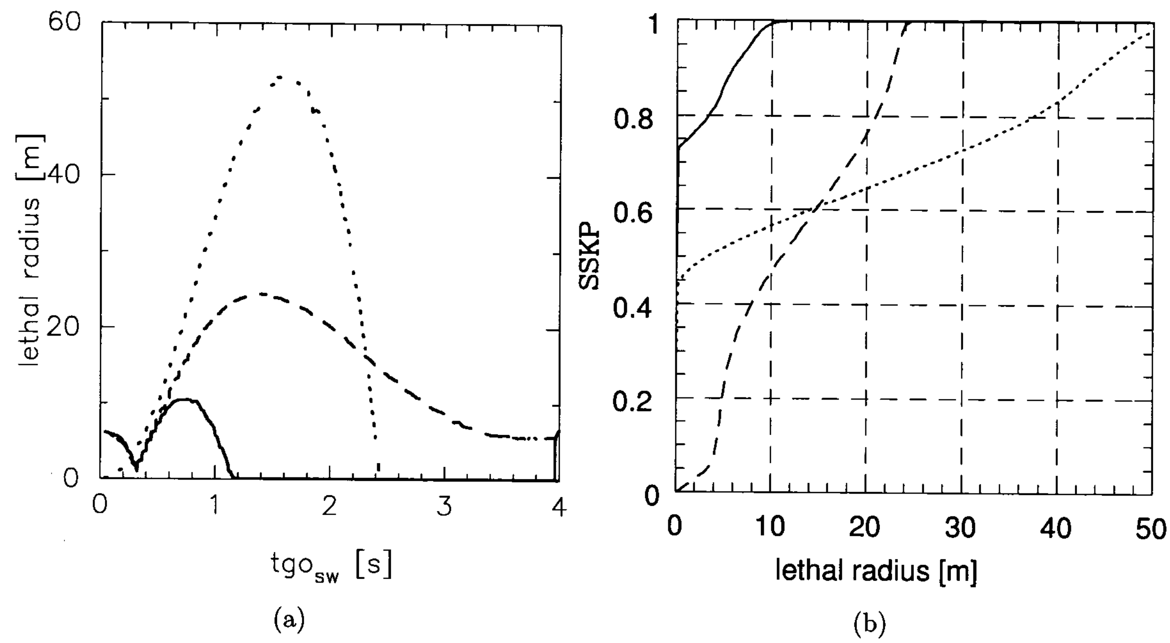

Figure 6.11: Homing accuracy of the adaptive scheme using the PN and MEL laws. Panel (a): Required lethal radius of the pursuer to guarantee SSKP = 0.95. Panel (b): Overall SSKP versus the interceptor lethal radius. Three curves are compared: solid line - decision directed adaptive scheme, dotted line - non-adaptive E_0 filter with a pure MEL law, and dashed line - non-adaptive E_0 filter with a pure PN law.

6.6 Homing Accuracy of the Discretized Guidance Laws

The pursuer's command acceleration history for a sample engagement is presented in Fig. 6.12 for two guidance laws: the discretized DGL/1 law and the sample and hold approximation of the continuous-time DGL/1 law. The sample run employs $\mathrm{tgo}_{\mathrm{sw}} = 2.0$ [s] and is carried out without noise. The sample and hold approximation is characterized by a discontinuous command history due to its bang-bang nature while the discretized DGL/1 law provides a smooth acceleration command.

The minimum R_k of the pursuer required to achieve a SSKP $= 0.95$ is shown in Fig. 6.13 for the DGL/0, DGL/1, and DGL/C laws and for the three considered types of implementations of the laws. As is seen from Fig. 6.13, the performance of the discretized laws is equivalent to the one of the the sample and hold approximation at an update rate of 100 KHz. By comparison, the implementation of the continuous-time laws using a sample and hold approximation at an update rate of 100 Hz degrades the miss distance of the pursuer.

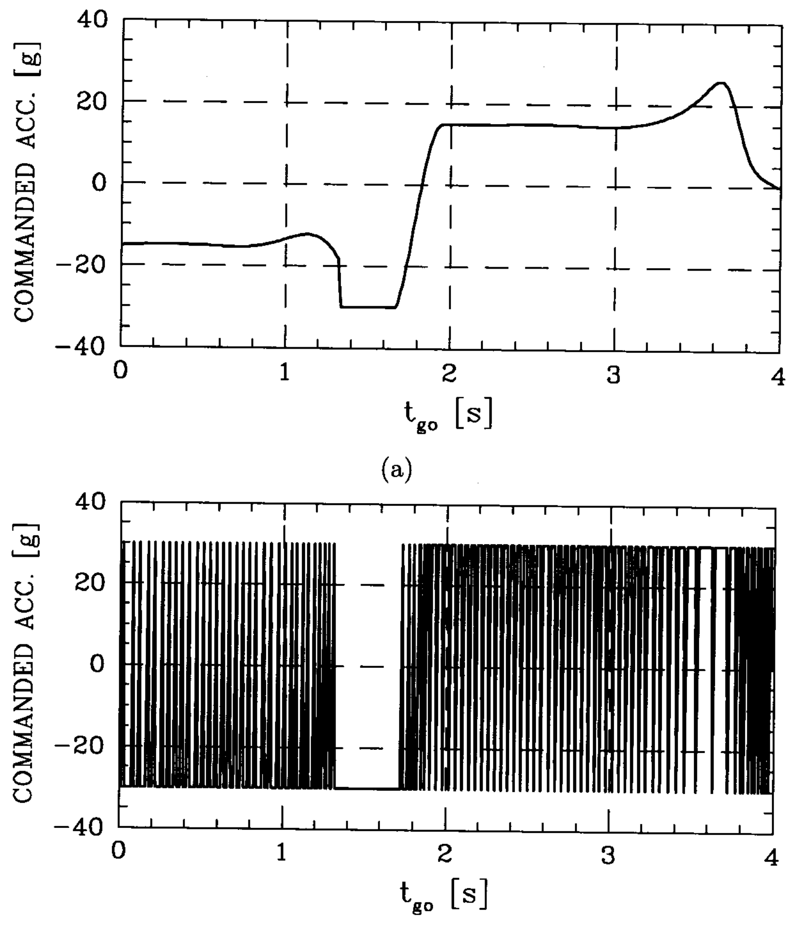

Figure 6.12: Pursuer's acceleration command: discrete vs continuous time. A sample engagement with no measurement noise is presented. The onset of the evasive maneuver is $tgo_{sw} = 2.0$ [s]. Panel (a): Discretized DGL/1 law. Panel (b): Sample and hold approximation of the DGL/1 law (update rate: 100 Hz)

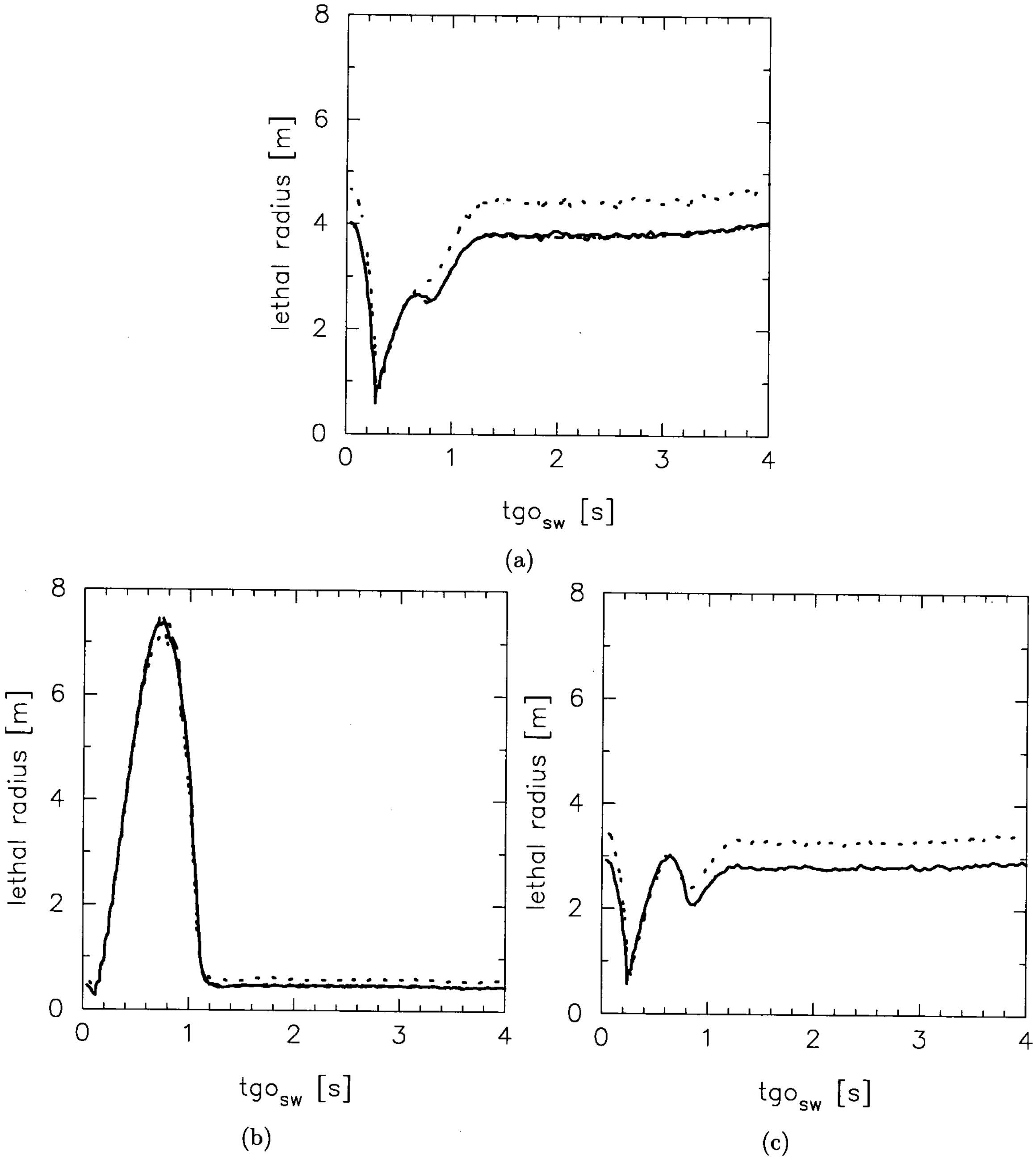

Figure 6.13: Required lethal radius to guarantee SSKP = 0.95: discrete vs continuous. Panel (a): DGL/0 law. Panel (b): DGL/1 law. Panel (c): DGL/C law. Solid line - sample and hold approximation (update rate: 100 KHz). Dotted line - sample and hold approximation (update rate 100 Hz). Dashed line - discretized DGL law.

Chapter 7

The Concluding Remarks

7.1 General Summary

This thesis presents a new guidance approach for the interception of a maneuvering target. The approach has been developed in several directions as the function of homing guidance relies on several subsystems, most notably the estimator and the guidance law. The main research contributions are:

1. The development of two novel maneuver detectors.
2. The development of two novel adaptive state estimators that employ ideas from detection theory.
3. The development of a novel adaptive Bayesian multiple model predictor of the ballistic miss that employs semi-Markov models and ideas from detection theory.
4. The presentation of a novel integrated estimation and guidance scheme that employs banks of estimators and guidance laws, a maneuver detector, and an on-line governor.

5. The introduction of a novel discretization scheme for a family of bang-bang guidance laws.

The development of the new detection algorithms was motivated by the absence of sufficiently fast and reliable sequential detection schemes that were capable of detecting and identifying abrupt changes in unknown input processes (such as the acceleration commands of randomly maneuvering targets). The first new algorithm in this category is a novel implementation of GLR detector for maneuver detection. The new implementation introduces a simpler formula to calculate the signature of an additive change in the innovation of a Kalman filter and employs a re-initialization scheme to compensate for the unknown reference realization of the maneuver. The novel adaptive-$\mathscr{H}_0$ GLR detector is presented next. The adaptive-$\mathscr{H}_0$ GLR detector employs a new adaptation scheme to estimate and update on-line the reference realization without discarding information. The adaptive-$\mathscr{H}_0$ GLR detector is hence more accurate than the GLR detector.

The development of the two novel adaptive state estimators employs by the ability of the GLR algorithm to constrain the evasive maneuver to be a member of a parametric family of functions. This ability permits for a more accurate modeling of the target behavior as compared with other estimators. The novel estimators employ banks of parametric families of input functions within a GLR scheme to yield a Bayesian state estimate. The estimators apply to linear systems with unknown inputs subject to additive abrupt changes. The two new state estimators differ by their assumption about the realization of the unknown input before an abrupt change (the so-called reference realization). The first state estimator assumes that the reference realization is a member of a finite set of pre-specified realizations while the second state estimator assumes it to be a member of a parametric family of functions.

Finally, the terminal guidance problem is approached in three different manners. First, a novel Bayesian multiple model predictor of the ballistic miss employing a bank of adaptive semi-Markov models is presented. The semi-Markov modeling permits for a more accurate modeling of the future evasive behavioral patterns than their Markovian counterparts while the Bayesian multiple model approach yields the pdf of the ballistic miss. As most terminal guidance laws are functions of the ballistic miss, the mean of this pdf is then employed for terminal guidance. A GLR algorithm is employed to adapt the semi-Markov models and to yield the required a posteriori probabilities to calculate the pdf of the ballistic miss.

A new integrated approach is also presented to improve the homing performance by adaptation of the state estimator and terminal guidance law to the characteristics of the pdf of the filtered state. Banks of estimators and guidance laws a provided and the effective estimator and guidance law are selected on-line by a governor on the basis of the outputs of a maneuver detector and a priori information about the number of maneuvers expected. The approach can be viewed as an on-line optimization scheme of the state estimator and of the guidance law. Lastly, a novel discretization scheme for a family of bang-bang guidance laws is presented.

The performance of the novel algorithms is assessed using an example benchmark scenario of a pursuit-evasion engagement between a randomly maneuvering ballistic missile and an interceptor. Extensive Monte Carlo simulations are employed to evaluate the main statistical properties of the algorithm. The results demonstrate the following:

- The adaptive-$\mathscr{H}_0$ GLR detector outperforms the GLR detector in that it achieves a lower observed false alarm rate (about four times smaller than that achieved by the GLR detector), a more consistent detection delay, characterized by a smaller standard deviation, and a more consistent input estimate, characterized by a smaller average error and a smaller standard deviation. Also, in contradistinction with the standard GLR detector, the observed false alarm rate of the novel detector matches its theoretical prediction (the pre-specified false alarm probability).

- The novel AMR-GLR estimator is compared to several implementations of the IMM estimator. The AMR-GLR delivers a better trade-off between the estimation reliability as expressed by the standard deviation of the error and speed of convergence after an abrupt change. None of the implemented IMM estimators is capable of delivering estimates characterized by a similar standard deviation error while simultaneously exhibiting comparable rate of convergence. The benefits of the AMR-GLR estimator are achievable at relatively modest computational expense as, unlike the IMM estimator, the AMR-GLR estimator employs only a single Kalman filter.

- The Bayesian multiple model prediction of the ballistic miss is compared to that employed by the game theoretic DGL/1 law. A terminal guidance law of the same form as the DGL/1 law but employing the Bayesian prediction of the ballistic miss decreases the achieved miss distance by 30%.

- The integrated estimation and guidance scheme demonstrates a significant decrease of the miss distance as compared with state-of-the-art approaches which are optimized off-line.

- The discretization of the bang-bang guidance laws known as DGL/0, DGL/1, and DGL/C is shown to deliver similar miss distances as their continuous-time counterpart.

7.2 Conclusions

The main conclusions are:

- The adaptive-$\mathscr{H}_0$ GLR detector delivers an efficient and reliable diagnosis of evasive maneuvers.
- The modeling of the target behavior by parametric families of functions permits to improve its state estimate. Moreover, the GLR algorithm delivers a numerically efficient implementation of an estimation procedure.
- The modeling of the future evasive maneuvers by semi-Markov models and their prediction by a Bayesian multiple model approach improves the homing accuracy of the terminal guidance.
- The optimization of the state estimator and the guidance law with respect to the pdf of the filtered state improves the homing performance.
- The discretization of the bang-bang guidance laws is an efficient procedure and facilitates their implementation.

Although primarily developed for a terminal interception problem, the algorithms presented in this thesis apply to the broader class of linear hybrid systems described in § 2. This class of systems is commonly encountered in several applications, most notably in quality control, recognition-oriented signal processing, fault detection, and monitoring and control of industrial plants.

7.3 Future Research Avenues

In spite of the broad coverage of this thesis (presented in 11 papers) many important topics could not be addressed. The list of such topics includes:

1. Analysis of the algorithms in application to problems other than terminal interception scenarios.

2. Application and evaluation of the algorithms to a three-dimensional non-linear time-varying interception scenario.

3. Development of interception algorithms in the presence of multiple targets or in presence of decoys. In such problems, the pdf of the filtered state is multimodal and algorithms based on the expected values tend to drive the pursuer into the space between the targets rather than to a target. The novel algorithms introduced in this thesis employ maximum likelihood estimates that could prove advantageous in presence of multiple targets or decoys.

4. Detection, estimation, and control in the presence of nonlinear dynamics and non-additive changes (realistic flight dynamics are inherently nonlinear in the state).

5. Integration with an autopilot. An autopilot should be able to compensate for uncertainties in the dynamics of the vehicles. These uncertainties vary with the flight conditions.

Appendix A

General Solution of the Normed Differential Game

A general solution for the normed differential game of Eq. (5.25) *with perfect information* is cited below. It appears in Ref. [64], pp. 26-28, and is based on the solution presented in Ref. [38].

A.1 Deterministic Cost Function

The natural cost function, $\tilde{J}$, of the perfect information game is the miss distance

$$\tilde{J} = \inf_{a_P^c \in \mathcal{A}_P^c} \sup_{a_E^c \in \mathcal{A}_E^c} |\mathbf{D}x(t_f)| = \inf_{a_P^c \in \mathcal{A}_P^c} \sup_{a_E^c \in \mathcal{A}_E^c} |x_1(t_f)| \tag{A.1a}$$

with

$$\mathcal{A}_P^c \triangleq \left\{a_P^c \in \mathcal{P} \,\middle|\, |a_P^c(t)| \leq (a_P^c)^{\max} \;\; a.e. \;\; t \in [0, t_f]\right\} \tag{A.1b}$$

$$\mathcal{A}_E^c \triangleq \left\{a_E^c \in \mathcal{P} \,\middle|\, |a_E^c(t)| \leq (a_E^c)^{\max} \;\; a.e. \;\; t \in [0, t_f]\right\} \tag{A.1c}$$

$$\mathbf{D} = \begin{bmatrix} 1 & 0 & 0 & 0 \end{bmatrix} \tag{A.1d}$$

For simplicity, assume that $(a_P^c)^{\max} = (a_E^c)^{\max} = 1$. The pursuer attempts to minimize the cost $\tilde{J}$ while the evader wants to maximize it. In this deterministic case, an SSKP=1 is guaranteed if the pursuer's warhead lethal radius is larger than the guaranteed miss distance of the game.

A.2 Reformulated Problem

In order to reduce the order of the problem, the following terminal projection transformation is introduced

$$Z(t) = \mathbf{D}\Phi(t_f, t)x(t) \tag{A.2}$$

where $\Phi(t_f, t)$ is the transition matrix of the original homogeneous system. The variable Z denotes the zero effort miss (or ballistic miss). The transformation (A.2) reduces the problem to a scalar dynamic equation of the form

$$\frac{dZ(t)}{dt} = B(t)a_P^c + C(t)a_E^c \tag{A.3a}$$

where

$$B(t) = \mathbf{D}\Phi(t_f, f)\mathbf{B}_1(t) \tag{A.3b}$$

$$C(t) = \mathbf{D}\Phi(t_f, f)\mathbf{B}_2(t) \tag{A.3c}$$

The matrices $\mathbf{B}_1$ and $\mathbf{B}_2$ are the input matrices of the pursuer and evader, respectively, in the linear system describing the engagement The cost function becomes

$$\tilde{J} = \inf_{a_P^c \in \mathcal{A}_P^c} \sup_{a_E^c \in \mathcal{A}_E^c} |Z(t)| \tag{A.4}$$

A.3 Necessary Conditions of Optimality

The Hamiltonian of the game is

$$\mathcal{H} = \lambda_z(t)\left[B(t)a_P^c + C(t)a_E^c\right] \tag{A.5}$$

where λ_z is the co-state variable satisfying

$$\dot{\lambda}_z = -\frac{\mathrm{d}\mathcal{H}}{\mathrm{dZ}} = 0 \tag{A.6a}$$

$$\lambda_z(t_f) = \left.\frac{\mathrm{d}\tilde{J}}{\mathrm{dZ}}\right|_{t_f} = \mathrm{sign}\left(\mathrm{Z}(t_f)\right), \qquad \mathrm{Z}(t_f) \neq 0 \tag{A.6b}$$

which means that

$$\lambda_z(t) = \mathrm{sign}\left(\mathrm{Z}(t_f)\right), \qquad \mathrm{Z}(t_f) \neq 0 \tag{A.7}$$

as long as λ_z is continuous. The optimal strategies of the pursuer and the evader, $(a_P^c)^*$ and $(a_E^c)^*$, respectively, are then expressed as follows

$$(a_P^c)^* = \arg\min \mathcal{H} = -\mathrm{sign}\left(B(t)\mathrm{Z}(\mathrm{t_f})\right), \tag{A.8a}$$

$$(a_E^c)^* = \arg\max \mathcal{H} = \mathrm{sign}\left(C(t)\mathrm{Z}(\mathrm{t_f})\right), \qquad \mathrm{Z}(t_f) \neq 0 \tag{A.8b}$$

Assuming $B(t) < 0$ and $C(t) > 0$, the optimal strategies become

$$(a_P^c)^* = (a_E^c)^* = \mathrm{sign}\left(\mathrm{Z}(\mathrm{t_f})\right), \qquad \mathrm{Z}(t_f) \neq 0 \tag{A.9}$$

The last assumption is satisfied for the interception scenario described in § 2.

Bibliography

[1] F. P. Adler. Missile guidance by three-dimensional proportional navigation. *Journal of Applied Physics*, 27(3):500–507, 1956.

[2] B. D. O. Anderson and J. B. Moore. *Optimal Filtering.* Prentice Hall, Englewood Cliffs, 1979.

[3] G. M. Anderson. Comparison of optimal control and differential game intercept missile guidance laws. *Journal of Guidance and Control*, 4(2):109–115, 1981.

[4] Y. Bar-Shalom. Stochastic dynamic programming: Caution and probing. *IEEE Transactions on Automatic Control*, 26(5):1184–1195, 1981.

[5] Y. Bar-Shalom and K. Birmiwal. Variable dimension filter for maneuvering target tracking. *IEEE Transactions on Aerospace and Electronic Systems*, 18:621–629, 1982.

[6] Y. Bar-Shalom and K. C. Chang. Tracking a maneuvering target using input estimation versus the interacting multiple model algorithm. *IEEE Transactions on Aerospace and Electronic Systems*, 25:296–300, 1989.

[7] Y. Bar-Shalom and X. R. Li. *Estimation and Tracking: Principles, Techniques and Software.* Artech House, Inc., Boston, U.S., 1993.

[8] T. Basar and G. J. Olsder. *Dynamic Noncooperative Theory.* Academic Press, New York, 1982.

[9] M. Basseville. Detecting changes in signals and systems, a survey. *Automatica*, 24:309–326, 1988.

[10] M. Basseville and I. V. Nikiforov. *Detection of Abrupt Changes—Theory and Applications.* Prentice-Hall, Englewood Cliffs, N.J., April 1993. ISBN 0-13-126780-9.

[11] J. Ben-Asher and I. Yaesh. *Advances in Missile Guidance Theory*, volume 180 of *Progress in Astronautics and Aeronautics.* American Institute of Aeronautics and Astronautics, Reston, Virginia, 1998. ISBN: 1-56347-275-9.

[12] J. Ben-Asher and I. Yaesh. Improved methodology for theater missile defense end-games. In *Theater Ballistic Missile Defense*, volume 192 of *Progress in Astronautics and Aeronautics*, pages 222–242. AIAA, 2001. ISBN: 1-56347-385-2.

[13] H. A. P. Blom. An efficient filter for abruptly changing systems. In *Proceedings of the Conference on Decision and Control*, pages 656–658, 1984.

[14] H. A. P. Blom and Y. Bar-Shalom. The interacting multiple model algorithm for systems with Markovian switching coefficients. *IEEE Transactions on Automatic Control*, 33:780–783, 1988.

[15] P. L. Bogler. Tracking a maneuvering target using input estimation. *IEEE Transactions on Aerospace and Electronic Systems*, 23:298–310, 1987.

[16] A. K. Caglayan and R. E. Lancraft. Reinitialization issues in fault tolerant systems. In *Proceedings of the American Control Conference*, pages 952–955, San Francisco, CA, June 1983.

[17] L. Campo, P. Mookerje, and Y. Bar-Shalom. State-estimation for systems with sojourn-time-dependent Markov model switching. *IEEE Transactions on Automatic Control*, 36:238–243, 1991.

[18] R. G. Cottrell. Optimal intercept guidance for short-range tactical missiles. *AIAA Journal*, 9:1414–1415, 1971.

[19] D. Dionne and H. Michalska. Cost-equivalent guidance laws. Submitted to AIAA Journal of Guidance, Control, and Dynamics.

[20] D. Dionne and H. Michalska. *An Adaptive, Variable Structure, Multiple Model Estimator.* NATO ASI Series Book. Kluwer, 2003.

[21] D. Dionne and H. Michalska. *Integrated Estimation and Guidance for Target Interception.* NATO ASI Series Book. Kluwer, 2003.

[22] D. Dionne and H. Michalska. An adaptive multiple reference GLR state estimator for hybrid systems. In *Proceedings of the International Conference on Computing, Communications and Control Technologies*, volume 4, pages 107–112, Austin, Texas, 2004.

[23] D Dionne and H. Michalska. A multiple reference GLR state estimator for hybrid systems. *WSEAS Transactions on Circuits and Systems*, 3:711–716, 2004.

[24] D Dionne and H. Michalska. A multiple reference GLR state estimator for hybrid systems. In *Proceedings of the WSEAS International Conference on Instrumentation, Measurements, Control, Circuits and Systems*, Miami, Florida, 2004. paper n. 484-360.

[25] D Dionne and H. Michalska. An adaptive GLR estimator for state estimation of a maneuvering target. In *Proceedings of the American Control Conference*, 2005. in press.

[26] D Dionne and H. Michalska. An adaptive proportional navigation law for interception of maneuvering targets. *CSME Transactions on Industrial Automation and Control*, 2005. in press.

[27] D. Dionne, H. Michalska, and Y. Oshman. Terminal missile guidance using a semi-Markov target model. In *Proceedings of the 16th IFAC Symposium on Automatic Control in Aerospace*, volume 2, pages 56–61, St-Petersburg, Russia, June 2004.

[28] D. Dionne, H. Michalska, Y. Oshman, and J. Shinar. A novel adaptive generalized likelihood ratio detector with application to maneuvering target tracking. *Journal of Guidance, Control, and Dynamics*, 2005. in press.

[29] D. Dionne, H. Michalska, J. Shinar, and Y. Oshman. Decision-directed adaptive estimation and guidance for an interception endgame. Submitted to AIAA Journal of Guidance, Control and Dynamics.

[30] J. R. Dowdle, A. S. Willsky, and S. W. Gully. Nonlinear generalized likelihood ratio algorithms for maneuver detection and estimation. In *Proceedings of the American Control Conference*, pages 985–987, Arlington, VA, June 1982.

[31] R. J. Elliot, L. Aggoun, and J. B. Moore. *Hidden Markov Models: Estimation, and Control.* Springer-Verlag, New York, 1995.

[32] R. J. Fitzgerald. Shaping filters for disturbances with random starting times. *Journal of Guidance and Control*, 2:152–154, 1979.

[33] R. J. Fitzgerald. Simple tracking filters: Closed-form solutions. *IEEE Transactions on Aerospace and Electronic Systems*, 17:781–785, 1981.

[34] V. Garber. Optimum intercept laws for accelerating targets. *Journal of Guidance and Control*, 6:2196–2198, 1968.

[35] S. J. Godsill, A. Doucet, and M. West. Maximum a posteriori sequence estimation using monte carlo particle filters. *Annals of the Institute of Statistical Mathematics*, pages 82–96, 2001.

[36] M. Guelman. Antiballistic missile interception guidance. In *Theater Ballistic Missile Defense*, volume 192 of *Progress in Astronautics and Aeronautics*, pages 222–242. AIAA, 2001. ISBN: 1-56347-385-2.

[37] F. Gustafsson. *Adaptive Filtering and Change Detection.* John Wiley and Sons, Inc., New York, October 2000. ISBN: 0-471-49287-6.

[38] S. Gutman. On optimal guidance for homing missiles. *Journal of Guidance and Control*, 3(4):296–300, 1979.

[39] S. Gutman and G. Leitmann. Optimal strategies in the neighborhood of a collision course. *AIAA Journal*, 14:1210–1212, 1976.

[40] H. Hablani and D. W. Pearson. Miss distance error analysis of exoatmospheric interceptors. *Journal of Guidance, Control, and Dynamics*, 27(2):283–289, 2004.

[41] R. Isaacs. *Differential Games: a Mathematical Theory with Applications to Warfare and Pursuit, Control, and Optimization.* John Wiley and Son, New York, 1965.

[42] A. J. Isaksson and F. Gustafsson. Comparison of some Kalman filter based methods for manoeuvre tracking and detection. In *Proceedings of the Conference on Decision and Control*, volume 2, pages 1525–1531, 1995.

[43] S. Kay. *Fundamental of Statistical Signal Processing, Volume 2: Detection theory.* Number ISBN 0-13-504135-X. Prentice-Hall, 1998.

[44] T. Kirubarajan and Y. Bar-Shalom. Kalman filter versus IMM estimator: when do we need the latter? *IEEE Transactions on Aerospace and Electronic Systems*, 39(4):1452–1457, 2003.

[45] T. Kirubarajan, Y. Bar-Shalom, K. R. Pattipati, and I Kadar. Ground target tracking with variable structure IMM estimator. *IEEE Transactions on Aerospace and Electronic Systems*, 36:26–46, 2000.

[46] J. Korn, S. W. Gully, and A. S. Willsky. Application of the generalized likelihood ratio algorithm to maneuver detection and estimation. In *Proceedings of the American Control Conference*, pages 792–798, 1982.

[47] H. J. Kushner. Robustness and convergence of approximations to nonlinear filters for jump-diffusions. *Computational and Applied Math.*, 16:153–183, 1997.

[48] T. L. Lai. Sequential changepoint detection in quality control and dynamical systems. *Journal of the Royal Statistical Society, Series B*, 57(4):613–658, 1995.

[49] T. L. Lai and Z. Shan. Efficient recursive algorithms for detection of abrupt changes in signals and systems. *IEEE Transactions on Automatic Control*, 44(5):952–966, 1999.

[50] A. Leon-Garcia. *Probability and Random Processes for Electrical Engineering.* Addison-Wesley, 1994. ISBN: 0-201-50037-X.

[51] S. Levinson, H. Weiss, and J. Z. Ben-Asher. Trajectory shaping and terminal guidance using linear quadratic differential games. In *Proceedings of AIAA Guidance, Navigation, and Control Conference*, Monterey, California, August 2002. AIAA paper 2002-4839.

[52] X. R. Li. *Hybrid Estimation Techniques*, volume 76 of *Control and Dynamic Systems*, pages 213–287. Academic Press, 1996.

[53] X. R. Li. Multiple-model estimation with variable structure - part ii: Model-set adaptation. *IEEE Transactions on Automatic Control*, 45:2047–2060, 2000.

[54] X. R. Li and Y. Bar-Shalom. Model-set adaptation in multiple model estimators for hybrid systems. In *Proceedings of the American Control Conference*, pages 1794–1799, 1992.

[55] S. S. Lim and M. Farooq. Maneuvering target tracking using jump processes. In *Proceedings of the Conference on Decision and Control*, pages 2049–2054, Boston, MA, June 1991.

[56] G. Lorden. Procedures to reacting to a change in distribution. *Annals of Mathematical Statistics*, 42:1897–1908, 1971.

[57] F. Martinerie and P. Forster. Data association and tracking using hidden Markov models and dynamic programming. In *in Proceedings of the Conference ICASSP*, 1992.

[58] R. J. McAulay and E. Denlinger. A decision-directed adaptive tracker. *IEEE Transactions on Aerospace and Electronic Systems*, 9(2):229–236, 1973.

[59] G. V. Moustakides. Optimal stopping times for detecting changes in distribution. *Annals of Statistics*, 14:1379–1387, 1986.

[60] E. S. Page. Continuous inspection schemes. *Biometrika*, 41:100–115, 1954.

[61] B. Ristic, A. Sanjeev, and N. Gordon. *Beyond the Kalman Filter.* Artech House, 2004. ISBN: 1-58053-631-x.

[62] Y. Ritov. Decision theoretic optimality of the CUSUM procedure. *Annals of Statistics*, 18:1464–1469, 1990.

[63] I. Rusnak. Multiple model-based terminal guidance law. *Journal of Guidance, Control, and Dynamics*, 23(4):742–746, 2000.

[64] T. Shima. *End-Game Guidance Against a Highly Maneuvering Target.* PhD thesis, Technion - Israel Institute of Technology, Haifa, Israel, 2001.

[65] J. Shinar. *Solution Techniques for Realistic Pursuit-Evasion Games*, pages 63–124. Advances in Control and Dynamic Systems, Ed.: C.T. Leondes. Academic Press, New York, 1981.

[66] J. Shinar. Interception of maneuvring targets in theater missile defense. In *Theater Ballistic Missile Defense*, volume 192 of *Progress in Astronautics and Aeronautics*, pages 257–297. AIAA, 2001. ISBN: 1-56347-385-2.

[67] J. Shinar and V. Y. Glizer. Solution of a delayed information linear pursuit-evasion game with bounded controls. *International Game Theory Review*, 1(3–4):197–217, 1999.

[68] J. Shinar and T. Shima. Non-orthodox guidance law development approach for intercepting maneuvering targets. *Journal of Guidance, Control, and Dynamics*, 25(4):658–666, 2002.

[69] J. Shinar, T. Shima, and A. Kebke. On the validity of linearized analysis in the interception of reentry vehicles. In *Proceedings of the AIAA Guidance, Navigation, and Control Conference and Exhibit*, pages 1050–1060, Boston, Massachusetts, August 1998.

[70] J. Shinar and D. Steinberg. Analysis of optimal evasive maneuvers based on a linearized two-dimensional model. *Journal of Aircraft*, 14:795–802, 1977.

[71] J. Shinar and V. Turetsky. On improved estimation for interceptor guidance. In *Proceedings of the American Control Conference*, volume 1, pages 203–208, Anchorage, AS, June 2002.

[72] J. Shinar and M. Zarkh. The guidance challenge in ballistic missile defense scenarios against maneuvring threats. In *Proceedings of the Multinational Conference on Theater Missile Defense*, 1996.

[73] A. N. Shiryaev. The problem of the most rapid detection of a disturbance in a stationary process. *Soviet Math. Dokl.*, 1(2):795–799, 1961.

[74] A. N. Shiryaev. On optimum methods in quickest detection problems. *Theory of Probability and its Applications*, 8:22–46, 1963.

[75] A. N. Shiryaev. Minimax optimality of the method of cumulative sums (CUSUM) in the case of continuous time. *Russian Mathematical Surveys*, 51:750–751, 1996.

[76] R. A. Singer. Estimating optimal tracking filter performance for manned maneuvering targets. *IEEE Transactions on Aerospace and Electronic Systems*, 5:473–483, 1970.

[77] A. Spencer and W. Moore. Design trade-offs for homing missiles. In *Proceedings of the AIAA SDIO Annual Interceptor Technology Conference*, Huntsville, Alabama, May 1992. AIAA paper 92-2755.

[78] C. Striebel. Sufficient statistics in the optimum control of stochastic systems. *Journal of Mathematical Analysis and Applications*, 12:576–592, 1965.

[79] R. M. Stuckey and M. J. Lewis. Hypersonic missile requirements and operational tradeoff studies. *Journal of Spacecraft and Rockets*, 40(2):292–293, 2003.

[80] V. Turetsky and J. Shinar. Missile guidance law based on pursuit-evasion game formulation. *Automatica*, 39:607–618, 2003.

[81] M. L. Vellekoop. *Rapid Detection and Estimation of Abrupt Changes by Nonlinear Filtering.* PhD thesis, Imperial College of Science, Technology and Medicine, UK, Department of Electrical and Electronic Engineering, 1997.

[82] A. J. Viterbi. Error bounds for convolutional codes and an asymptotically optimum decoding algorithm. *IEEE Transactions on Information Theory*, pages 260–269, 1967.

[83] A. Wald. *Sequential Analysis.* Wiley, New York, 1947.

[84] A. S. Willsky. *Detection of abrupt changes in dynamic systems*, pages 27–49. Detection of Abrupt Changes in Signals and Systems, M. Basseville, A Benveniste, eds., Lecture Notes in Control and Information Sciences, v. 77. Springer, NY, 1986.

[85] A. S. Willsky and H. L. Johns. A generalized likelihood ratio approach to the detection and estimation of jumps in linear systems. *IEEE Transactions on Automatic Control*, AC-21:108–112, 1976.

[86] H. S. Witsenhausen. Separation of estimation and control for discrete time systems. In *Proceedings of the IEEE*, volume 69, pages 1557–1566, 1971.

[87] B. Yakir. *Optimal Detection of a Change in Distribution when the Observations Form a Markov-Chain with a Finite State-Space*, pages 346–358. Change-Point Problems, E. Carlstein, H. Muller, and D. Siegmund, Eds., Hayward. Inst. Math. Stastistics, CA, 1994.

[88] C. L. Yuan. Homing and navigational courses of automatic target seeking devices. *Journal of Applied Physics*, 19:1122–1128, 1948.

[89] P. Zarchan. Representation of realistic evasive maneuvers by the use of shaping filters. *Journal of Guidance, Control, and Dynamics*, 2:290–295, 1979.

[90] P. Zarchan. *Tactical and Strategic Missile Guidance*, volume 176 of *Progress in Astronautics and Aeronautics.* American Institute of Aeronautics and Astronautics, Reston, Virginia, 3 edition, 1997.